

**Functional consequences of ϵ AChR subunit truncating mutations
linked to Congenital Myasthenic Syndrome**

Dissertation

zur

Erlangung des Doktorgrades (Dr. rer. nat.)

der

Mathematisch-Naturwissenschaftlichen Fakultät

der

Rheinischen Friedrich-Wilhelms-Universität Bonn

vorgelegt von

Cristian Gurgui

aus

Bukarest, Rumänien

Bonn 2004

The work for this PhD thesis was performed from September 2002 to October 2004 in the laboratory of Prof. Dr. Dieter Swandulla at the Institute of Physiology II, Bonn, Germany

Angefertigt mit Genehmigung der Mathematisch-Naturwissenschaftlichen Fakultät der Rheinischen Friedrich-Wilhelms-Universität Bonn

1. Referent: Prof. Dr. Dieter Swandulla

2. Referent: Prof. Dr. Volker Herzog

Tag der Promotion: 06.04.05

Diese Dissertation ist auf dem Hochschulschriftenserver der ULB Bonn http://hss.ulb.uni-bonn.de/diss_online elektronisch publiziert

Erscheinungsjahr: 2005

Acknowledgements

Thanks to Prof. Dr. Dieter Swandulla for helpful discussion, for advice, for revising the thesis and evaluating it, and for his true friendship. Thank you very much for giving me the opportunity to pursue my PhD thesis in Electrophysiology.

I would also like to express my gratitude to my supervisor Dr. Michael Hans for the kind support throughout the thesis. You started by teaching me the first steps in Electrophysiology, and made me discover the vast world of the Patch-clamp technique. Thanks for your patience in the time you have spent next to me during recordings, analysis and writing, while answering to my questions, making suggestions, correcting my errors, and guiding me to achieving this goal. Without your kind support and friendship, this work would not have been possible.

I wish to express my sincere thanks to Prof. Dr. Volker Herzog for kindly accepting to be a co-referee of my major exam, for the support, and for evaluating the thesis.

I am greatly indebted to PD Dr. Gerhild van Echten-Deckert for being examiner of my PhD defence, for practical and moral support, suggestions, comments, and friendship.

Special thanks also go to Prof. Dr. Gabriele König, who also kindly agreed to be the examiner of my minor exam.

I am very grateful to Prof. Dr. Peter Propping for the kind support and true friendship throughout the time I was member of Graduiertenkolleg GRK 246 (“Pathogenesis of Diseases of the Central Nervous System”) in Bonn.

I acknowledge with thanks and appreciation the role of Joachim Sternberg and Hanne Bock for their excellent technical assistance and friendship.

Thanks to my girlfriend Mihaela Dragusin for patience and moral support throughout the time we have spent together. Thank you for proofreading the thesis and for the useful comments and suggestions. I would not have reached here without your support either.

Special thanks go to my family in Romania who spiritually supported and trusted me in all these years. Also, many thanks to all my friends (you all know who you are).

Scientific Work

Publications

Dragusin M., Gurgui C., Schwarzmann G., Hoernschemeyer J., and van Echten-Deckert G. (2003) Metabolism of the unnatural anticancer lipid safingol (L-threo-dihydrosphingosine) in cultured cells. *J Lipid Res*: 44(9): 1772-9.

Poster sessions

03/04: “Functional consequences of ϵ AChR subunit truncating mutations linked to Congenital Myasthenic Syndrome”, at the 83rd Annual Congress of the “Deutsche Physiologische Gesellschaft e.V.”, Leipzig, Germany. Authors: Gurgui C., Kraner S., Steinlein O. K., Swandulla D., and Hans M.

05/03: “Functional consequences of ϵ AChR subunit truncating mutations linked to Congenital Myasthenic Syndrome”, at the 29th Göttingen Neurobiology Conference, Göttingen, Germany. Authors: Gurgui C., Kraner S., Steinlein O. K., Swandulla D., and Hans M.

06/03: “Metabolism of the unnatural anticancer lipid safingol (L-threo-dihydrosphingosine) in cultured cells”, at the 2nd International Charleston Ceramide Conference, Como, Italy. Authors: Dragusin M., Gurgui C., Schwarzmann G., Hoernschemeyer J., and van Echten-Deckert G. (*Poster Prize*)

09/01: “Impedance Spectrometry in Electrodes Characterization“, at the 12th Romanian International Congress on Chemistry and Chemical Engineering, Bucharest, Romania. Authors: Popescu A., Lisca G., Gurgui C., Voinea C., and Vasilco R.

Presentations

12/03: Presentation “Functional consequences of ϵ AChR subunit truncating mutations linked to Congenital Myasthenic Syndrome”, at the Graduiertenkolleg Joint Meeting of the Neuroscience Research Training Groups 246 (“Pathogenesis of Diseases of the Central Nervous System”, Bonn University) and 320 (“Pathological Processes of the Nervous System: From Gene to Behavior”, Heinrich-Heine-Universität Düsseldorf), Bornheim-Walberberg, Germany

Table of Contents

Abbreviations.....	8
Abstract.....	10
1 Introduction	11
1.1 Neurological diseases. Congenital myasthenic syndromes. General remarks	11
1.2 Ligand-gated ion channels of fast chemical synapses.....	13
1.2.1 Nicotinic acetylcholine receptors (AChRs).....	14
1.2.1.1 Subtypes of nicotinic muscle AChR	15
1.2.1.2 Size and shape of the receptor molecule	15
1.2.1.3 The AChR topology	16
1.2.1.4 Mechanisms of ACh receptor activation.....	18
1.3 The neuromuscular junction (NMJ)	21
1.3.1 From nerve action potential to muscle action potential	21
1.3.2 CMS caused by defects in AChR.....	24
1.3.2.1 Slow-channel CMS	24
1.3.2.2 Fast-channel CMS	25
1.3.2.3 CMS caused by low-expressor mutations	26
1.4 The goal of the study.....	28
2 Materials and Methods	29
2.1 Cell culture	29
2.2 Transient transfection.....	29
2.3 Patch-clamp recordings	30
2.3.1 Data analysis of the patch-clamp recordings.....	31
2.3.1.1 Analysis of whole-cell recordings.....	31
2.3.1.1.1 Dose-response curves	31
2.3.1.1.2 AChR desensitization kinetics and current density.....	32
2.3.1.2 Analysis of single-channel recordings	32
2.4 Materials and suppliers.....	34

3	Results	37
3.1	Pharmacological and biophysical properties of wild-type, ϵ -subunit lacking, and ϵ -mutant AChRs inferred from whole-cell recordings.....	37
3.1.1	Introduction to whole-cell recordings	37
3.1.2	The properties of wild-type receptor	38
3.1.3	The properties of ϵ -subunit lacking receptor.....	39
3.1.4	The properties of ϵ -mutant receptors.....	42
3.1.5	Summary of the whole-cell data.....	48
3.2	Single-channel recordings	49
3.2.1	Introduction to single-channel recordings and data kinetic analysis.....	49
3.2.2	Unitary current and slope conductance	51
3.2.3	Kinetic analysis	52
3.2.3.1	Gating-kinetics of wild-type receptor	52
3.2.3.2	Gating-kinetics of ϵ -subunit lacking receptor	55
3.2.3.3	Gating-kinetics of ϵ -mutant receptors	58
3.2.3.4	The spontaneous activity of AChR	63
3.2.4	The correlation between the whole-cell- and the single-channel data	66
3.2.5	Summary of the single-channel data	68
4	Discussion.....	69
4.1	CMS mutations and their localization.....	69
4.2	Structure, formation and membrane insertion of the AChR	70
4.3	Mutation ϵ 911delT in the M ₃ segment leads to loss of function.....	71
4.4	Mutations within the TM3-4 cytoplasmic loop.....	72
4.4.1	Mutation ϵ 1101insT	72
4.5	Structural elements within the TM3-4 loop that influence channel-gating.....	73
4.5.1	Role of mutations ϵ 1293insG and ϵ 1206ins19.....	73
4.6	Mutation ϵ 1030delC elicits switch in gating pattern.....	75
4.7	Outlook for treatment of CMS patients.....	76
4.8	Summary	77

Appendix	79
The patch-clamp technique	79
i. General remarks	79
ii. Five patch-clamp measurement configurations.....	80
iii. The patch-clamp setup	82
iv. The main steps during a patch-clamp experiment.....	83
References	84
Eidesstattliche Erklärung	99
Curriculum Vitae	100

Abbreviations

A	Agonist
Å	Angstrom
AcCoA	Acetyl-Coenzyme A
ACh	Acetylcholine
ACHE	Acetylcholinesterase
AChR	Nicotinic Acetylcholine Receptor
AD	Analog-Digital
AP	Action Potential
BCS	Bovine Calf Serum
bp	Base pairs
CAP	Cell-Attached Patch
cDNA	Complementary DNA
CHAT	Choline Acetyltransferase
CHRNE	Cholinergic Receptor, Nicotinic, ϵ -polypeptide gene
CMAP	Compound Muscle Action Potential
CMS	Congenital Myasthenic Syndrome
ColQ	Collagenic tail subunit of Acetylcholinesterase
D	Desensitization
3,4-DAP	3,4-Diaminopyridine
Del	Deletion
DMEM	Dulbecco's Modified Eagle Medium
DNA	Deoxyribonucleic Acid
EC ₅₀	Effective Concentration 50
EGTA	Ethylene Glycol-1,2-bis(aminoethylether)-Tetraacetic Acid
EMG	Electromyography
ENaC	Epithelial Na ⁺ Channel
EPC	Patch-clamp Amplifier
EPP	Endplate Potential
ER	Endoplasmic Reticulum
Exp	Exponential
FEP	Fluorine Ethylene Propylene
g	Slope Conductance
GABA	γ -Aminobutyric Acid
GFP	Green Fluorescence Protein
HA	Amphipathic α -Helix
HACHT	High-Affinity Choline Transporter
HEK	Human Embryonic Kidney
HEPES	2-[4-(2-Hydroxyethyl)-1-Piperazinyl]-Ethanesulfonic Acid
Hz	Hertz
i	Unitary Current
Ins	Insertion
IOP	Inside-Out Patch
kbp	Kilo base pairs
kDa	Kilo Daltons
LEM	Lambert-Eaton Myasthenic Syndrome
LSS	Leading Signal Sequence
MEPP	Miniature Endplate Potential

MG	Myasthenia Gravis
Min	Minutes
mRNA	Messenger RNA
MTS	Methanethiosulfonate
MTSET	[2- (Trimethylammonium) Ethyl] MTS Bromide
n	Number of Cells
N	Number of Channels
NMJ	Neuromuscular Junction
Norm	Normalization
OOP	Outside-Out Patch
P_c	Close Probability
P_o	Open Probability
ppWC	Permeabilized-patch Whole-Cell
R	Receptor
RAPSYN	Receptor-Associated Protein at the Synapse
Rec. time	Recording time
RNA	Ribonucleic Acid
rpm	Rotations per minute
SCCMS	Slow-Channel Congenital Myasthenic Syndrome
Sec	Seconds
SEM	Standard Error of the Mean
τ_c	Close Time
τ_o	Open Time
τ_D	Time constant of Desensitization
TM	Transmembrane domain
VACHT	Vesicular ACh Transporter
V_{mp}	Membrane Potential
W	Weight
WC	Whole-Cell
WT	Wild-Type

Abstract

Congenital myasthenic syndromes (CMS) are inherited disorders due to presynaptic, synaptic, or postsynaptic defects of neuromuscular transmission. Some previously described kinships with typical signs of postsynaptic CMS showed a marked deficiency of nicotinic acetylcholine receptors (AChRs) as well as biochemical and morphological changes at the neuromuscular junctions (Shen et al., 2003; Engel et al., 1996a,b; Ohno et al., 1997; Ohno et al., 1998a; Abicht et al., 1999; Middleton et al., 1999; Croxen et al., 1999; Sieb et al., 2000a,b; Shen et al., 2002). Recently, five truncating (ϵ 911delT, ϵ 1030delC, ϵ 1101insT, ϵ 1206ins19, and ϵ 1293insG) and one missense mutation (ϵ V448L) in the muscular AChR ϵ -subunit gene (*CHRNE*) were identified in patients with CMS symptoms (Engel et al., 1996a; Ohno et al., 1998b; Sieb et al., 2000a,b). We introduced the six mutations into the human ϵ -subunit and investigated their functional consequences by the means of patch-clamp technique after co-expression with human α , β and δ -subunits in HEK 293 cells.

Whole-cell recordings revealed that with the exception of ϵ V448L AChR all mutants exhibited altered biophysical properties, with acceleration of the macroscopic current decay and enhanced degree of desensitization, similar to $-\epsilon$ receptor. Furthermore, the receptors carrying the truncating mutations showed a significantly reduced current density. Mutant ϵ V448L exhibited biophysical properties similar to those of wt receptor.

Single-channel recordings revealed that mutants ϵ 911delT and ϵ 1101insT opened with brief and isolated events, similarly to $-\epsilon$ receptor. In contrast, mutant ϵ 1030delC switched between two distinct gating modes, one resembling the gating pattern of wt AChR, with bursts of single-channel openings and a second one with very low probability of opening, as observed with $-\epsilon$ receptor. Mutant ϵ V448L exhibited gating kinetics that were similar to wt receptor.

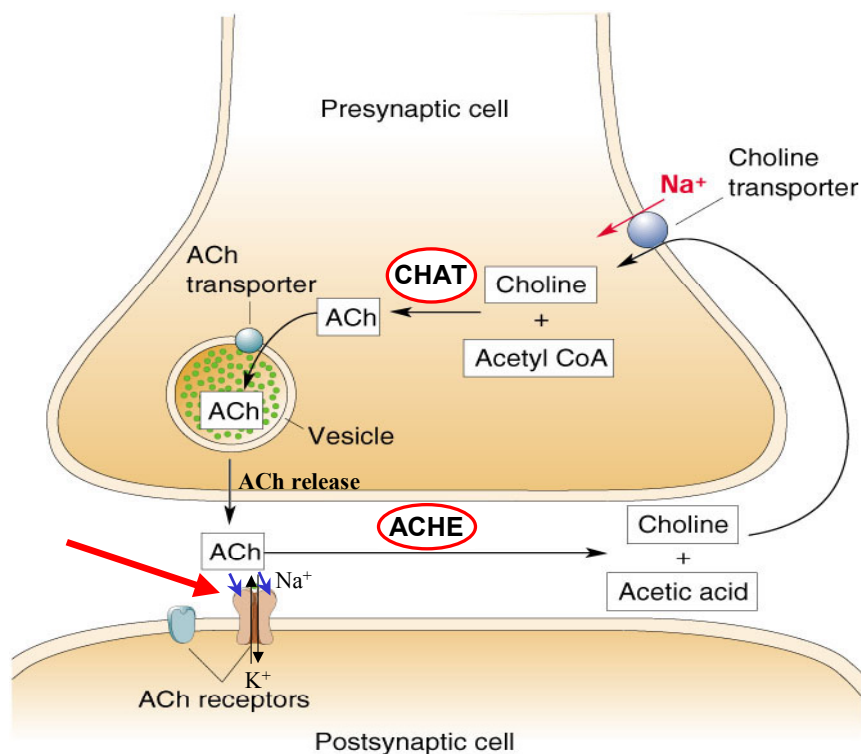
From whole-cell- and single-channel studies, we conclude that the missense mutation ϵ V448L is very unlikely to alter the receptor function significantly. Only mutation ϵ 911delT, located at the end of the third transmembrane domain, completely prevented formation of functional receptors at the neuromuscular junction. All the other mutations result in functional channels, however, with altered biophysical properties and reduced current density. Furthermore, our data suggest that the low open probability observed with the receptors carrying the ϵ -truncating mutations is most probably the main factor that results in the drastic reduction of their current density. The changes in receptor function associated with the truncating mutations are very likely to result in the defects in neuromuscular transmission observed in postsynaptic CMS.

1 Introduction

1.1 Neurological diseases. Congenital myasthenic syndromes. General remarks

Congenital myasthenic syndromes (CMSs) are inherited disorders that cause muscle weakness (myasthenia) by affecting the connection between nerve cells and muscle cells, called the neuromuscular junction (NMJ). The origins and symptoms of CMS sometimes resemble those of two other NMJ disorders, myasthenia gravis (MG) and Lambert-Eaton myasthenic syndrome (LEM). While these disorders occur when the immune system attacks the NMJ, CMS is caused by defects in genes that are essential at the NMJ, at presynaptic, synaptic, or postsynaptic level. For example, mutations in the ϵ -acetylcholine receptor (ϵ -AChR) subunit gene cause congenital myasthenic syndromes (CMS) with postsynaptic neural transmission defects. The myasthenic symptoms vary with the type of CMS and the specific genetic defect, but in general, CMS has its onset after birth or during early childhood, and involves ocular, facial, bulbar, and limb muscles. Some CMSs are sporadic or appear later in life (Croxen et al., 2002). Clinically, the most typical symptoms are: generalized weakness (unusual fatigue that worsen with activity), weakness in the muscles of the eyes and face, inducing partial paralysis of eye movements (ophthalmoparesis), facial diplegia, droopy eyelids (ptosis), and an open-mouthed expression. There also can be weakness in the mouth and throat, causing in neonates feeble cry and feeding difficulties due to poor sucking and swallowing (dysphagia). In some children, there can also be weakness in the respiratory muscles that may lead to sudden respiratory insufficiency often precipitated by infections, fever, excitement or vomiting. In contrast to autoimmune myasthenia gravis, tests for AChR antibodies are negative. Most patients with postsynaptic transmission defects respond well to treatment with acetylcholinesterase (ACHE) inhibitors (Engel, 1994; Engel et al., 2003a,b,c; Middleton, 1996). The clinical phenotypes of CMS are often similar; therefore, precise diagnosis requires correlation of clinical (serologic tests, electromyographic – EMG – stimulation studies), *in vitro* electrophysiological (microelectrode studies, patch-clamp recordings), morphological (immunocytochemical localizations of ACHE, AChR at the endplate, α -bungarotoxin binding studies), and, whenever possible, molecular genetic studies (mutation analysis, expression studies). The corroboration of all these studies has made it possible to identifying defects in the endplate-associated proteins (Beeson et al., 1998; Engel, 1994; Engel, 1999a).

To date, genetically identified defects include mutations in a gene encoding the choline acetyltransferase (CHAT) (Ohno et al., 2001), which were classified as ‘presynaptic CMS’ (see also Fig. 1). This type of CMS accounts for 7 % of all CMS cases, and is due to decreased synthesis or release of ACh at the NMJ. Secondly, there are defects in the ColQ gene that encodes for the collagenic tail subunit of acetylcholinesterase (ACHE) (Donger et al., 1998; Ohno et al., 1998a), the enzyme that breaks down ACh molecules in the synaptic space. This form of CMS was termed as ‘synaptic CMS’, and represents approximately 14 % of the cases. Finally, but not the least, there are also mutations at the postsynaptic level in the genes encoding the acetylcholine receptor (AChR) subunits (Engel et al., 1999; Kraner et al., 2002; Sieb et al., 2000a,b), as well as in a gene encoding RAPSYN (Receptor-associated Protein at the Synapse; Ohno et al., 2002), the protein responsible for clustering of AChRs at the postsynaptic membrane. This so-called ‘postsynaptic CMS’ accounts for about 79 % of all CMS cases, and is caused mainly by mutations in the AChR (Engel et al., 2003b).



(Modified from Bear et al., 2001)

Fig. 1 The neuromuscular endplate and the three different levels of occurrence of defects underlying CMS: presynaptic defects (in the ACh synthesis by CHAT or ACh release), synaptic defects (in the ACh cleavage by ACHE), and postsynaptic defects (in the AChR or RAPSYN).

The majority of mutations underlying postsynaptic CMS have been reported for the gene encoding the ϵ -subunit of the AChR (ϵ -AChR). Some missense mutations of the AChR ϵ gene lead to kinetic abnormalities of the channel, e.g. the so-called slow-channel congenital myasthenic syndrome (SCCMS). SCCMSs are inherited in autosomal-dominant traits. However, most ϵ -AChR mutations reported to date are frameshifting, missense, nonsense, splice site or promoter mutations that result in a deficiency of functional AChR at the postsynaptic membrane. Severe deficiency of the adult AChR at the neuromuscular junction as a result of decreased or absent protein expression leads to the clinical phenotype of CMS and is usually inherited in autosomal-recessive traits (Croxen et al., 2001; Engel et al., 1999; Vincent et al., 2000). Genotype-phenotype correlations carried out in CMS patients suggested some peculiar clinical and electrophysiological findings as the diagnostic hints at certain forms of CMS (Engel et al., 2003a,b,c; Middleton, 1996). For example, a selective weakness of cervical and wrist extensor muscles has been reported in patients with SCCMS (Engel et al., 2003b). Furthermore, a frequent mutation of the ϵ -subunit of AChR found in South-Eastern European Gypsy populations (ϵ 1267delG) usually results in ophthalmoplegia and a relatively mild phenotype (Abicht et al., 1999; Croxen et al., 1999). However, many CMS patients carry “private” mutations in one of the above-mentioned candidate genes, detected in few or single kinships, only. The clinical phenotype that they produce may vary largely.

1.2 Ligand-gated ion channels of fast chemical synapses

The ligand-gated ion channels are channels specialized for mediating fast chemical synaptic transmission. These channels gate ion movements and generate electrical signals in response to a specific chemical neurotransmitter, such as acetylcholine, glutamate, glycine, or γ -aminobutyric acid.

The superfamily of ligand-gated ion channels is also known as the class of Cys-loop receptors because all family subunits contain in their amino-terminal extracellular halves a pair of disulphide-bonded cysteines, which are separated by 13 residues (Kao and Karlin, 1986; Karlin and Akabas, 1995; Ortells and Lunt, 1995; Tsunoyama and Gojobori, 1998). The superfamily includes muscle-type and neuronal-type nicotinic ACh receptors, 5-hydroxytryptamine type 3 (5-HT₃) receptors, γ -aminobutyric acid type A (GABA_A) and GABA_C receptors, glycine receptors, and invertebrate glutamate (Cully et al., 1994) and histidine (Zheng et al., 2002) receptors.

1.2.1 Nicotinic acetylcholine receptors (AChRs)

Nicotinic acetylcholine receptors (AChRs) are the first and the best characterized ligand-gated ion channels and have served as an archetype for studying other ligand-gated ion channels. Binding of the small-molecule neurotransmitter acetylcholine to two sites on the extracellular surface of the AChR protein triggers a concerted conformational change in the AChR. This causes a cation-specific channel through the center of the protein to flicker open repeatedly for a millisecond or two at a time. If exposure to acetylcholine or other nicotinic agonists persists for seconds or minutes, AChRs assume a desensitized conformation characterized by a closed ion channel and high affinity for agonists. The passive flow through activated AChRs of Na^+ ions into the cell and K^+ ions out results in a net excitatory depolarization of the cell. This can trigger an action potential (AP) that can be conducted along a nerve cell, trigger contraction in a muscle cell or facilitate transmitter release from a nerve ending. Some types of AChRs are especially permeable to Ca^{2+} ions. Entry of Ca^{2+} ions to the cell may, for example, further facilitate transmitter release at nerve endings, activate inhibitory or excitatory Ca^{2+} -sensitive ion channels in the postsynaptic membrane, or trigger signaling cascades that can regulate gene transcription in the cell nucleus. The ACh receptors are impermeable to all anions (Takeuchi and Takeuchi, 1960; Sine et al., 1990).

AChRs of the type found in skeletal muscle are the best characterized. These receptors form a critical link in signaling between spinal motor neurons and skeletal muscles to produce all voluntary movements. Inhibition of their function by toxins, such as curare or cobra venom toxins, by autoantibodies in the disease myasthenia gravis (MG), or by mutations in congenital myasthenic syndromes causes weakness or death. The homogeneity and accessibility of AChRs at neuromuscular junctions have permitted electrophysiological, pharmacological, and developmental studies that are difficult or impossible in the central nervous system. The relatively huge amounts of AChRs at the modified neuromuscular junctions that form the electric organs by which electric eels and rays produce their electrical discharges have provided a unique source of AChRs for structural studies.

AChRs of types found in neurons are widely distributed in the nervous system. However, in contrast to the peripheral skeletal neuromuscular system and autonomic ganglia where AChRs are the dominant receptors, in the central nervous system of mammals, AChRs play a minor role and receptors for glutamate function represent the major excitatory receptors. Genetic deficits in AChRs have been found to cause rare forms of epilepsy. Autoantibodies to AChRs have been implicated in causing rare dysautonomias. Loss of AChRs is associated with

Alzheimer's disease and Parkinson disease. AChR dysregulation is associated with schizophrenia, and nicotinic investigational drugs have been found to have beneficial effects on Tourette syndrome and chronic pain, among other possible benefits including cognitive enhancement and weight loss (Lindstrom, 2001).

1.2.1.1 Subtypes of nicotinic muscle AChR

The muscle-type ACh receptor is a glycoprotein complex (~ 290 kDa), which consists of five subunits arranged around a central membrane-spanning pore. In electrolytes (Reynolds and Karlin, 1978) and fetal muscle, the receptor composition is $(\alpha_1)_2 \beta_1 \gamma \delta$, whereas in adult muscle (Mishina et al., 1986), the γ -subunit is replaced by an ϵ -subunit. The subunits are arranged in the circular order of $\alpha \epsilon \alpha \beta \delta$ (Fig. 2), like barrel staves around a central channel (Karlin et al., 1983; Stroud et al., 1990; Unwin, 1993; Miyazawa et al., 1999).

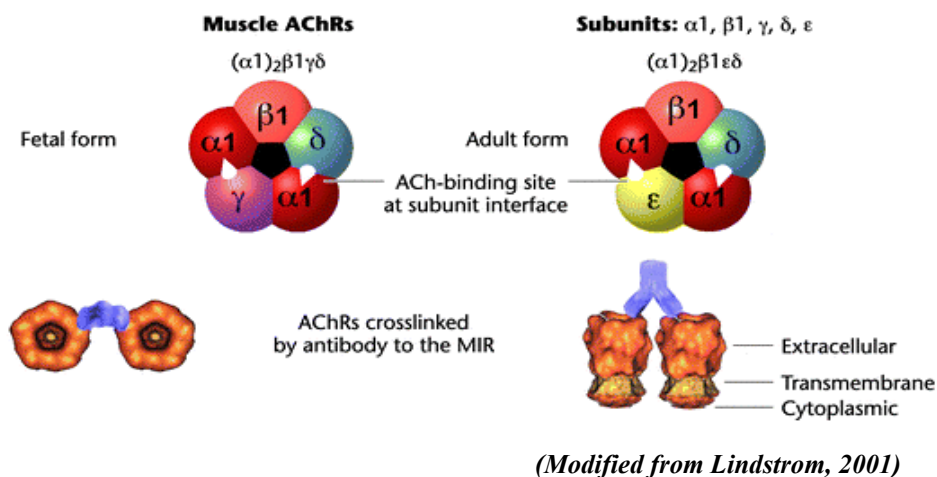


Fig. 2 The muscle (embryonic and adult) subtypes of nicotinic AChR.

1.2.1.2 Size and shape of the receptor molecule

Electron-crystallographic studies of *Torpedo californica* electric organ AChRs have achieved resolutions of 9 Å (Unwin, 1993), and 4.6 Å (Miyazawa et al., 1999). The AChR is about 80 Å in diameter and 120 Å long with 65 Å extending on the extracellular surface, 40 Å crossing the lipid bilayer, and 15 Å extending beneath the bilayer into the cytoplasm. The extracellular vestibule of the channel is about 25 Å in diameter, surrounded by walls about 25 Å thick. The gate of the channel is thought to be at its cytoplasmic end. The acetylcholine-binding sites,

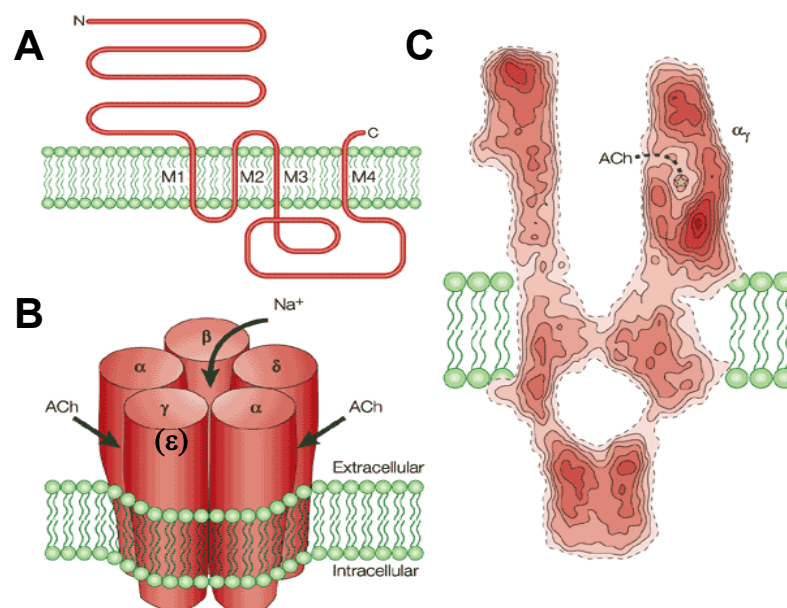
which control the opening of the channel, are thought to be halfway up the sides of the extracellular domain, about 35 Å from the bilayer (see Fig. 3 C).

1.2.1.3 *The AChR topology*

All AChR subunits share a high degree of homology, and have the same topology (Karlin and Akabas, 1995; Lindstrom, 2000; Corringer et al., 2000). The *transmembrane topology* of the AChR has been inferred from *hydrophobicity plot analysis* and *secondary structure prediction* of the primary sequence (Schofield et al., 1987). So-called hydropathy plots indicate the grouping of five hydrophobic stretches in the sequences that are identified as spanning the membrane, usually in the form of α -helices. The first peak is a leading signal sequence (LSS) that is cleaved off during synthesis. During protein synthesis from this N-terminal end, the initial signal sequence guides the nascent peptide chain across the endoplasmic reticulum (ER) to the luminal side so that the mature N-terminus of these subunits ends up on the extracellular side of the cell membrane (Anderson et al., 1983). The orientation of the receptor within the postsynaptic membrane has been modeled as having the large N-terminal domain outside the cell facing the synaptic cleft. The N-terminal extracellular domain consists of about 220 amino acids and contains a disulfide bond between Cysteines C192 and C193. These residues form part of the extracellular binding sites for agonist and competitive antagonists including α -bungarotoxin. In most AChR subunits, there is an N-glycosylation site at asparagine 141, and some subunits contain additional glycosylation sites in the large extracellular domain. All subunits contain at least one such site. Three transmembrane domains ($M_1 - M_3$) extend between the large extracellular domain and the large cytoplasmic domain (Fig. 3 A). These are closely spaced, highly conserved, and largely α -helical. A fourth transmembrane domain (M_4), also of about 20 amino acids, is not especially conserved in sequence. It extends between the large cytoplasmic domain and a short extracellular C-terminal tail of 10 – 20 amino acids (Fig. 3 A). The large cytoplasmic domain of 110 – 127 amino acids is the most variable region in sequence between subunits. The N-terminal third of M_1 and one side of M_2 comprise each subunit's contribution to the lining of the channel. Each of the five subunits of the receptor contributes its M_2 segment to the channel thus forming a 5-fold symmetry. In cryo images, this is visible as five rod-like densities lining the pore. The rods slope towards the axis of the pore and then are kinked in a knee halfway through the membrane (Fig. 3 C). Thus, the actual lumen of the channel through the lipid bilayer is quite narrow but sufficiently wide to permit the rapid passage of hydrated cations. Almost 50 Å

away, the rode-like knees at the membrane level turn so they no longer point so directly into the pore axis (Unwin, 1993, 1995). The inner vestibule of the channel does not open up as an axial hole directly to the cytoplasm. Instead, it ends in a colonnade of five rods that converge and are covered by a cupola (Miyazawa et al., 1999). This results in a lattice containing acidic amino acids that contribute to the cation selectivity of the AChR. The rods of the colonnade are thought to derive from the major cytoplasmic loop (M3-4 loop) of the receptor subunits, whereas the distal part of the cupola seems to represent the receptor-aggregating protein RAPSYN attaching to the receptor complex (Fig. 3 C). RAPSYN is a 43000 Da peripheral membrane protein that links AChRs to the cytoskeleton and contributes to the normal tight packing of muscle AChRs at the tips of folds in the postsynaptic membrane which are adjacent to sites of acetylcholine release from the presynaptic terminal.

Opening of the channel occurs upon binding of ACh to both α -subunits at sites that are at, or close to, the interfaces made with neighboring ϵ - (or γ - in fetal muscle) and δ -subunits (α_{ϵ} (γ) and α_{δ} ; see Fig. 3 B; Karlin, 1993; Sine et al., 1995; Xie and Cohen, 2001).



(Modified from Karlin, 2002)

Fig. 3 The structure of the nicotinic acetylcholine receptor (AChR); **A**: The threading pattern of receptor subunits through the membrane; each subunit is composed by a large extracellular N-terminus, four membrane-spanning segments, a long cytoplasmic loop, and a short extracellular C-terminus; **B**: Schematic representation of the pentameric structure, showing the arrangement of the subunits in the muscle-type receptor, the location of the two acetylcholine (ACh)-binding sites (between α - and ϵ -subunits (or γ -subunit in the embryonic muscle), and α - and δ -subunits), and the axial cation-conducting channel; **C**: Cross-section through the 4.6-Å structure of the receptor determined by electron microscopy of tubular crystals of *Torpedo* membrane embedded in ice.

1.2.1.4 Mechanisms of ACh receptor activation

The structural transition from the closed to the open-channel state of the receptor has been analyzed at 9 Å resolution (Unwin, 1995). Since the ACh-binding sites are distant from the pore itself, ACh binding must trigger channel-opening via propagated conformational changes. Indeed, Unwin has shown that binding of ACh initiates two interconnected events in the extracellular domain. One is a local disturbance, involving all five subunits, in the region of the binding sites, and the other an extended conformational change, involving predominantly the two α -subunits, which communicates to the transmembrane portion. However, this describes the receptor in either of the two states, in the closed and in the open states, but does not take into account the possibility that binding to one site might affect binding to the other before the channel opens (Hatton et al., 2003).

A simple mechanistic picture is as follows: first, ACh triggers a localized disturbance in the region of the binding sites. Second, the effect of this disturbance is communicated by axial rotations, involving mainly the α -subunits, to the M₂ helices in the membrane. Third, the M₂ helices transmit the rotations to the gate-forming side-chains, drawing them away from the central axis; the mode of association near the middle of the membrane is thereby disfavored, and the helices switch to the alternative side-to-side mode of association, creating an open pore. The first attempts to investigate the mechanism of action of acetylcholine (ACh) were made by Colquhoun and Sakmann (1981; 1985). Single-channel measurements showed that the channel could open, though much less efficiently, with only one ACh molecule bound. This cannot be detected from whole-cell measurements.

Two reaction schemes that have been widely used to represent the activation of the nicotinic receptor are shown in Figure 4. The first proposed activation mechanism of AChR (Fig. 4 A) assumes that the two ACh binding sites are equivalent before ACh binds, and when two agonist molecules are bound they have equal rates of dissociation. The closed channel R can bind ACh molecules in two steps of relatively low affinity but with high forward rate constants almost at the diffusion limit. Agonist binding profoundly increases the probability that the channel will become open (R*). However, there may be cooperativity in the process of binding to the shut receptor, and binding of the second ACh molecule may not have the same rate constants as binding of the first. The doubly occupied closed receptor (A₂R) opens with a rate of β_2 , and the doubly occupied open receptor (A₂R*) closes with a rate of α_2 , while the singly occupied closed receptor (AR) opens with a rate of β_1 , and AR* closes with a rate of α_1 . The closed \rightleftharpoons open reaction ("gating") of the diliganded AChR is much more favorable

thermodynamics requires that desensitized states will bind agonists more tightly than closed states. The affinity increases by more than 1000-fold here. Desensitization is a complex and ill-understood phenomenon, because it develops on many different time scales, from milliseconds to minutes (Katz and Thesleff, 1957; Cachelin and Colquhoun, 1989; Butler and McNamee, 1993; Franke, et al 1993), with fast- and slow-desensitized states, and therefore it is hard to describe an adequate reaction mechanism for it. Recently, it has been shown by single-channel methods (Elenes and Auerbach, 2002) that there are multiple desensitized states, but there is nothing yet known about the structural differences between these states.

The second proposed activation mechanism of AChR (Fig. 4 B), which in most cases is more realistic, assumes that the two binding sites for ACh are different from the start; so, two distinguishable open mono-liganded states exist: $AR_a-R_b^*$ and $R_a-AR_b^*$. This mechanism allows for cooperativity of the binding reaction, because the rates for binding to site a may depend on whether or not site b is occupied (and *vice versa*). Different studies (Jackson, 1986; Grosman and Auerbach, 2000) showed that the unliganded, singly-liganded, and doubly-liganded states all can indeed open.

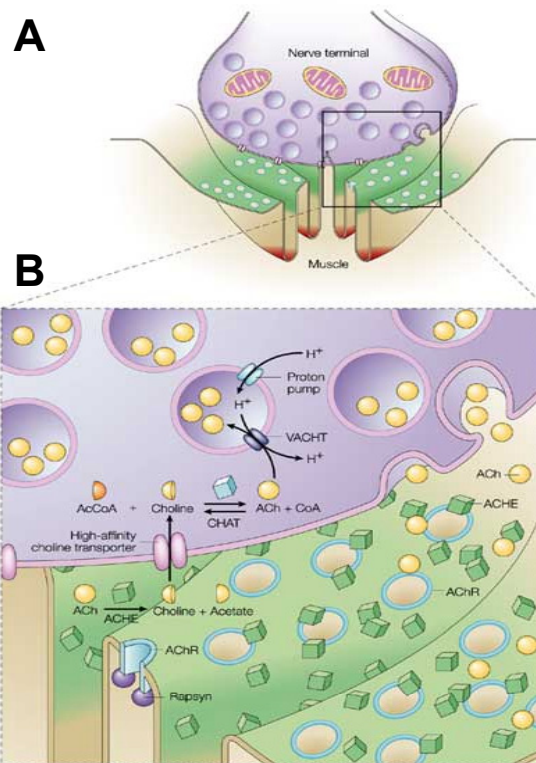
When looking at the structure-function relationships of proteins, the difference between the two ACh binding sites is of great interest. However, from the physiological point of view it is not very important. It is clear that the two ACh binding sites differ, and this has been found to be the case for most subtypes of the receptor. Binding of a single ACh molecule is sufficient to produce very brief openings of the channel, though with very low efficacy (Colquhoun and Sakmann, 1981). In the adult human receptor, the most obvious sign that the sites differ lies in the fact that two classes of singly-liganded openings are detectable, one much briefer than the other (Hatton et al., 2003). However, singly-liganded openings contribute next to nothing to the endplate current that is responsible for neuromuscular transmission. From the physiological point of view, the rates that matter most are the open and closed rate constants for the doubly-liganded channel (α_2 and β_2) and the total rate at which agonist dissociates from the doubly-liganded receptor ($k_{-2a} + k_{-2b}$; see Fig. 4 B). After exposure to the transient high concentration of ACh released from a nerve ending, most receptor molecules will be in the doubly-liganded states, and these three values determine the length of each individual opening, the number of reopenings and the lengths of the short shut periods that separate each opening. In conclusion, they are sufficient to determine the characteristics of the predominant doubly-liganded bursts of openings (channel ‘activations’) that are responsible for neuromuscular transmission (Colquhoun et al., 2003).

Because the different conformations of the muscle AChR interconvert and the ACh-association / dissociation rate constants are exceedingly fast, there is no prospect of being able to measure directly (that is, with binding assays) the kinetics of the agonist-binding steps in a conformation-specific manner. A reasonable alternative is to postulate an appropriate kinetic model and to estimate the agonist-association / dissociation rate constants from single-channel recordings. Both desensitization and ACh dissociation from the open state significantly contribute to the time course of the endplate current decay in patients with congenital myasthenic syndrome (Grosman and Auerbach, 2001).

1.3 The neuromuscular junction (NMJ)

1.3.1 From nerve action potential to muscle action potential

To understand the mechanism underlying congenital myasthenic syndrome (CMS), it is of great importance to know how the neuromuscular junction (NMJ) functions in healthy individuals. Thus, an action potential, having propagated along the axon of the α motor nerve, from the ventral horn of the spinal chord to the muscle, invades the pre-junction membrane or endplate. The depolarization (voltage changing from negative towards zero and even becoming positive to zero) caused by the invading action potential is detected by voltage-gated Ca^{2+} channels which open, admitting Ca^{2+} ions, raising the concentration of Ca^{2+} within the endplate and causing release (Ca^{2+} -dependent mechanism) of the neurotransmitter vesicles (Aidley, 1989; Hille, 2001). The neurotransmitter diffuses from the pre-junction release site to the post-junctional membrane, a distance of some 20 nm. After exocytotic release from the nerve terminal, some acetylcholine (ACh) molecules are hydrolyzed by acetylcholinesterase (ACHE) before they bind to the AChR and the remaining ACh molecules are hydrolyzed by ACHE after dissociation from AChR. Choline is transported into the nerve terminal by a high-affinity choline transporter (HACHT). ACh is resynthesized from choline and acetyl-coenzyme A (AcCoA) by choline acetyltransferase (CHAT) and is then transported into the synaptic vesicle by the vesicular ACh transporter (VACHT) in exchange for protons delivered to the synaptic vesicle by a proton pump (Fig. 5).



(Modified from Engel et al., 2003b)

Fig. 5 The neuromuscular junction (NMJ); **A**: Schematic diagram of an endplate region showing the general locations of the acetylcholinesterase (ACHE), the acetylcholine receptor (AChR) (green), and the voltage-gated Na^+ channels of the $\text{Na}_v 1.4$ type (red); **B**: After exocytotic release from the nerve terminal, some acetylcholine (ACh) molecules are hydrolyzed by ACHE before they bind to the AChR and the remaining ACh molecules are hydrolyzed by ACHE after dissociation from AChR. Choline is transported into the nerve terminal by a high-affinity choline transporter (HACHT). ACh is resynthesized from choline and acetyl-coenzyme A (AcCoA) by choline acetyltransferase (CHAT) and is then transported into the synaptic vesicle by the vesicular ACh transporter (VACHT) in exchange for protons delivered to the synaptic vesicle by a proton pump.

ACh binds to receptor (2 molecules of ACh per AChR), causing it to open. The channels can pass both K^+ and Na^+ ions, but in reality, the ions of only one species move in any quantity. One AChR opens and allows $1.5 \times 10^4 \text{ Na}^+$ ions / ms of open time. The channel opens on average 1 ms, and therefore one open channel causes a depolarization of about $0.3 \mu\text{V}$. The amount of neurotransmitter contained in one vesicle causes a postsynaptic potential of $\sim 1 \text{ mV}$. Therefore, one vesicle contains enough neurotransmitter to open ~ 3000 receptors, and because two molecules of ACh are needed to open one receptor, there must be a minimum of ~ 6000 molecules of ACh per vesicle. If the average depolarization generated at a NMJ of a muscle fiber is 40 mV then there must be at least 40 vesicles released and in the order of 133000 receptors activated at the NMJ (Aidley, 1989; Hille, 2001). The movement of ions tends to push the membrane potential of the post-junctional membrane towards 0 mV, and this

triggers an endplate potential (EPP) that activates the voltage-gated Na⁺ channels of the Na_v 1.4 type (Flucher and Daniels, 1989; Ruff, 1996), which are higher in density in the bottom of the synaptic folds. The interior of a resting muscle fiber has a resting potential of about -95 mV. If the EPP reaches the threshold voltage (approximately -50 mV), Na⁺ ions flow in with a rush and an action potential is generated, which then propagates away from the NMJ to depolarize the entire muscle fiber. In the NMJ, the AChR density is highest at the tops of the synaptic folds, $\sim 7500 - 10000 / \mu\text{m}^2 = 1 \text{ AChR} / 100 - 133 \text{ nm}^2$. This gives a spacing of $\sim 10 - 12 \text{ nm}$ between each AChR molecule. The AChR density drops off sharply as one reaches the bottoms of the folds. A high concentration of AChRs on the crests of the synaptic folds (Salpeter, 1987) and of Na_v 1.4 in the depth of the folds (Flucher and Daniels, 1989; Ruff, 1996) ensures that excitation is propagated beyond the endplate (Martin, 1994; Wood and Slater, 2001). The safety margin of neuromuscular transmission is a function of the difference between the depolarization that is caused by the EPP and the depolarization that is required to activate Na_v 1.4 channels. All CMSs that have been identified so far have been traced to one or more factors that render the EPP subthreshold for activating Na_v 1.4 channels (Engel et al., 1999b). No visible change occurs in the muscle fiber during (and immediately following) the action potential. This period, called the latent period, lasts from 3 – 10 ms. Before the latent period is over, the enzyme acetylcholinesterase breaks down the ACh in the neuromuscular junction (at a speed of 25000 molecules per second), the voltage-gated Na⁺ channels close, and the field is cleared for the arrival of another nerve impulse. The resting potential of the fiber is restored by an outflow of K⁺ ions. The brief (1 – 2 ms) period needed to restore the resting potential is called the refractory period.

In each CMS, the safety margin of neuromuscular transmission is impaired by one or more specific mechanisms. Thus, the factors that govern the safety margin can be grouped into the following main categories: factors that affect the number of acetylcholine (ACh) molecules per synaptic vesicle, factors that affect neurotransmitter release mechanisms, and factors that affect the efficacy of individual quanta (Wood and Slater, 2001; Katz, 1966). Therefore, a clear understanding of the mechanisms that operate in the CMS requires an analysis of the different ways in which these synaptic properties can be modified. They include variations in the number of AChRs per endplate, in the synaptic localization of AChR and acetylcholinesterase (ACHE), in the fine structure of the endplate, in the amplitude of miniature endplate potentials (MEPPs), in the number of quanta released by nerve impulse, in the number of readily releasable quanta, in the probability of release and in the kinetic properties of single AChRs. Combined electrophysiological and morphological tests can

probe the involvement of these different mechanisms in CMSs. If these tests point to a candidate molecule, then genetic analysis becomes feasible. If a mutation is discovered in the candidate gene, then expression studies with the recombinant mutant molecule can be used to confirm its involvement in pathology and to analyze the properties of the abnormal molecule (Engel, 1993a; Engel et al., 1993b). The candidate-gene approach has pointed to defects in choline acetyltransferase (CHAT), ACHE, AChR and the postsynaptic molecule RAPSIN as causes of CMS (Fig. 5). These defects lead to failure of neuromuscular transmission. In humans, the extent to which the EPP normally exceeds the threshold, the 'safety factor', is quite small and neuromuscular transmission is sensitive to pathological changes. By contrast, in mice the safety factor appears higher, and mouse models of neuromuscular diseases do not always demonstrate obvious weakness (Vincent et al., 1997; Bhattacharyya et al., 1997). However, in two studies by Gomez and co-workers (1997 and 2002), transgenic mice expressing different mutations that induce severe forms of SCCMS in humans also developed myasthenic symptoms highly reminiscent to those of the patients. Therefore, such transgenic animal models are actively contributing to our understanding of the complex genotype-phenotype relationship in CMS.

1.3.2 CMS caused by defects in AChR

Our study focuses on mutations in the AChR channel, which are genetic defects that induce postsynaptic CMS. Such mutations have now been discovered in all AChR subunits and in different domains of the subunits (Engel et al., 2003a,b,c). The mutations fall into two groups: mutations that alter the kinetic properties of AChR and mutations that reduce its expression (low-expressor mutations). The kinetic mutations can be further divided into two types: slow-channel mutations that increase the synaptic response to ACh, and fast-channel mutations that decrease it. The slow- and fast-channel mutations represent physiological opposites in both their phenotypic consequences and alterations of fundamental steps that underlie receptor activation.

1.3.2.1 Slow-channel CMS

It was recognized two decades ago by its distinct phenotypic features. Five patients showed dominant inheritance and selective weakness of cervical, scapular and finger extensor muscles, mild ophthalmoparesis and variable weakness of other muscles. Single-nerve

stimulation evoked a repetitive compound muscle action potential (CMAP), rather than the expected single CMAP, and the normally constant amplitude of the CMAP attenuated with repetitive nerve stimulation. Synaptic potentials decayed abnormally slowly, showing normal or reduced amplitudes, but the evoked ACh release was normal. The disease left an anatomical trace – termed endplate myopathy – which is associated with postsynaptic Ca^{2+} accumulation, as well as focal degeneration of the junctional folds with corresponding loss of AChRs, and degenerating membranous organelles and small vacuoles in junctional fiber regions (Engel and Biesecker, 1982; Engel et al., 2003b). The repetitive CMAP was attributed to the EPP outlasting the absolute refractory period of the muscle fiber, and the endplate myopathy was credited to excessive Ca^{2+} influx into the postsynaptic region during prolonged episodes of synaptic activation. The slow decay of the synaptic potentials was attributed to prolonged openings of the AChR channel (Anderson and Stevens, 1973). The presence of normal amounts and activity of the enzyme at the synapse excluded the alternative explanation that a defect in ACHE prolonged the lifetime of ACh in the synaptic space. However, formal proof of a kinetic defect in AChR came only in the mid of '90s, with the recording of markedly prolonged synaptic and single-channel currents from the endplate of other patients with slow-channel CMS (Ohno et al., 1995; Engel et al., 1996b).

1.3.2.2 Fast-channel CMS

The name 'fast-channel CMS' originates from the abnormally fast decay of the synaptic response, which is caused by abnormally brief channel-opening events. The disorder was first recognized in 1993 in a patient with moderately severe myasthenic symptoms from birth, which responded partially to cholinesterase inhibitors. Endplate studies showed a normal structure, no deficiency of ACHE or AChR, a normal neurotransmitter release by nerve impulse, but small miniature endplate potentials (MEPPs) (Uchitel et al., 1993a,b). Analysis of the ACh-induced current noise pointed to a normal conductance of the AChR channel but with abnormally short-lived openings. The diminished synaptic response, in face of normally abundant AChRs, indicated a decreased ACh content of the synaptic vesicles, ACHE overactivity or an abnormality in AChR. Morphometric analysis showed that synaptic vesicles were of normal size, pointing away from reduced vesicular ACh content (Jones and Kwanbunbumpen, 1970a,b), and ACHE overactivity seemed unlikely, as cholinesterase inhibitors did not fully restore the synaptic response. The findings therefore implied a kinetic

defect in AChR in which opening of the channel was impaired and its closing was enhanced (Uchitel et al., 1993a,b; Shen et al., 1999, 2000, 2001; Maselli et al., 2002; Sine et al., 2002).

1.3.2.3 CMS caused by low-expressor mutations

In this category, most of the CMS cases that have been identified so far are caused by homozygous or heterozygous low-expressor mutations in AChR subunit genes, and these mutations are concentrated in the ϵ -subunit of the receptor (for a detailed table with low-expressor mutations in AChR subunits, please refer to *Engel et al., 2003a*). Patients harboring low-expressor or even homozygous null mutations in the ϵ -subunit might have mild symptoms. Conversely, patients with low-expressor mutations in non- ϵ -subunits are severely affected, and so far, no patients with null mutations in both alleles of a non- ϵ -subunit have been observed. A probable explanation is that persistent low-expression level of fetal AChR harboring γ -subunit can partially compensate for the absence of the ϵ -subunit (Milone et al., 1998b; Engel et al., 1996a,b; Ohno et al., 1997). Null mutations in subunits other than ϵ -subunit might be lethal, presumably owing to the lack of a substituting subunit. In patients with null mutations of both ϵ -alleles, all AChR channels recorded from the endplate have the reduced conductance and prolonged time course that are typical of γ -subunit-containing AChRs (Ohno et al., 1997), and immunostaining confirms the presence of the γ -subunit at the endplate (Engel et al., 1996a,b). Targeted deletion of the ϵ -subunit in mice showed that either the γ - or ϵ -subunit is essential for survival. Thus, the AChR $\epsilon^{-/-}$ mice express the γ -subunit instead of the ϵ -subunit at birth (as in human fetus), but die two to three months later when the γ -subunit mRNA is no longer transcribed (Witzemann et al., 1996). Humans, however, continue to express low-levels of the γ -subunit at the endplate (Croxen et al., 2001), and so this subunit rescues the ϵ -null phenotype.

Morphological studies of endplates with low-expressor mutations show an increased number of endplates distributed over an increased span of individual muscle fibers. The integrity of the junctional folds is preserved, but some endplate regions are simpler and smaller than normal. The distribution of AChRs on the junctional folds is patchy, and the density of the receptors is reduced. The immunocytochemical reaction for RAPSIN, the molecule that clusters the AChRs at the postsynaptic membrane, is decreased in proportion to the decreased expression of AChR. The quantal response at the endplate is reduced, but neurotransmitter release by nerve impulse is frequently higher than normal. Different types of recessive

mutations that cause severe endplate AChR deficiency have been identified in the gene encoding the ϵ -subunit of the receptor (Engel et al., 2003a; see Fig. 6).

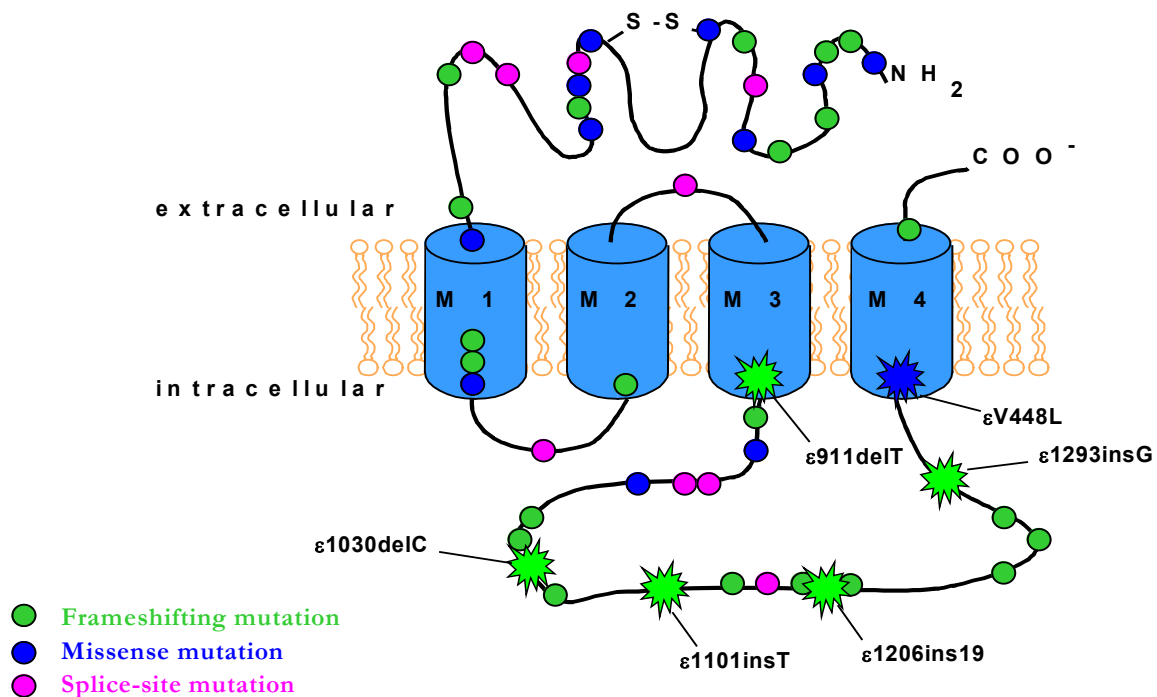


Fig. 6 Sites of occurrence of different types of ϵ -mutations (frameshifting, missense, and splice-site) identified in patients with postsynaptic CMS. The ϵ -mutations assigned with stars are the object of the present study.

Some mutations cause premature termination of the translational chain. These mutations are frameshifting (Shen et al., 2003; Engel et al., 1996a,b; Ohno et al., 1997; Ohno et al., 1998a; Abicht et al., 1999; Middleton et al., 1999; Croxen et al., 1999; Sieb et al., 2000a,b; Shen et al., 2002), occur at a splice site (Ohno et al., 1998a; Middleton et al., 1999) or produce a stop codon (Ohno et al., 1997). All these mutations can reduce the AChR cell surface expression by causing premature termination of the translational chain, and thus resulting in a truncated protein product. A second type of recessive mutations are point mutations in the Ets binding site, or N-box, of the promoter region of the ϵ -subunit gene (Abicht et al., 2002; Ohno et al., 1999; Nichols et al., 1999). In addition to these mutations, there are also missense mutations in a signal-peptide region (Ohno et al., 1996; Middleton et al., 1999), and missense mutations that involve residues that are essential for the assembly of the pentameric receptor (Fig. 6).

1.4 *The goal of the study*

Recently, several mutations within the ϵ -subunit of the human muscle AChR have been described that impair the normal function of the neuromuscular synaptic transmission. While there is considerable amount of information on morphological changes in the neuromuscular synapse associated with these mutations, little is known about the functional alterations of the mutations.

The aim of this study was to investigate the molecular mechanism underlying postsynaptic CMS, in the presence of two frameshifting mutations, ϵ 911delT and ϵ 1030delC, and a missense mutation ϵ V448L (Sieb et al., 2000a; see Fig. 6). Additionally, three related CMS-linked mutations all located within the ϵ -cytoplasmic loop of AChR, namely the insertion mutations ϵ 1101insT (Engel et al., 1996a), ϵ 1206ins19 (Ohno et al., 1998b), and ϵ 1293insG (Engel et al., 1996a; Sieb et al., 2000b; see Fig. 6) were also included in the study to identify the role of specific regions in the TM3-4 loop for the functionality of the receptor.

The approach we took was to express recombinant wild-type and ϵ -mutant AChRs in HEK 293 cells and characterize the functional properties of these receptors with electrophysiological techniques.

We asked the following questions:

Do the mutations influence the affinity of the receptor for its natural ligand?

Do the mutations alter the kinetic properties of ACh-induced current responses, e.g. alter speed and degree of receptor activation and desensitization?

Do the mutations impair the cell surface expression of the AChR channel?

The mutation(s) that showed in whole-cell recordings functional changes were further investigated on the single-channel level.

There we determined the size of the ion flux through the open channel (the single-channel conductance), the frequency of opening events (the open probability), and the open and close lifetimes of the AChR.

The combined results from whole-cell- and single-channel recordings from these ϵ -mutants should provide insight into the mechanism underlying postsynaptic CMS.

2 Materials and Methods

2.1 Cell culture

Human Embryonic Kidney 293 cells (HEK 293), kindly provided by Prof. Dr. T. Schneider (Institute of Neurophysiology, Köln), were used as expression system for the present study. Cells were grown in Dulbecco's Modified Eagle Medium (DMEM; Invitrogen) supplemented with 10 % bovine calf serum (BCS), 100 µg/ml of streptomycin, and 100 U/ml of penicillin. For plating-out the HEK 293 cells, confluent cells were collected from 25 cm² Petri dishes by pipetting up and down, and after a 3 min centrifugation at 1000 rpm, they were resuspended in DMEM HEK medium, and replated on 8 cm² dishes. Cells were incubated at 37°C for ~ 48 h, and they were approximately 70 % confluent on the day of the transfection.

2.2 Transient transfection

Dr. S. Kraner (Institute of Human Genetics, Bonn) generated AChR ϵ -subunit mutations: ϵ V448L, ϵ 911delT, ϵ 1030delC, ϵ 1293insG, ϵ 1206ins19, and ϵ 1101insT (Sieb et al., 2000a,b; Engel et al., 1996a; Ohno et al., 1998b) by „QuikChangeTM Site-Directed Mutagenesis“ (Stratagene). The resultant ϵ -subunit cDNAs were sequenced to check for the presence of the mutations and absence of any additional sequence changes (Kraner et al., 2003). The cDNAs were subcloned into the CMV-based expression vector pCDNA 3.1 (+) (5.4 kbp) (Invitrogen). HEK 293 cells were transiently cotransfected with cDNAs encoding the wild-type (α , β , δ , and ϵ), ϵ -lacking (α , β , and δ), and ϵ -mutated AChR subunits by TransFastTM transfection reagent (Promega) together with green fluorescence protein (GFP) using a subunit ratio of 2:1:1:1 (α : β : δ : ϵ). Initial experiments using Ca²⁺ - phosphate precipitation method had lower transfection efficiency on our HEK 293 cell line, and therefore TransFastTM transfection was further used. This method has some advantages being faster (it takes round about 1 h), easy-to-use (after resuspending the reagent in water, freezing, thawing, and mixing with DNA, everything is simply added to cells), more efficient (high-efficiency transfection – transient and stable – in many cell lines), and, finally, more robust (it requires less optimization than other systems). Additionally, it allows transfection of cell types such as primary cell cultures that require continuous exposure to serum, as it can be used in the presence of serum (see TransFastTM transfection reagent technical bulletin at www.promega.com).

Transfection was started two days after plating-out the HEK 293 cells on 8 cm² Petri dishes, by pipetting the AChR cDNAs and the GFP cDNA together. GFP (green fluorescent protein; Invitrogen) was used to identify transfected cells for electrophysiological studies. It followed a dilution of the cDNAs in DMEM HEK medium, on which thawed TransFast™ reagent was added, and this mixture was vortexed for a short time. After a 10 – 15 min incubation of the cDNAs / TransFast™ reagent mixture, and after the removal of the old growth medium from the 70 % - confluent HEK 293 cells on the 8 cm² Petri dishes, the transfection mixture was added onto the cells, and cells were incubated at 37°C for ~ 48 – 96 h. After this period, the transfected cells were plated in fresh DMEM HEK medium on poly-D-lysine-coated glass coverslips (Labomedic). For this purpose, cells were collected from 8 cm² Petri dishes by pipetting up and down, and after a 3 min centrifugation at 1000 rpm, they were resuspended in DMEM HEK medium. A small volume (usually 20 µl) was mixed with the same amount of Tripin Blue for counting the cells. Cell suspension was diluted in a way that 1 ml of it always contained a density of 1 x 10⁶ cells on average. A small volume of transfected cells (30 µl) was used for plating the cells on coverslips in 8 cm² Petri dishes. After 30 min of incubation at 37°C, 2 ml of DMEM HEK medium were added over the coverslips in 8 cm² Petri dishes. Four coverslips were used for each 8 cm² Petri dish. Whole-cell- and cell-attached patch-clamp recordings were started 2 – 3 h after plating the cells on coverslips.

2.3 Patch-clamp recordings

Whole cell currents were recorded using an EPC 9 patch-clamp amplifier and Pulse Software (HEKA Elektronik). Recordings were filtered at 5 kHz (Bessel, 4-pole), digitized using an ITC-16 AD / DA interface (HEKA Elektronik) at a rate of 25 kHz, and stored on hard disk. Patch pipettes were pulled from borosilicate capillary tubes (Kimble Products), on a horizontal programmable puller (Zeitz-Instrumente), and had resistance between 1.5 and 3 MΩ, when filled with internal solution. The pipette solution contained (in mM): 2.5 NaCl, 110 KCl, 0.5 CaCl₂, 10 EGTA, and 10 HEPES (pH = 7.3, adjusted with KOH). The external solution contained (in mM): 145 NaCl, 2.5 KCl, 2 CaCl₂, 1.3 MgCl₂, 10 HEPES, and 20 Glucose (pH = 7.3, adjusted with NaOH). ACh-induced currents were elicited by application of ACh (a 2 sec pulse of 0.03, 0.1, 0.3, 0.5, 1, 3, 10, 30, 100 or 300 µM ACh) using a fast pressure-application system (ALA Scientific Instruments). Flow from the pressurized reservoirs was computer-controlled via Lee solenoid valves. The output from the valves was connected via FEP tubing (Fluorinated Ethylene Propylene Tubing) to the micromanifold.

The application system consisted of quartz glass tubes (8 or 12 x 100 μm application tubes + 1 x 200 μm flush tube) that communicated with the application tip of 100 μm . The agonist solution was applied at intervals of 3 – 5 min. ACh solutions were prepared daily from a 100 mM stock solution. All whole-cell recordings were performed at a holding potential of –60 mV.

Cell-attached patch-clamp recordings were performed at room temperature (19 – 24°C), using an EPC 9 patch-clamp amplifier (HEKA Elektronik). Recordings were filtered at 10 or 5 kHz (Bessel, 4-pole), digitized using an ITC-16 AD / DA interface (HEKA Elektronik) at a rate of 25 kHz, and stored on hard disk. Patch pipettes were pulled from borosilicate capillary tubes (Kimble Products) and coated with Sylgard 184 (Dow Corning) to reduce the noise interference during recordings. The pipette resistance ranged from 5 to 10 M Ω . In the cell-attached experiments, the pipette solution contained (in mM): 0.001, 0.01, 0.03 or 0.1 ACh in 142 KCl, 5.4 NaCl, 10 HEPES, 1.8 CaCl₂, 1.7 MgCl₂, pH = 7.3. The external solution contained (in mM): 142 KCl, 5.4 NaCl, 10 HEPES, 1.8 CaCl₂, 1.7 MgCl₂, pH = 7.3. In cell-attached recordings, the holding potential was –100 mV, unless otherwise indicated. Slope conductance curves were determined from continuous recording protocol performed at various membrane potentials (from –60 to –220 mV).

(For a detailed description of the patch-clamp technique, see also the Appendix section!)

2.3.1 Data analysis of the patch-clamp recordings

2.3.1.1 Analysis of whole-cell recordings

2.3.1.1.1 Dose-response curves

Analysis of the macroscopic currents was carried out using Pulse + PulseFit software (HEKA Elektronik) and GraphPad Prism software (GraphPad Software Inc.). Using Pulse + PulseFit software, the macroscopic currents (I_{max}) were manually measured at different ACh concentrations ranging from 0.03 to 300 μM , for wt, ϵ -lacking, and ϵ -mutant AChRs. To construct dose-response curves, the currents were normalized to the maximum response and plotted as a function of log of the agonist concentration (in M). Making use of GraphPad Prism software, EC_{50} values and *Hill slopes* were obtained by fitting the data points to a logistic equation in the form: $y = y_{min} + [(y_{max} - y_{min}) / 1 + (x / EC_{50})^n]$.

2.3.1.1.2 AChR desensitization kinetics and current density

Analysis of the desensitization process was carried out using PulseFit, IGOR Pro (Wavemetrics), and GraphPad Prism software. The time course of the current decay was fitted using the following exponential function: $y = A + y_0 \cdot \exp(-x / \tau_{D})$ in the IGOR Pro and PulseFit software. The values obtained for the time constants of desensitization (τ_{D} , in seconds) were plotted as a function of the ACh concentration in the GraphPad Prism software. The fraction of residual current ($y_0 = I_{ACh \text{ residual}}$, pA) was also obtained by this fit and plotted vs. the ACh concentration in the GraphPad Prism software. In the text, values are given as degree of desensitization: 100 % - X % residual current.

To correct for variation in current magnitude due to differences in cell size, we normalized current responses to the cell surface and expressed them as current density in pA / pF. Current density was deducted from the peak current response obtained at 30 or 100 μM ACh concentration, by dividing the maximum current amplitude (I_{max} , pA) to the slow component of the membrane capacitance (C_s , pF) in the GraphPad Prism software. Values are given as mean \pm SEM, and n represents the number of cells taken in analysis.

2.3.1.2 Analysis of single-channel recordings

Single-channel recordings were first inspected visually and corrected for baseline drift. Noisy sections and those containing simultaneous openings of two or more channels were excluded from analysis. Single-channel events were automatically or manually fitted using the TAC software (Bruxton), being detected by the fixed threshold criterion and using a rise time of 0.08 ms. Amplitude histograms were built by plotting the single-channel current (i , pA) vs. the number of events (bin counts), and mean amplitude values were obtained for wt and ϵ -mutant AChRs, at 1, 10, 30, and 100 μM ACh, between -60 and -220 mV. Slope conductance curves of single channels were constructed from linear regression of single-channel current (i , pA) vs. membrane potential (V_{mp} , mV). Bursts of channel-openings from single receptors elicited at high concentrations of agonist (Sakmann et al., 1980) were defined as a series of openings separated by close intervals shorter than a critical duration and followed by long closings corresponding to dwells in the desensitized state. Typically, the analysis focused on close and open intervals within clusters, the durations of which reflect agonist binding and channel-gating processes. The limit duration of the shut times within clusters of events was estimated by selecting multiple stretches with bursts of openings (with > 5 events and lasting

more than 100 ms) and after fitting them, a mean value of 30 ms was determined. We assume that periods longer than 30 ms represent intervals when all of the channels in the patch were desensitized. Therefore, two datasets called “bursts analysis” and “total recording time analysis” were obtained by including only opening events between 0.04 and 30 ms duration or by including all the events longer than 0.04 ms, respectively. In some experiments, for example, at low ACh concentrations (1 μ M, in the case of wt receptor), the currents were not clustered and all open intervals in the record were measured. Open and close duration histograms were constructed using a logarithmic abscissa of the duration (in *seconds*) and a square root ordinate of the number of events, and fitted to the sum of exponentials by maximum likelihood (Sigworth and Sine, 1987), using TACFit software (Bruyton). After a visual inspection, we built histograms by merging similar open and close time distributions obtained at different holding potentials (between -60 and -220 mV), and at the same ACh concentration (1, 10, 30 or 100 μ M). Mean open and close time values were extracted for wt, ϵ -lacking, and ϵ -mutant AChRs.

Open and close probability values (P_O and P_C) in bursts and within the total recording time were obtained in the TACFit software from each individual cell, and subsequently they were averaged at each ACh concentration tested, and at -100 mV holding potential. The percentage of cells that responded to ACh application was also estimated from whole-cell- and single-channel recordings.

2.4 Materials and suppliers

Chemicals	Supplier
Acetylcholine chloride	Sigma-Aldrich Chemie GmbH, Munich, Germany
Trypan Blue	Sigma-Aldrich Chemie GmbH, Munich, Germany
Sylgard 184	Dow Corning Co., Midland, MI, USA
NaCl	Merck KGaA, Darmstadt, Germany
KCl	Merck KGaA, Darmstadt, Germany
CaCl ₂	Merck KGaA, Darmstadt, Germany
EGTA	Sigma-Aldrich Chemie GmbH, Munich, Germany
HEPES	Sigma-Aldrich Chemie GmbH, Munich, Germany
MgCl ₂	Merck KGaA, Darmstadt, Germany
Glucose	Merck KGaA, Darmstadt, Germany

Reagents and kits	Supplier
Green fluorescent protein (GFP)	Invitrogen Ltd., San Diego, CA, USA
CMV-based expression vector pCDNA3.1 (+) (5.4 kbp)	Invitrogen Ltd., San Diego, CA, USA
QuikChange TM Site-Directed Mutagenesis kit	Stratagene Co., La Jolla, CA, USA
TransFast TM transfection reagent	Promega Co., Madison, WI, USA

Medium and Supplements	Supplier
Dulbecco's Modified Eagle Medium (DMEM)	Invitrogen Ltd., San Diego, CA, USA
Bovine Calf Serum (BCS)	Invitrogen Ltd., San Diego, CA, USA
Streptomycin, Penicillin	Invitrogen Ltd., San Diego, CA, USA

Other materials	Supplier
Poly-D-lysine-coated glass coverslips	Labomedic GmbH, Bonn, Germany
Counting chamber	Fuchs-rosenthal, Germany
8, 25 cm ² Petri dishes	Becton, Dickinson and Co., NJ, USA
10, 50 ml Polypropylene conical tubes	Becton, Dickinson and Co., NJ, USA
10, 20 ml serological pipettes	Sarstedt AG and Co., Nümbrecht, Germany
10 – 1000 µl Pipettes	Eppendorf AG, Hamburg, Germany
10, 200, 500 µl Pipette tips	Eppendorf AG, Hamburg, Germany
0.5, 1.5 ml Eppendorf tubes	Eppendorf AG, Hamburg, Germany
Pipette boy	Integra Biosciences AG, Chur, Switzerland
0.2 µm Syringe filters	Nalge Nunc International Co., NY, USA
1, 5, 10 ml Syringes	B. Braun Melsungen AG, Melsungen, Germany
Gloves	Kimberly-Clark Co., GA, USA
Parafilm M	American National Can TM , Chicago, IL, USA

Apparatuses	Supplier
Laminar flow hood	Kojair [®] Tech Oy, Vilppula, Finland
MGW M20 Water bath	Lauda-Königshofen, Germany
Carl Zeiss IM35 microscope	Carl Zeiss, Göttingen, Germany
Refrigerator LiebHerr Premium	LiebHerr-Holding GmbH, Germany
Megafuge 1.0R centrifuge	Kendro Laboratory Products GmbH, Germany
HERACell CO ₂ incubator	Kendro Laboratory Products GmbH, Germany

Patch-clamp setup component	Supplier
EPC 9 patch-clamp amplifier	HEKA Elektronik Dr. Schulze GmbH, Lambrecht, Germany
ITC-16 AD / DA interface	HEKA Elektronik Dr. Schulze GmbH, Lambrecht, Germany
Computer system: Power Mac G4	Apple Computer Inc., CA, USA
Head-stage (or probe)	HEKA Elektronik Dr. Schulze GmbH, Lambrecht, Germany
Axiovert 135 or 200 microscope	Carl Zeiss, Göttingen, Germany
Cell chamber	Custom made

Micromanipulator LN mini25	Luigs and Neumann GmbH, Ratingen, Germany
Ag / AgCl recording electrode	HEKA Elektronik Dr. Schulze GmbH, Lambrecht, Germany
Pipette holder	HEKA Elektronik Dr. Schulze GmbH, Lambrecht, Germany
Vibration isolation table	Technical Manufacturing Co., MA, USA
Perfusion pump	Ismatec SA, Glattbrugg, Switzerland
Faraday cage	Custom made
HBO 100 W Fluorescence lamp	Carl Zeiss, Göttingen, Germany
Borosilicate capillary tubes	Kimble Products, KIMAX-51 [®] , New Jersey, USA
Fast pressure-application system	DAD-VM-8SP Superfusion System, ALA Scientific Instruments, NY, USA
DMZ-Universal pipette puller	Zeitz-Instrumente Vertriebs GmbH, Augsburg, Germany
Oscilloscope	Tektronix Inc., OR, USA

Analysis Software	Supplier
Pulse + PulseFit Software	HEKA Elektronik Dr. Schulze GmbH, Lambrecht, Germany
GraphPad Prism 3.03 Software	GraphPad Software Inc.
IGOR 4.01 Pro Software	Wavemetrics, Lake Oswego, OR, USA
TAC X 4.1.3 + TACFit X 4.1.3 Software	Bruxton Corporation

3 Results

3.1 Pharmacological and biophysical properties of wild-type, ϵ -subunit lacking, and ϵ -mutant AChRs inferred from whole-cell recordings

3.1.1 Introduction to whole-cell recordings

Mutations of the ϵ -subunit (ϵ V448L, ϵ 911delT, ϵ 1030delC, ϵ 1101insT, ϵ 1206ins19, and ϵ 1293insG), identified in patients with CMS symptoms were introduced in ϵ -subunit of adult human muscle nicotinic acetylcholine receptor (AChR). We transiently expressed the ϵ -subunits in HEK 293 cells together with α , β , and δ -subunits, and investigated functional properties of the ϵ -mutated AChRs using the patch-clamp technique, with two of its approaches: whole-cell- and single-channel recordings.

In the whole-cell recording mode, a so called “whole-cell current” (or macroscopic current; I_{max}) is obtained (Fig. 7), which is a measure of the total number of functional channels (N), the probability that a channel is open (P_O), and the ionic current through each individual channel (i), according to the formula $I_{max} = N \cdot P_O \cdot i$ (see also section 3.2.1).

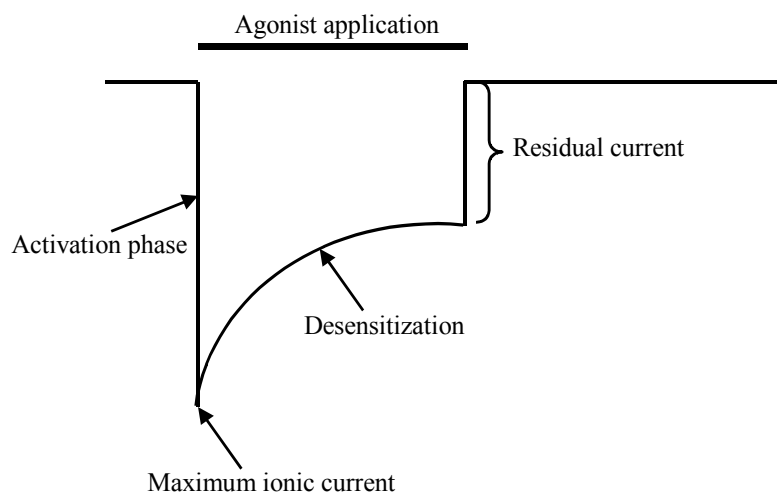


Fig. 7 Idealized representation of a whole-cell current.

The whole-cell current elicited by ACh application consists of an *activation phase*, until a *maximum ionic current* is reached, and an exponential current decay over time, in the continuous presence of the agonist, which represents the *desensitization* process. The fraction of ionic current that remains at the end of the agonist application period is the *residual current*

representing the fraction of receptors that have not desensitized yet (Fig. 7). These properties of wt and ϵ -mutant receptors were first addressed by whole-cell recordings.

To resolve fast ACh responses during whole-cell recordings, we used a fast pressure-application system that allowed applications within milliseconds. ACh-induced currents were elicited every 3 – 5 min by 2 sec-applications of different concentrations of agonist (between 0.03 and 300 μ M ACh). The agonist was applied in random order. The inter-pulse interval of 3 – 5 min ensured that the receptors fully recovered from desensitization (data not shown).

3.1.2 The properties of wild-type receptor

First, we investigated the properties of wt AChR by applying ACh at concentrations between 0.3 and 100 μ M. A representative set of current responses is shown in Figure 8. At lower concentrations (0.3 – 3 μ M), the onset of the current response was initially fairly slow and became increasingly faster at higher ACh concentrations. At higher concentrations (10 – 100 μ M), the desensitization of the receptor was most pronounced, and was visible as current decay in the continuous presence of ACh (Fig. 8 and 10 A). However, the desensitization was incomplete and after 2 sec application of ACh at 100 μ M, the residual current fraction was $21.5 \pm 5.17\%$ ($n = 6$). This indicates that $\sim 21.5\%$ of the wt AChRs were still available after 2 sec application of 100 μ M ACh and $\sim 78.5\%$ ($100 - 21.5\%$, represents the *degree of desensitization*) have entered the desensitized state (Fig. 8 and 10 B).

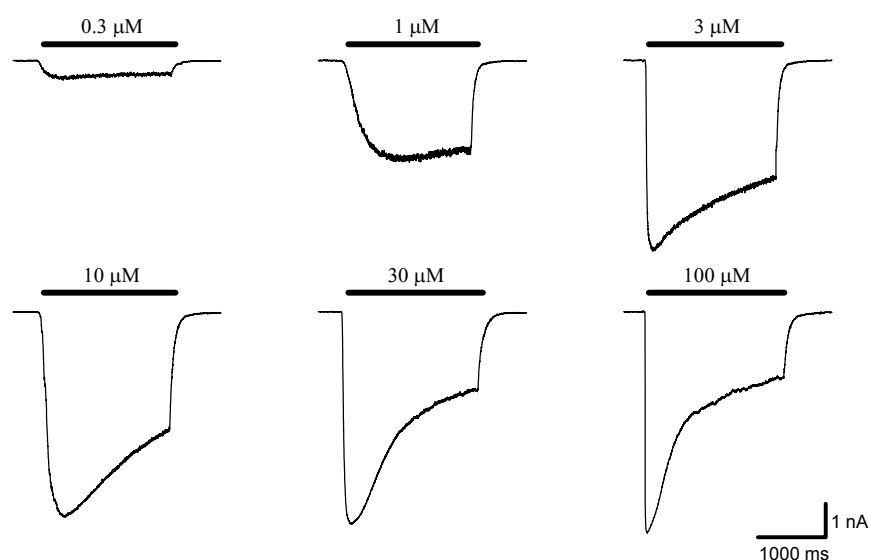


Fig. 8 Whole-cell currents obtained from wt AChRs transiently expressed in a HEK 293 cell, at different concentrations of ACh (between 0.3 and 100 μ M ACh). The bar on the top of each trace indicates the ACh application period (2 sec). The holding potential was -60 mV.

The maximum ionic current at the highest concentration tested (300 μM ; not shown) was -5445 ± 450.54 pA ($n = 24$).

We also studied the pharmacological properties of wt receptor and from the concentration-dependence of the ionic current (shown in Fig. 11) we constructed dose-response relationships from each individual cell recorded. After fitting the curves, a mean EC_{50} value of 1.42 ± 1.11 μM , with a *Hill slope* of 1.05 ± 0.098 ($n = 9$) was extracted.

3.1.3 The properties of ϵ -subunit lacking receptor

We next characterized receptors lacking the ϵ -subunit. In the absence of the ϵ -subunit ($-\epsilon$ AChR), the receptor showed a significantly altered biophysical profile. The most prominent features were the acceleration in the desensitization kinetics and the increase in the degree of desensitization (Fig. 9).

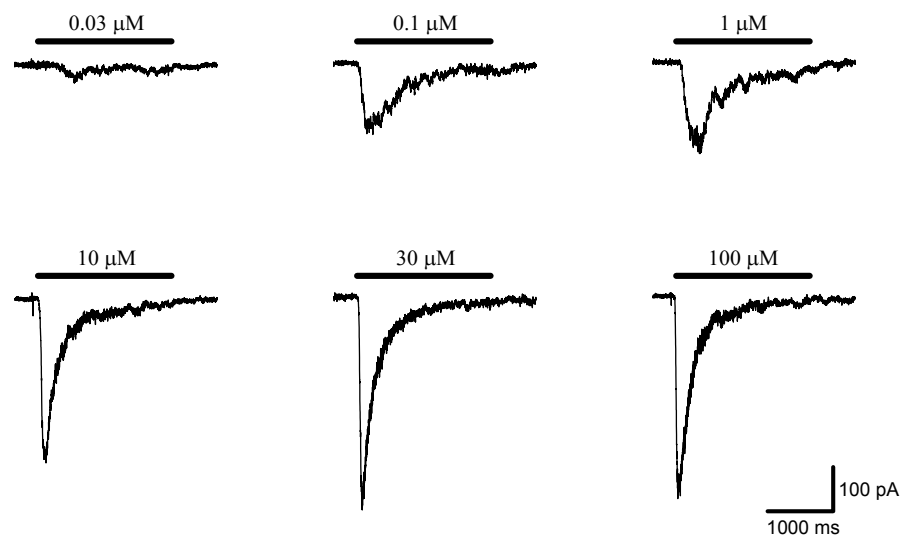


Fig. 9 Whole-cell currents obtained from a single cell expressing ϵ -subunit lacking AChRs. Currents were elicited by the indicated ACh concentrations.

Currents elicited at ACh concentrations of 0.03 and 1 μM declined with a time course that could be fitted to a single exponent function with a time constant (Tau_D) of 1.14 ± 0.04 s ($n = 3$), and 0.46 ± 0.02 s ($n = 5$), respectively. At low ACh concentrations (0.03 and 1 μM), there was a 3-fold, and, respectively, a 2-fold speed-up of the current decay compared to wt receptor (3.4 s, $n = 1$, and 0.98 ± 0.06 s, $n = 9$, respectively). However, at larger ACh concentration (30 to 300 μM), the time constants for desensitization were similar for wt and $-\epsilon$ receptors (Fig. 10 A).

The degree of desensitization was ~ 2.5 -fold increased in the absence of the ϵ -subunit. At ACh concentrations of 0.03 and 1 μM , the desensitization for $-\epsilon$ AChR was $69.3 \pm 0.64\%$ ($n = 3$), and $80.25 \pm 0.87\%$ ($n = 7$), whereas for wt receptor the desensitization was only $19.83 \pm 3.88\%$ ($n = 5$) and $44.05 \pm 5.61\%$ ($n = 8$), respectively (Fig. 10 B).

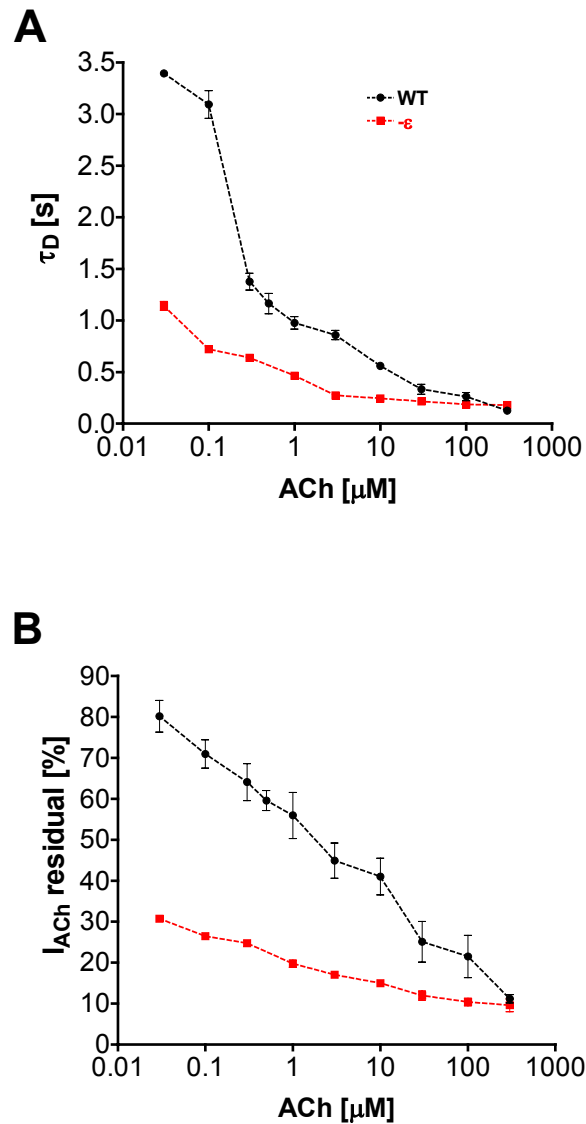


Fig. 10 Desensitization kinetics of wt and $-\epsilon$ AChRs. The time constant for desensitization (τ_{D} , **A**) and the fraction of residual current (I_{ACh} residual, **B**) for wt (black circles) and $-\epsilon$ (red squares) were plotted as a function of the ACh concentration. τ_{D} and I_{ACh} residual were obtained by fitting the current decay in *Fig. 8* and *9* to an exponential equation in the form: $y = A + y_0 * \exp(-x / \tau_{D})$.

In contrast to the large differences in kinetic properties, sensitivity to ACh for $-\epsilon$ AChR was similar to wt receptor, with values for EC_{50} and *Hill slope* of $1.65 \pm 1.05 \mu\text{M}$ ($n = 3$), and 1.11 ± 0.05 , respectively (Fig. 11). This data suggests that omitting the ϵ -subunit of AChR does not alter affinity to ACh of the receptor but rather its kinetic properties, namely time course and degree of desensitization.

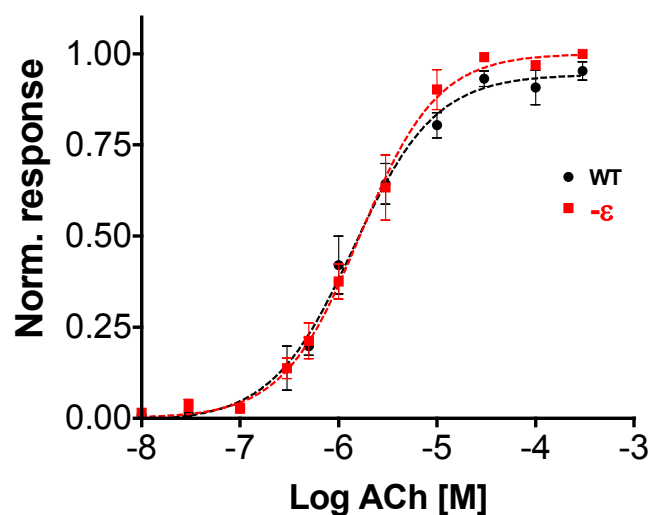


Fig. 11 Dose-response relationships obtained for wt and $-\epsilon$ AChRs. The ionic currents elicited by the different ACh concentrations were normalized to the maximal response and plotted as a function of log of the agonist concentration (in M). The data points were fitted to a logistic equation in the form: $y = y_{\min} + [(y_{\max} - y_{\min}) / 1 + (x / EC_{50})^n]$, and mean EC_{50} and *Hill slope* values were extracted. Best fits are represented by dashed lines.

The maximum current magnitude elicited by $300 \mu\text{M}$ (not shown) was about 9-fold smaller for $-\epsilon$ AChR than for wt receptor: $-598.4 \pm 166.04 \text{ pA}$ ($n = 8$), vs. $-5445 \pm 450.54 \text{ pA}$, $n = 24$ ($P < 0.0001$), respectively.

To correct for variation in current magnitude due to differences in cell size, we normalized current responses to the cell surface and expressed them as current density in pA / pF .

A comparison of the AChR current density (pA / pF) for wt and $-\epsilon$ AChRs is illustrated in Figure 12. The current density was ~ 8 -fold reduced ($P < 0.0001$) for $-\epsilon$ compared to wt receptor: $36.5 \pm 9.1 \text{ pA} / \text{pF}$ ($n = 24$) vs. $292.5 \pm 2.64 \text{ pA} / \text{pF}$ ($n = 58$), respectively. The reduction in the current density might be the result of a decrease in cell surface expression, and / or altered gating properties of the individual $-\epsilon$ AChR.

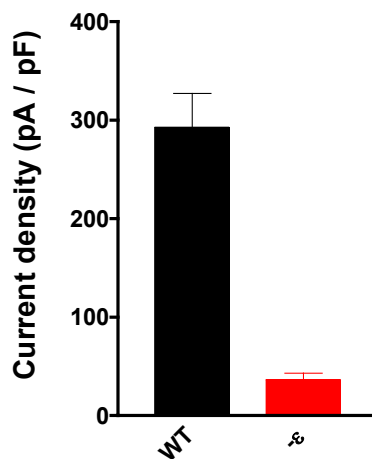


Fig. 12 Comparison of current density for wt and ϵ AChRs.

3.1.4 The properties of ϵ -mutant receptors

First, we addressed the functional consequences of missense ϵ V448L mutation. Mutant ϵ V448L exhibited gating properties that were similar to wt receptor: little desensitization at low concentrations (0.5 μ M), and at increase of ACh concentration, faster but incomplete desensitization (Fig. 13).

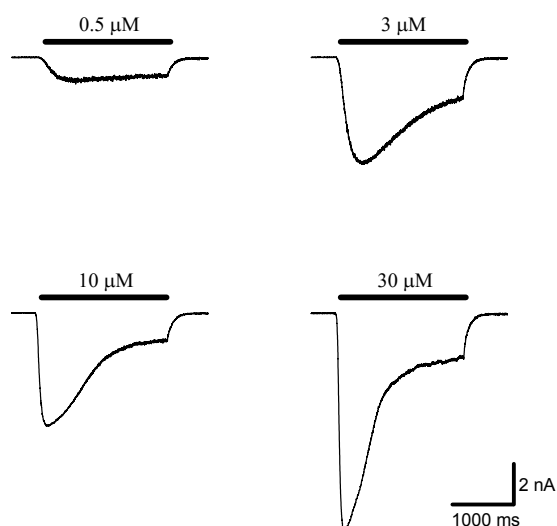


Fig. 13 Representative whole-cell currents obtained from a single cell expressing ϵ V448L AChRs. Currents were elicited by the indicated ACh concentrations.

The time constant for desensitization (Tau_D) had values that were similar to those obtained for wt receptor (Fig. 16 A). The degree of desensitization was somewhat increased at higher ACh concentrations (10 to 100 μ M) compared to wt, with values of: $83 \pm 1.4 \%$ ($n = 5$), and 91% ($n = 1$) vs. $59 \pm 4.47 \%$ ($n = 11$), and $21.5 \pm 5.17 \%$ ($n = 6$), respectively (Fig. 16 B).

The maximum current density for mutant ϵ V448L was 223.3 ± 30 pA / pF ($n = 14$). This value is similar to that obtained with wt AChR ($P = 0.364$; Fig. 17), suggesting that ϵ V448L mutation is very unlikely to impair cell surface expression of the receptor.

In contrast to ϵ V448L mutation, the properties of the receptor were altered by mutation at position 1030 (ϵ 1030delC). Mutation ϵ 1030delC leads to a shift in the reading frame and produces after 20 residues a stop codon. The resulting protein carries only 1/3 of the cytoplasmic loop between TM₃ and TM₄. This may underlie the 2-fold increase in receptor desensitization (Tau_D : 1.86 ± 0.11 s, $n = 2$, and 0.53 ± 0.01 s, $n = 3$) compared to wt, at ACh concentrations between 0.03 and 1 μ M, respectively (Fig. 14 and 16 A). At larger agonist concentration (1 to 300 μ M), the desensitization process became faster, with values for Tau_D similar to those of $-\epsilon$ AChR (Fig. 16 A).

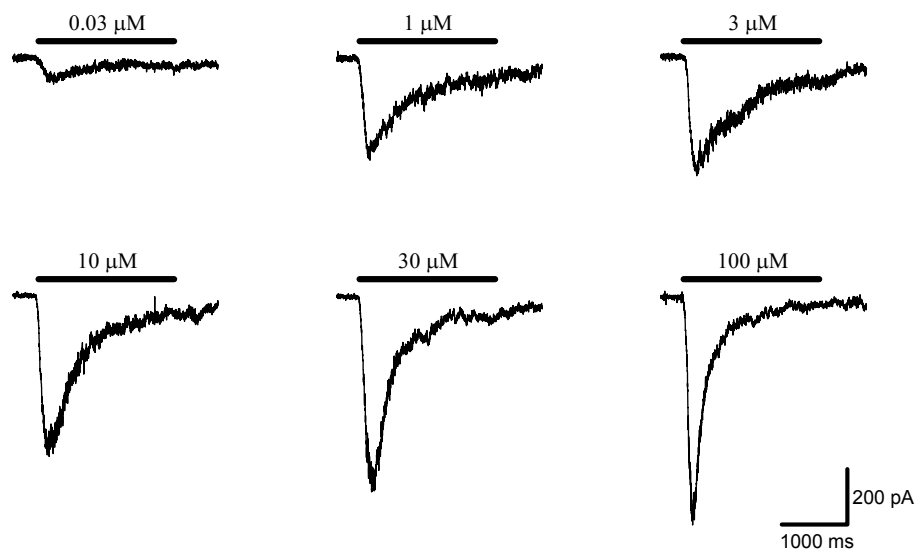
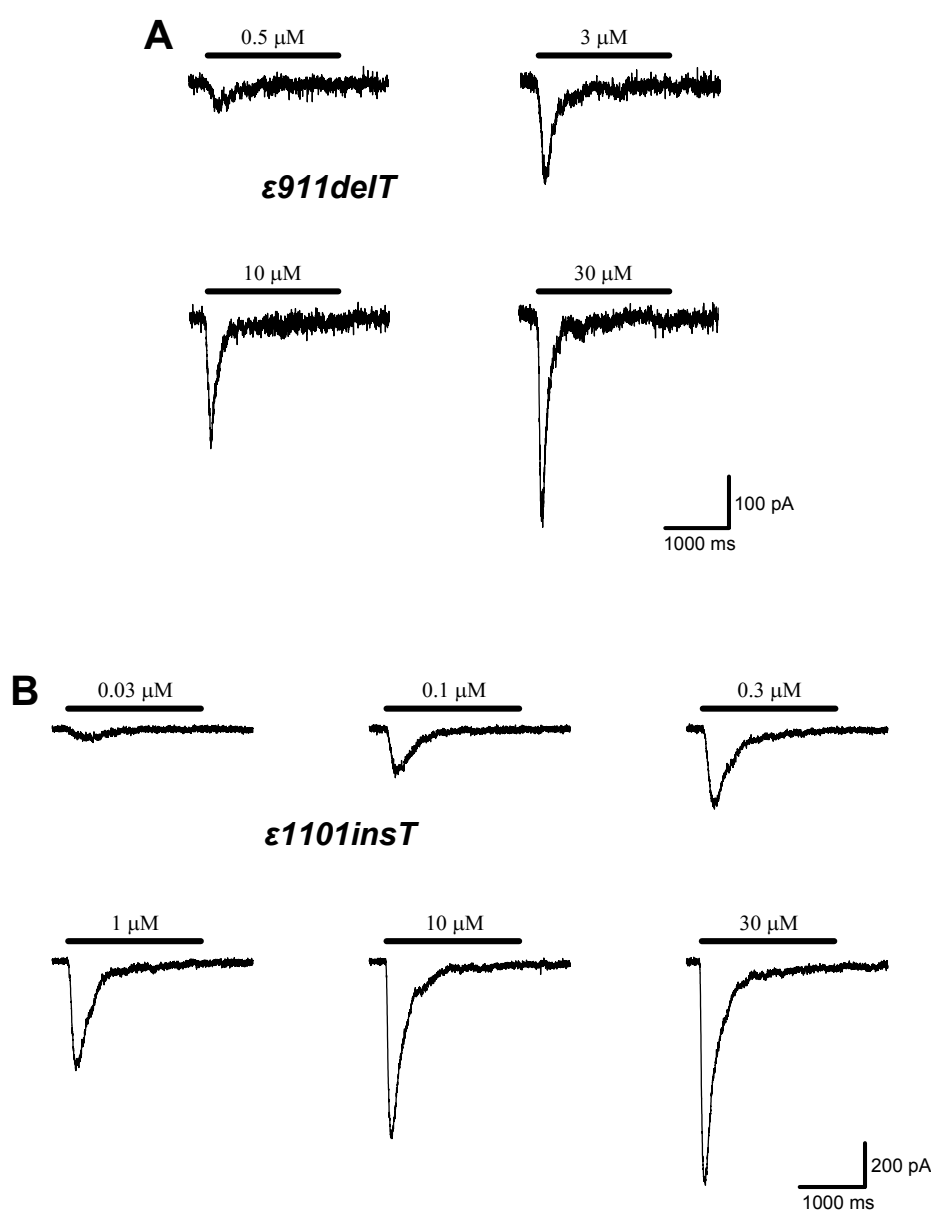


Fig. 14 Whole-cell currents obtained from a single cell expressing ϵ 1030delC AChRs. Currents were elicited by the indicated ACh concentrations.

Mutation ϵ 1030delC not only altered the kinetic of the time course of the desensitization process but also affected the degree of desensitization. Thus, between 0.03 and 1 μ M there was a 2-fold increase of desensitization in comparison to wt receptor ($54.9 \pm 3.5 \%$, $n = 3$, and $68.4 \pm 1.1 \%$, $n = 5$, respectively). However, at higher ACh concentrations (10 to 300 μ M),

the degree of desensitization was similar to $-\epsilon$ receptor (Fig. 16 B). Mutant $\epsilon 1030\text{delC}$ exhibited 3.5-fold reduced current density compared to wt receptor ($82.85 \pm 11.2 \text{ pA / pF}$, $n = 25$; $P = 0.0003$; Fig. 17), and therefore, unlike $\epsilon V448L$, the $\epsilon 1030\text{delC}$ mutation is likely to affect the cell surface expression of AChR.

The deletion mutation $\epsilon 911\text{delT}$, as well as the three insertion mutations $\epsilon 1101\text{insT}$, $\epsilon 1206\text{ins19}$, and $\epsilon 1293\text{insG}$ caused acceleration of the desensitization process (time course and degree of desensitization). The properties of these receptors were similar in all cases to those observed with $-\epsilon$ AChR (Fig. 15 and 16).



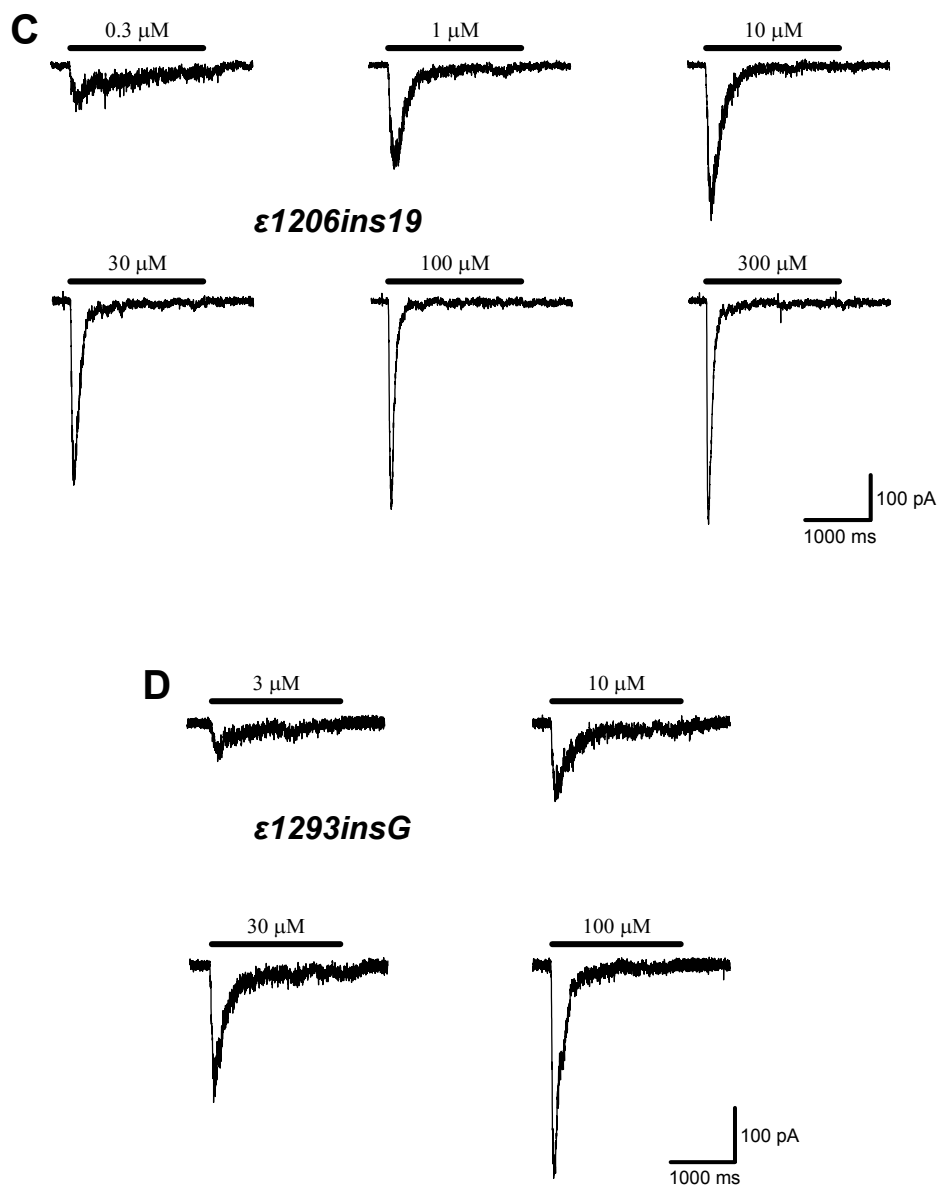


Fig. 15 Representative whole-cell currents in response to the indicated ACh concentrations obtained from single cells expressing $\epsilon 911delT$ (*A*), $\epsilon 1101insT$ (*B*), $\epsilon 1206ins19$ (*C*), and $\epsilon 1293insG$ AChRs (*D*), respectively.

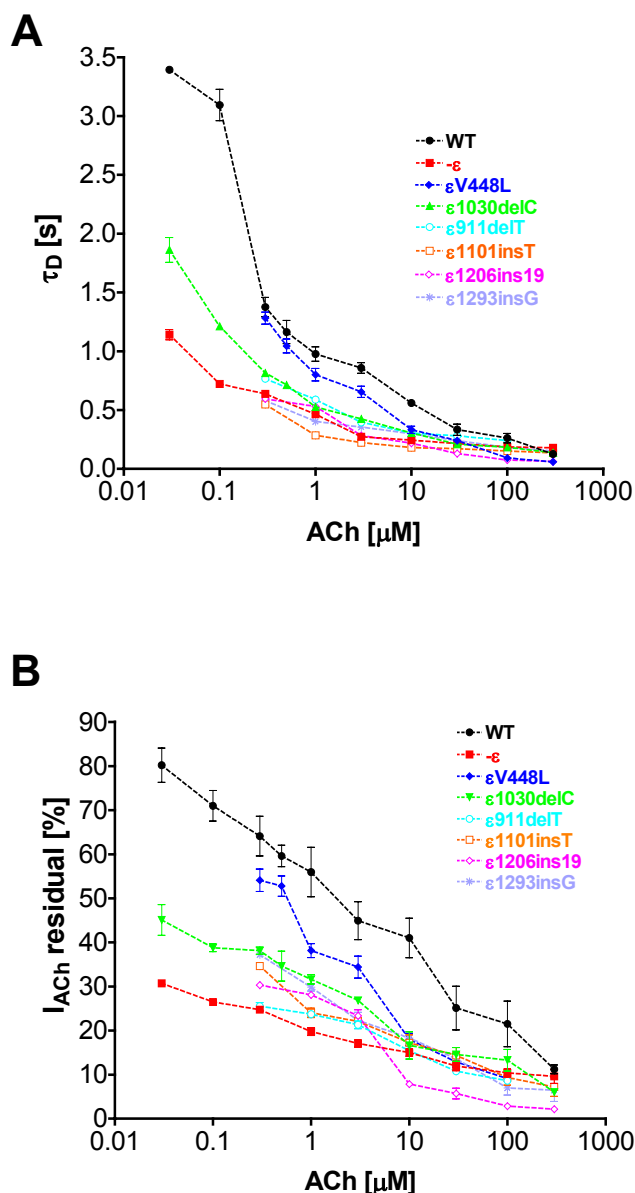


Fig. 16 Desensitization kinetics: current decay (**A**) and residual current fraction (**B**) of ϵ -mutant AChRs in comparison to wt and $-\epsilon$ receptors.

The maximum current amplitude (I_{max}) observed with these mutants was significantly reduced compared to wt receptor, with values similar to those observed in AChR lacking the ϵ -subunit ($P > 0.05$ vs. $-\epsilon$ receptor; compare Fig. 15 A-D vs. Fig. 9).

Mutant ϵ 911delT exhibited ~ 2.5 -fold reduced current density compared to $-\epsilon$ receptor (13.57 ± 1.83 pA / pF, $n = 17$; $P = 0.009$ vs. $-\epsilon$ AChR), whereas all three insertion mutations (ϵ 1101insT, ϵ 1206ins19, and ϵ 1293insG) resulted in slight, but statistically not significant, increase in current density (see Fig. 17). Thus, the very likely reduction in cell surface expression observed with these mutants suggests a loss of function of AChR at the neuromuscular junction.

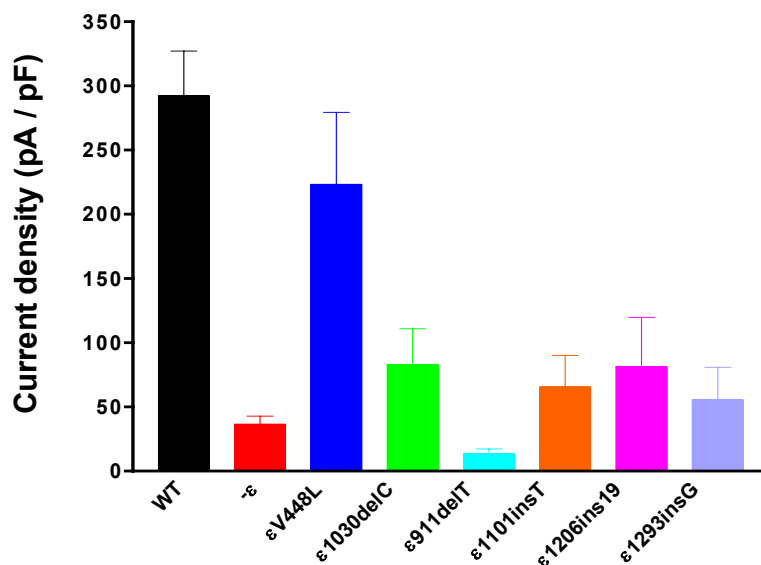


Fig. 17 Comparison of current density for wt, $-\epsilon$, and ϵ -mutant AChRs.

We also studied the affinity for ACh of these ϵ -mutant AChRs in comparison to wt and $-\epsilon$ receptors. Except for mutant $\epsilon 1293\text{insG}$, which resulted in 5-fold increase in the EC_{50} value ($17.71 \pm 1.14 \mu\text{M}$ with a *Hill slope* of 1.29 ± 0.20 , $n = 2$; $P < 0.05$), all the other mutant AChRs had EC_{50} and *Hill slope* values similar to wt and $-\epsilon$ AChRs ($P > 0.05$), ranging from 1.01 to $3.7 \mu\text{M}$ ACh, with *Hill slopes* between 0.85 and 1.07 (Fig. 18).

In summary, these findings suggest that only $\epsilon 1293\text{insG}$ mutation shows its effects by both decreasing sensitivity to ACh and altering desensitization kinetics of the receptor.

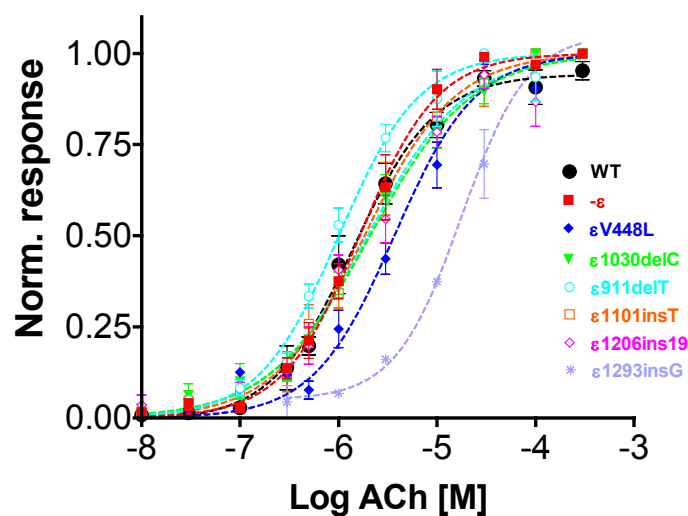


Fig. 18 Dose-response relationships obtained for ϵ -mutant AChRs in comparison to wt and $-\epsilon$ receptors.

3.1.5 Summary of the whole-cell data

With the exception of ϵ V448L receptor, all investigated ϵ -mutant AChRs exhibited acceleration of the macroscopic current decay and enhanced degree of desensitization, compared to wt receptor. Furthermore, their current density was significantly reduced, suggesting that these receptors might be expressed at low levels at the cell surface. Statistical analysis also indicated that the EC_{50} value obtained with mutant ϵ 1293insG was significantly different from the value exhibited by wt AChR, and thus mutation ϵ 1293insG is also likely to affect the ACh affinity of the receptor. The other mutations had no effect on the sensitivity to agonist of AChR.

3.2 Single-channel recordings

3.2.1 Introduction to single-channel recordings and data kinetic analysis

From whole-cell recordings, one can extract only average properties of large populations of ion channels in the membrane (Hille, 2001). The whole-cell current is described by formula $I_{max} = N \cdot P_O \cdot i$, where I_{max} represents the macroscopic current, N is the number of functional channels, P_O the probability that a channel is open, and i represents the ionic current through one single channel. It is possible to obtain this information from one individual channel by performing single-channel recordings.

In a single-channel recording, each opening event is a transition from the closed state (zero current) to the open state and has defined *unitary current* (i , pA) and *duration* (time, ms). An example of such recordings from wt AChR is illustrated in Figure 19 A.

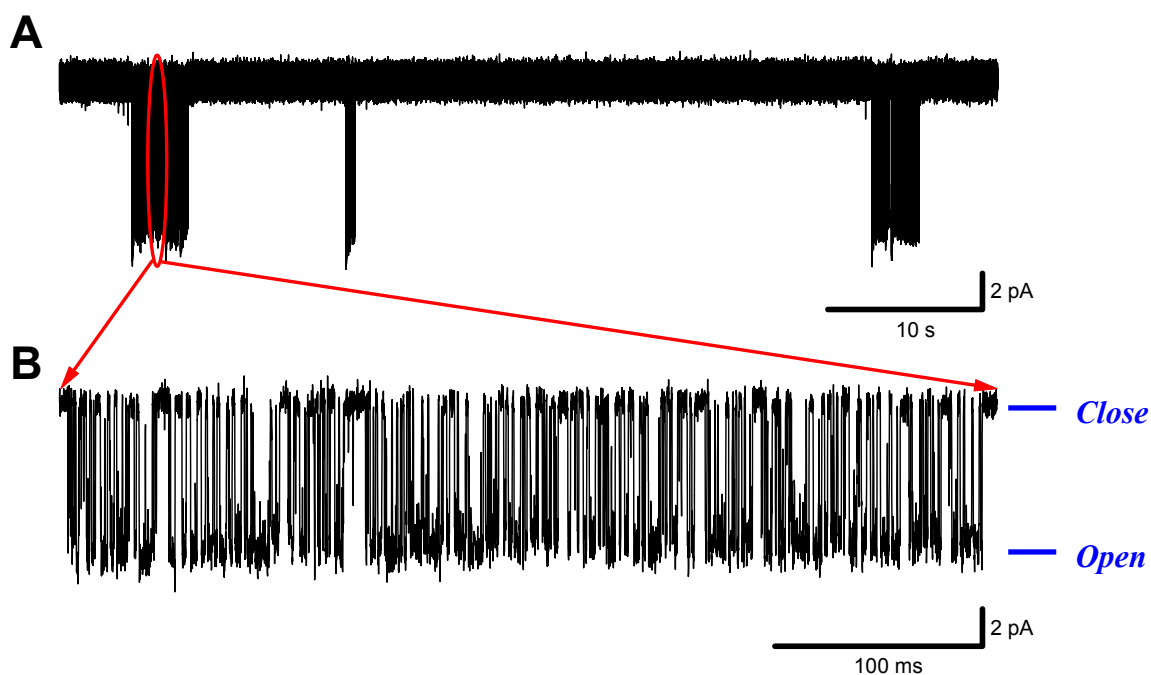


Fig. 19 Single-channel bursts of openings recorded from a wt AChR at -100 mV and $30 \mu\text{M}$ ACh; **A** shows few clusters with channel-opening events (bursts of openings) separated by periods with no channel activity when all AChRs are desensitized. Channel-openings are presented as downward deflections of the membrane current; **B** represents the magnification of a cluster of opening events, when the AChR undergoes many cycles of agonist association / dissociation. The horizontal bars on the right of **B** represent the closed and the open states of the receptor.

Channel-openings and ionic flux through these channels are represented by the rapid transient changes in the membrane current in the order of several picoampere (pA). The channel-openings in Figure 19 are visible as downward deflections. Upon closing of the channel, the membrane current returns to its baseline value, and these transitions are visible as upward deflections in Figure 19. The transitions between the closed and the open states occur in the microsecond range. In the record, channel-openings occur in clusters followed by periods with no channel activity. This clustering of channel-openings and closings has been termed “bursts” (Sakmann et al., 1980).

Binding of the agonist to the channel results initially in opening of the channel. However, the channel undergoes further conformational changes in the continued presence of the agonist that result in closing of the channel. In this state, the agonist can no longer activate the channel. This condition has been described as desensitization of the receptor (Katz and Thesleff, 1957). The long-lived closed intervals between the bursts of openings reflect times when all AChRs in the patch are desensitized (Fig. 19 A). A cluster starts when one AChR spontaneously recovers from desensitization, and continues with the protein molecule undergoing many cycles of agonist association / dissociation (Fig. 19 B). A cluster ends when that receptor again becomes desensitized.

The process of opening and closing of single-channels is termed as channel-gating and reflects conformational changes of the AChR. Gating of one channel is a stochastic process, and to derive information from such measurements requires analysis of many open-close events using statistical methods. Major parameters that are unique to an individual ion channel are the *amplitude* of the unitary current (i) and the *mean lifetime* (duration) of the open or the close state. The *open lifetime* is the time between the opening of one channel and its next closing, whereas the *close lifetime* represents the time between two opening events in succession. The binding of the two agonists brings the receptor into an equilibrium state between the closed and the open channel. This equilibrium is described by the *open probability* (P_o), a measure that an ion channel will be open under given conditions.

To understand whether for example the reduction in current density observed with the insertion / deletion mutations (see Fig. 17) is due to changes in any of the above-described parameters, we performed single-channel recordings in cell-attached configuration and analyzed the properties of individual receptors.

3.2.2 Unitary current and slope conductance

The ionic current that flows through an individual channel depends on the driving force (V_{EMF}) for the ions passing through the channel. According to Ohm's law: $I = V / R$, the size of the unitary current (i) can be calculated as $i = V_{EMF} \times g$, where $V_{EMF} = V_{mp} - V_{REV}$ (V_{EMF} is the electromotive force, V_{mp} is the membrane potential, V_{REV} represents the reversal potential of the permeating ion, and g , the conductance of the ion channel). The differences in whole-cell current densities between wt and ϵ -mutant AChRs may be caused by alteration in levels of expression of functional channels and / or by alteration in their single-channel properties (e.g. changes in the conductance of the AChR and / or channel-gating).

We first evaluated the *unitary current* size (i) and the *slope conductance* (g) of these receptors. The unitary current of wt receptor was -7.24 ± 0.22 pA ($n = 22$), at a membrane potential of -100 mV. A similar value for the unitary current was obtained for the AChR lacking the ϵ -subunit ($P > 0.05$). In contrast, mutations $\epsilon V448L$, $\epsilon 911delT$, and $\epsilon 1030delC$ exhibited different unitary current values, thus suggesting an alteration of the permeation properties of the channel (Table 1). However, the changes in the unitary current size observed with the mutants were statistically not different from that observed with wt receptor.

Type	i (pA)	g (pS)	n
WT	-7.24 ± 0.22	60.92 ± 1.32	22
$-\epsilon$	-7.73 ± 0.31	63 ± 0.97	12
$\epsilon V448L$	-6.56 ± 0.35	61.94 ± 1.88	6
$\epsilon 1030delC$	-8.01 ± 0.31	63.13 ± 0.9	9
$\epsilon 911delT$	-6.44 ± 0.23	63.21 ± 0.74	7

Table 1 Unitary current (i ; pA) and slope conductance (g ; pS) values for wt, $-\epsilon$, and ϵ -mutant AChRs. The unitary current values are given at a membrane potential of -100 mV. Data represent mean \pm SEM. n represents the number of cells.

We obtained the slope conductance for these receptors from linear regression fit to the current-voltage relationship of the individual receptors (Fig. 20). The slope conductances for wt, $-\epsilon$, and ϵ -mutant receptors were very similar, with values ranging from 60.92 to 63.21 pS (Table 1 and Fig. 20). The values for wt, as well as for the ϵ -mutant AChRs are similar to those reported previously by Newland et al. (1995; 62 pS) or Ohno et al. (1997; 60 pS) for human ACh receptors. These data suggest that the mutations within the ϵ -subunit have no measurable effect on the size of the ion flux through the open receptors. We next investigated the gating kinetic properties of the ϵ -mutant AChRs.

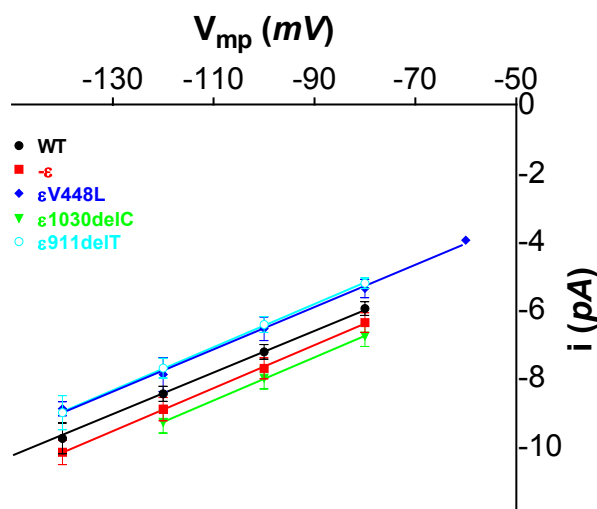


Fig. 20 Slope conductance curves were constructed for wt, $-\epsilon$, and ϵ -mutant AChRs by plotting the unitary current (i ; pA) vs. the membrane potential (V_{mp} ; mV).

3.2.3 Kinetic analysis

3.2.3.1 Gating-kinetics of wild-type receptor

We analyzed the gating properties of the receptors by analysis of the channel-opening events within the bursts of openings. Bursts were defined as a series of openings with closing intervals shorter than a critical duration of 30 ms (see Materials and Methods section 2.3.1.2). Periods longer than 30 ms very likely represent intervals when all of the channels in the patch are desensitized. The kinetic analysis focused on close and open intervals within clusters (termed as “Burst analysis”). Only stretches of bursts that contained more than 5 events of channel-openings were selected one by one and analyzed (see also Fig. 19 B). However, at low ACh concentrations (1 μ M, for wt receptor), we observed mostly isolated channel-openings and only very rarely a burst of openings (Fig. 21 A).

Using burst analysis, we addressed the gating parameters *open* and *close lifetime*, and *open probability* of wt, $-\epsilon$, and ϵ -mutant AChRs.

The gating pattern of wt AChR, at different agonist concentrations (between 1 and 100 μ M) is shown in Figure 21. At concentration of 1 μ M, the channel-opening events occurred only infrequently and for brief periods, followed by long closing intervals (Fig. 21 A). With increasing agonist concentration (10 – 100 μ M) the frequency of channel-opening events increased (Fig. 21). The opening events occurred mainly in bursts, and the receptor exhibited a dose-response increase in the open probability (P_o), because the time required for binding of

the agonist reduced, thus shortening the close time durations. The P_o values were: 0.30 ± 0.025 ($n = 3$), 0.44 ± 0.026 ($n = 7$), 0.66 ± 0.021 ($n = 9$), and 0.82 ± 0.043 ($n = 4$), at 1, 10, 30, and, 100 μM , respectively. In contrast, the open duration of the channel remained similar at all agonist concentrations (Fig. 21 A-D and 22 A).

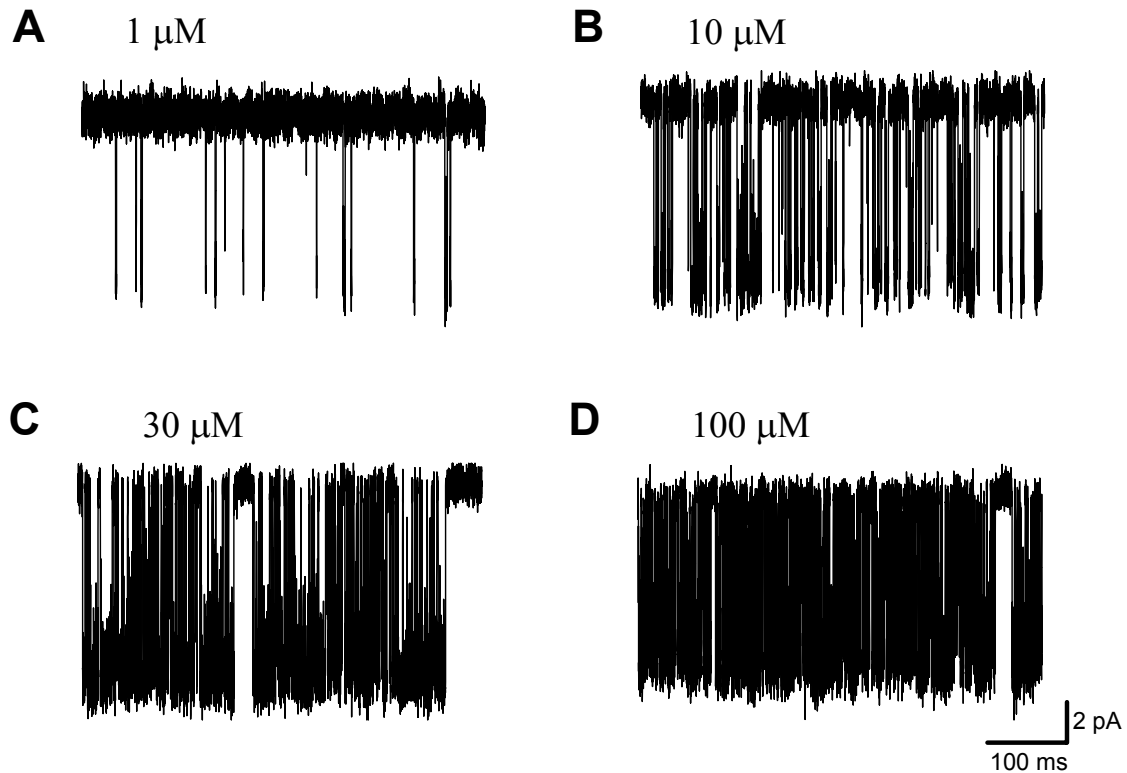


Fig. 21 Single-channel bursts of openings of wt AChR recorded at the indicated ACh concentrations. Currents are shown at bandwidth of 10 kHz, with channel-openings as downward deflections. Holding potential: -100 mV.

The distribution of the open and close time durations from several recordings obtained at different ACh concentrations are shown in Figure 22. The fit of open duration revealed two major components with time constants for opening of ~ 1 and 3 ms ($\text{Tau}_{\text{open1}}$ and $\text{Tau}_{\text{open2}}$). For example, at an ACh concentration of 30 μM , $\text{Tau}_{\text{open1}}$ and $\text{Tau}_{\text{open2}}$ had values of 1.25 ± 0.17 ms, and 2.7 ± 0.4 ms ($n = 9$), respectively (Fig. 22 A). The fractions of channel-openings associated with the two open time constants were: 64 ± 2.3 %, and 36 ± 2.3 %, respectively. Similar values were obtained at concentrations of 10 and 100 μM ACh. However, at agonist concentration of 10 μM , the opening events occurred at about equal levels at the two open time constants. At lower concentrations (1 μM), there was a shift towards shorter openings ($\text{Tau}_{\text{open1}}$: 0.52 ± 0.06 ms; $\text{Tau}_{\text{open2}}$: 1.74 ± 0.26 ms; $n = 3$). However, the major open duration was similar to those observed at higher concentrations (Fig. 22 A).

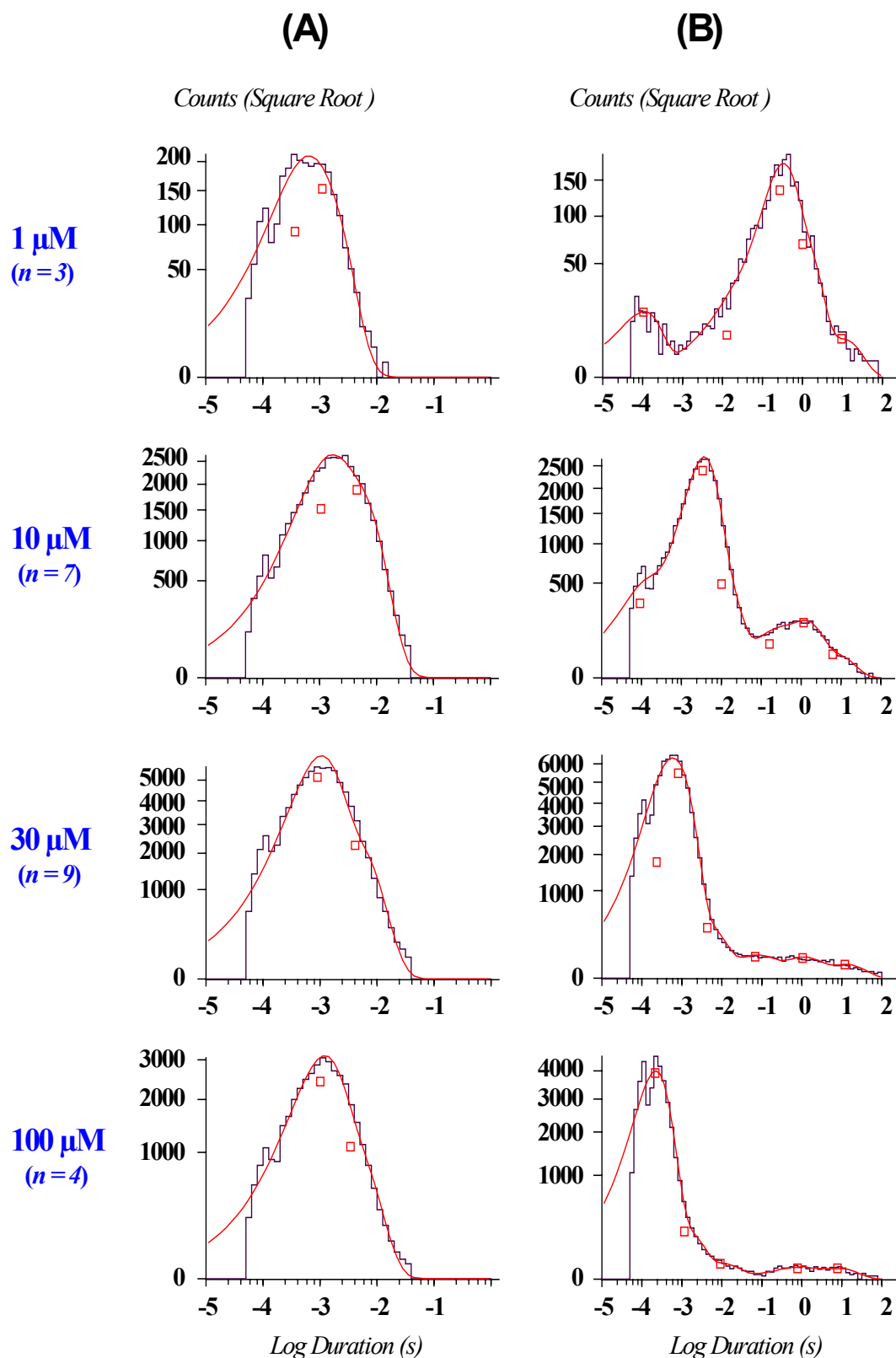


Fig. 22 Summary of open (A) and close (B) time distributions obtained for wt AChR at the indicated agonist concentrations. Histograms were constructed using a logarithmic abscissa (log of duration, s) vs. the square root ordinate of the number of events (bin counts); n represents the number of cells.

In contrast, the distribution of the channel close times shifted in a concentration-dependent manner towards shorter close time durations. The fastest component ($\text{Tau}_{\text{close1}}$) had an average value of 0.2 ± 0.02 ms ($n = 4$), and described more than 95 ± 0.8 % of channel-closing duration at $100 \mu\text{M}$ (Fig. 22 B). At lower concentrations (10 and $30 \mu\text{M}$), the dominant close time constants ($\text{Tau}_{\text{close2}}$) were 3.6 ± 0.18 ms ($n = 7$) and 0.75 ± 0.04 ms ($n = 9$), respectively. They accounted for about 75 % of the closing intervals exhibited by wt receptor, at both concentrations. At the lowest concentration tested ($1 \mu\text{M}$), $\text{Tau}_{\text{close1}}$ had a value of 0.12 ± 0.009 ms ($n = 3$), and represented only a small fraction of 8.4 ± 1.5 % of all shut times (Fig. 22 B). The majority of the closings were longer than 30 ms, reflecting low open probability at this concentration (0.30 ± 0.025 , $n = 3$).

3.2.3.2 Gating-kinetics of ϵ -subunit lacking receptor

The AChR lacking the ϵ -subunit exhibited a different gating kinetic pattern, consisting of fewer and briefer opening events than wt receptor, and longer intervals with no channel activity (Fig. 23 A-D).

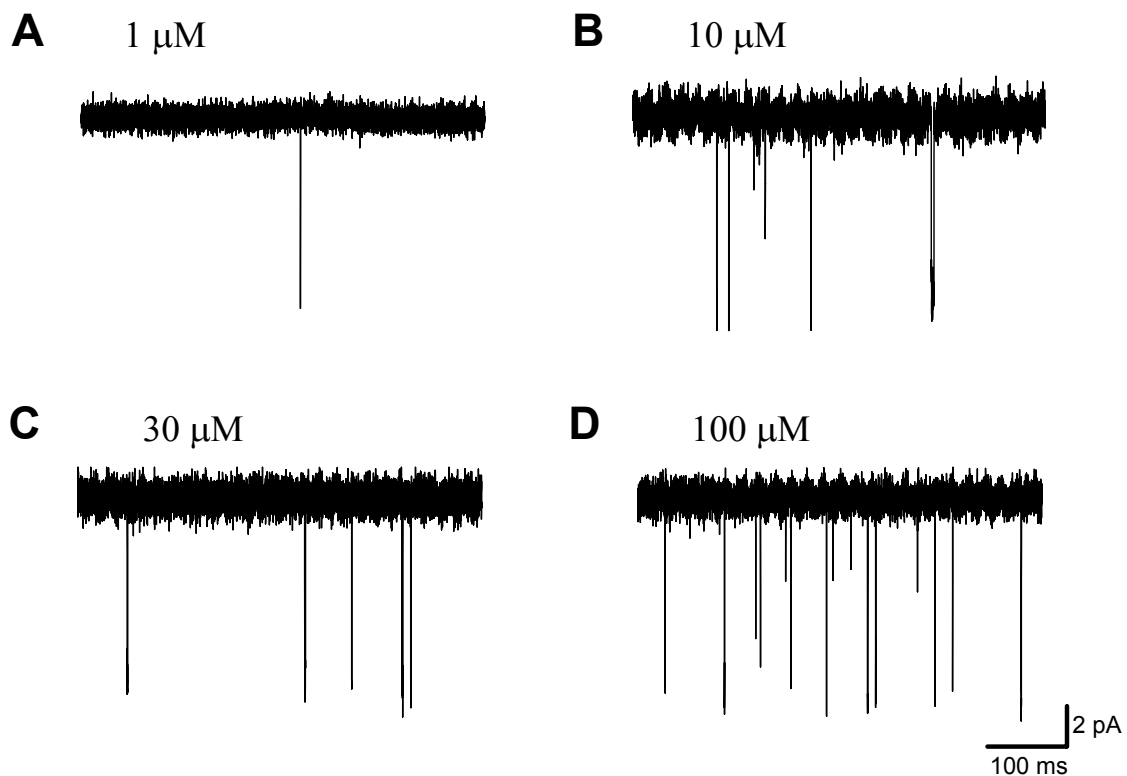


Fig. 23 Single-channel opening events of ϵ -lacking AChR recorded at the indicated ACh concentrations. Holding potential: -100 mV.

The absence of the ϵ -subunit resulted in a drastic reduction of the open probability of the receptor. For example, at a concentration of 30 μM the open probability of $-\epsilon$ receptor within the total recording time was ~ 40 -fold reduced compared to wt AChR ($9.8 \pm 3.5 \cdot 10^{-4}$, $n = 6$ vs. $432 \pm 52.2 \cdot 10^{-4}$, $n = 9$; see Table 3 and Fig. 32). This is also illustrated by the reduction in the overall number of channel-openings (Fig. 23).

The drastic changes in the gating kinetics are also reflected in the open and close time distributions for the ϵ -subunit lacking receptor (Fig. 24). The most visible change was the increase in the close time distribution, with a large increase in the number of long-lasting closings (> 30 ms) compared to wt receptor (Fig. 24 B vs. 22 B).

Fitting the open time distribution revealed a fast component ($\text{Tau}_{\text{open1}}$) with a time constant of ~ 0.2 ms (Fig. 24 A). At an agonist concentration of 1 μM , this fast component had a value of 0.14 ms ($n = 1$) and was the only gating component observed. At higher agonist concentrations, the values for $\text{Tau}_{\text{open1}}$ were very similar (10 μM : 0.21 ± 0.014 ms, $n = 4$; 30 μM : 0.18 ± 0.02 ms, $n = 6$; 100 μM : 0.24 ± 0.022 ms, $n = 7$) and were associated with ~ 85 % of all channel-openings. In addition to the fast component, two slower gating components ($\text{Tau}_{\text{open2}}$ and $\text{Tau}_{\text{open3}}$) were observed at agonist concentrations between 10 and 100 μM , with values of ~ 0.8 and ~ 5 ms, respectively. The fraction of opening events associated with $\text{Tau}_{\text{open2}}$ was ~ 10 % and that associated with $\text{Tau}_{\text{open3}}$ was ~ 5 % (Fig. 24 A).

As observed, in the AChR lacking the ϵ -subunit there is a 5-fold shortening of the major open time constant ($\text{Tau}_{\text{open1}}$), in comparison to wt receptor. At all concentrations, most of the closings were longer than 30 ms (Fig. 24 B), reflecting a low open probability for $-\epsilon$ receptor. Furthermore, the fraction of channel close times that occurred during the burst of openings, at agonist concentration of 30 μM was only 7.4 ± 2.7 %, and 12 ± 4.8 % ($n = 6$), for $\text{Tau}_{\text{close1}}$ and $\text{Tau}_{\text{close2}}$, respectively ($\text{Tau}_{\text{close1}}$: 0.45 ± 0.13 ms; $\text{Tau}_{\text{close2}}$: 2.55 ± 0.36 ms). Similar values were observed at agonist concentrations of 10 and 100 μM (Fig. 24 B). At the lowest concentration tested (1 μM), $\text{Tau}_{\text{close1}}$ weighted only 3% of all close times, whereas $\text{Tau}_{\text{close2}}$ was not observed.

Together, these findings indicate that the AChR lacking the ϵ -subunit is still functional, however, it is less functional than the wt receptor. This suggests that mutations that truncate the ϵ -subunit are likely to generate a receptor with similarly altered gating properties as observed with $-\epsilon$ AChR.

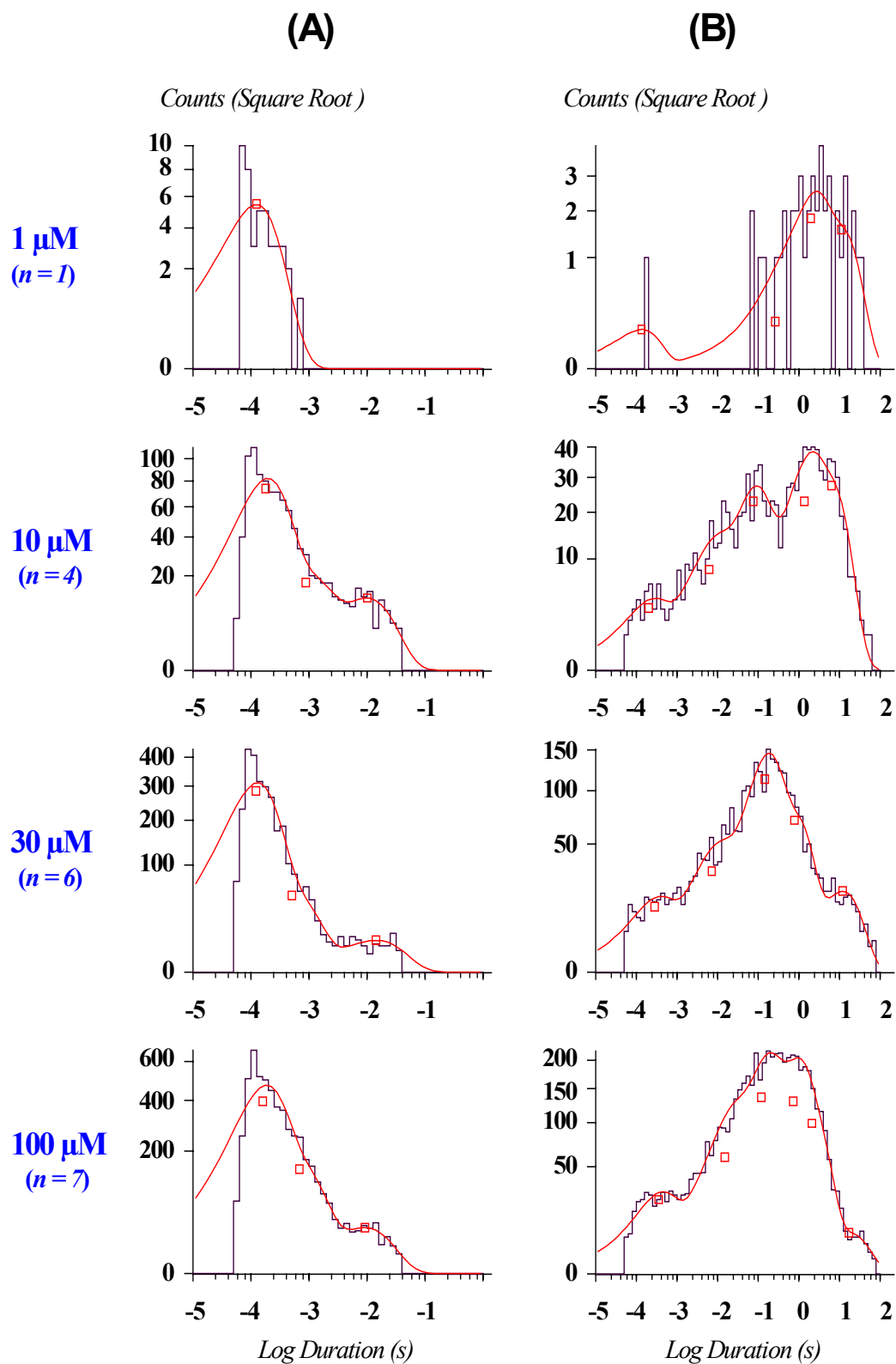


Fig. 24 Summary of open (A) and close (B) time distributions obtained for $-\epsilon$ AChR at the indicated agonist concentrations.

3.2.3.3 Gating-kinetics of ϵ -mutant receptors

To investigate the gating properties of AChR containing mutated ϵ -subunit, we performed recordings only at an agonist concentration of 30 μM . This concentration is optimal to eliciting bursts of channel-openings from single receptors, and, at the same time, does not induce desensitization of AChR (Sakmann et al., 1980).

As predicted by the properties observed at whole-cell level (see also section 3.1.4), mutant ϵV448L exhibited open and close time distributions similar to wt receptor (Fig. 25).

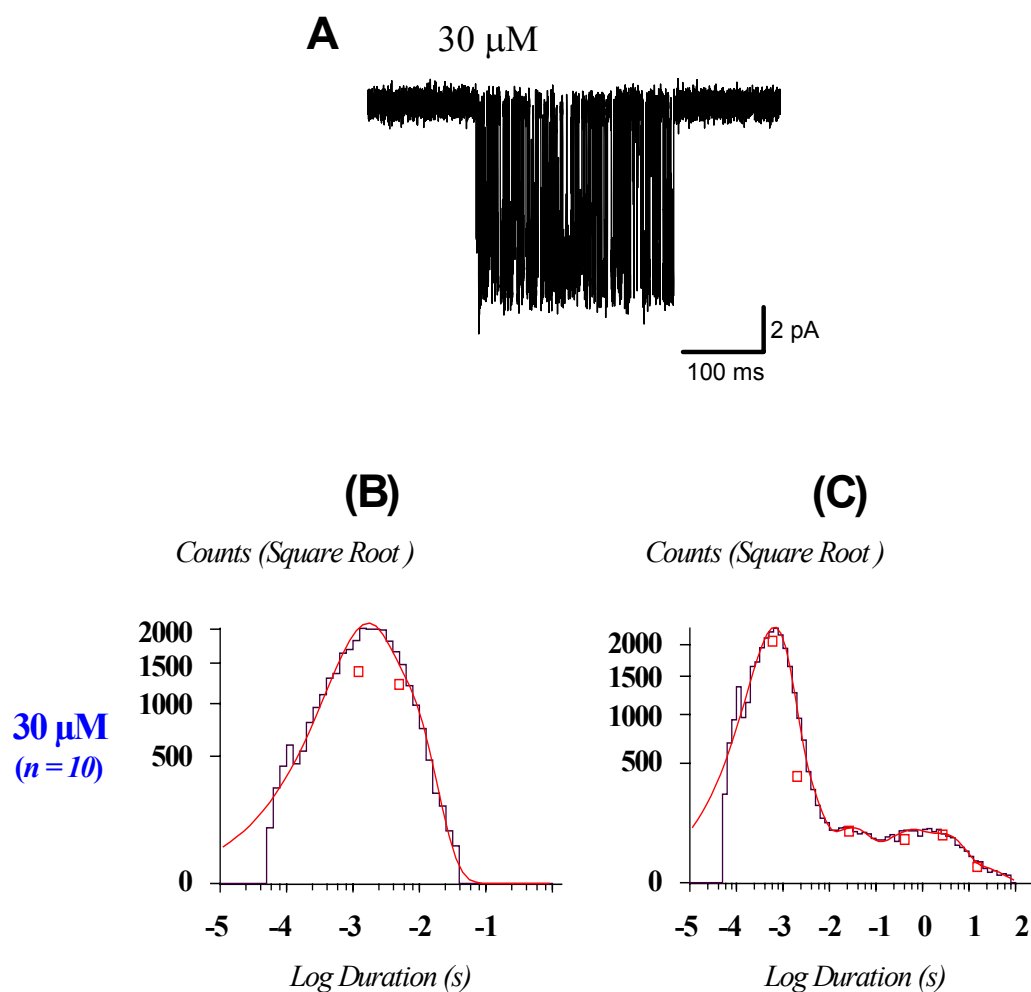


Fig. 25 Single-channel bursts of openings recorded at -100 mV from a ϵV448L AChR, elicited by 30 μM ACh (**A**), and summary of open (**B**) and close (**C**) time distributions.

The open time constants, $\text{Tau}_{\text{open1}}$ and $\text{Tau}_{\text{open2}}$, had values of 1.4 ± 0.15 ms, and 4.48 ± 0.24 ms ($n = 10$), respectively. The opening events occurred at about equal levels at the two open time constants (Fig. 25 B). Furthermore, the majority of closings occurred in clusters (Fig. 25

A), as indicated by the fastest component of the close time distribution, τ_{close1} (Fig. 25 C), which had a value of 0.71 ± 0.04 ms ($n = 7$). This close time constant described more than 75.3 ± 3.5 % of channel-closing duration. These values were similar in all cases to those obtained with wt receptor. The open probability in clusters was high ($P_O : 0.68 \pm 0.022$, $n = 10$, at $30 \mu\text{M}$). This value is statistically not different from that obtained for wt AChR ($P > 0.05$; see also Fig. 31). In conclusion, the gating kinetics of AChR were not altered by the ϵV448L mutation located within the fourth transmembrane domain of the ϵ -subunit.

The deletion mutation $\epsilon\text{911delT}$, located in the third membrane-spanning segment of the ϵ -subunit, is predicted to truncate the entire M_3 - M_4 – cytoplasmic loop of the subunit (see also Introduction section 1.3.2.3, Fig. 6). Recordings from $\epsilon\text{911delT}$ -containing receptors revealed gating kinetics similar to those observed with $-\epsilon$ AChRs (Fig. 26 vs. Fig. 23 and 24).

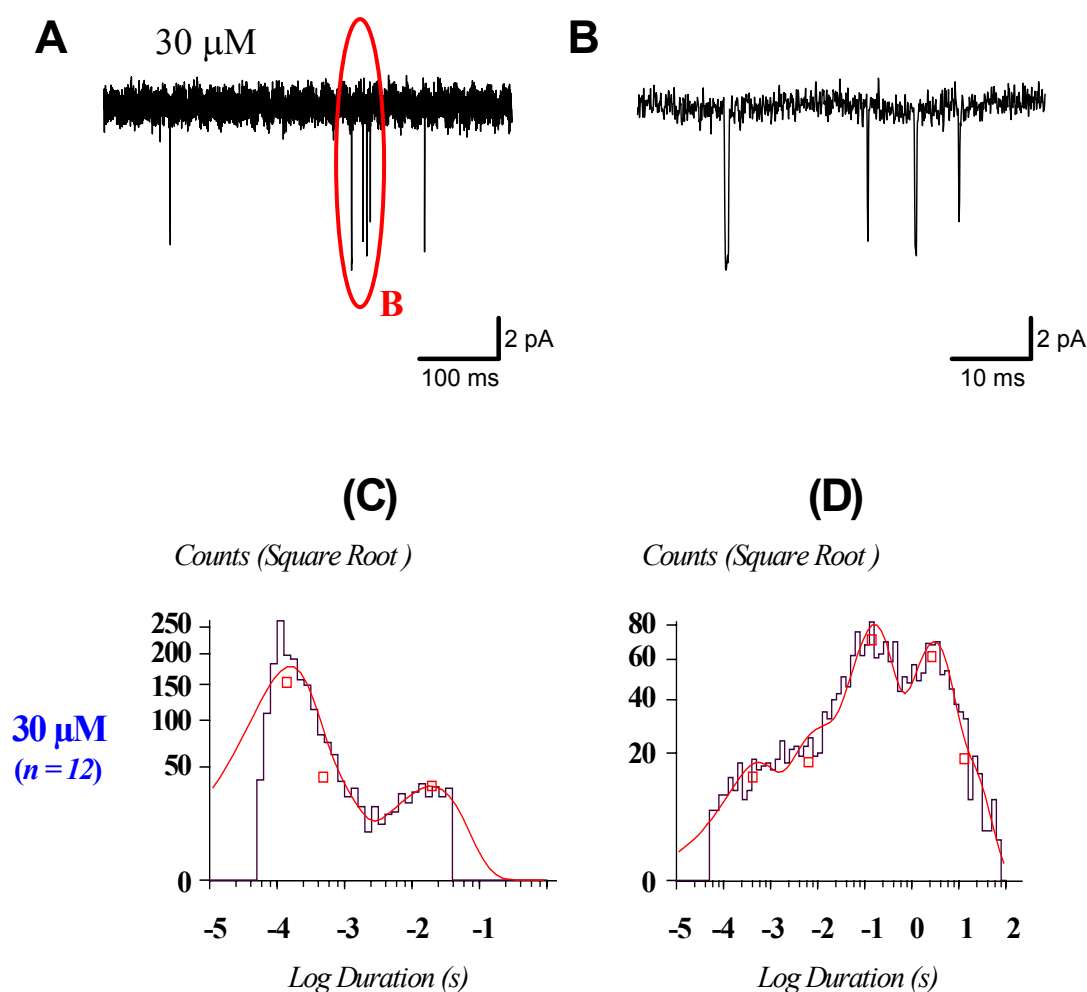


Fig. 26 Single-channel opening events recorded from a $\epsilon\text{911delT}$ AChR, elicited by $30 \mu\text{M}$ ACh (**A** and **B**), and summary of open (**C**) and close (**D**) time distributions; **B** represents the magnification of the encircled area of **A**. Holding potential: -100 mV.

The mutant showed only rarely openings that were very brief in duration ($\text{Tau}_{\text{open1}} : 0.17 \pm 0.01 \text{ ms}$; $n = 12$) in $78 \pm 3.5 \%$ of the apparent open time (Fig. 26 A-C). A second open time constant ($\text{Tau}_{\text{open2}}$) was similar to that observed with $-\epsilon$ receptor at a concentration of $30 \mu\text{M}$. Additionally, $\sim 9 \%$ of the openings were longer than 10 ms ($\text{Tau}_{\text{open3}}$, Fig. 26 C).

The distribution of the channel close times exhibited a reduction in the fraction of closings during burst gating (see $\text{Tau}_{\text{close1}}$ in Fig. 26 D), and the majority of the closings were longer than 30 ms . The open probability within the total recording time for mutant $\epsilon 911\text{delT}$ was $11 \pm 3.8 \cdot 10^{-4}$ ($n = 12$, at $30 \mu\text{M}$; see Fig. 32). Compared to wt receptors, this is almost a 40-fold reduction in the open probability, however, this value is similar to that observed in receptors lacking the ϵ -subunit ($P > 0.05$).

Mutant $\epsilon 1030\text{delC}$ exhibited only few and brief channel-openings at an agonist concentration of $1 \mu\text{M}$ (recording not shown), and spent long periods in the closed state (see Fig. 28). At higher agonist concentrations (30 and $100 \mu\text{M}$ ACh), the frequency of opening / closing events increased. During prolonged recordings, we observed in 3 out of 8 recordings a distinct switch in the gating mode of the receptor, as illustrated in Figure 27.



Fig. 27 Single-channel bursts of openings elicited by $30 \mu\text{M}$ ACh from a $\epsilon 1030\text{delC}$ AChR. The recording shows the switch between the two distinct gating modes during a recording time of 60 s . Holding potential: -100 mV .

The first gating mode (termed as ‘a’) resembled the gating pattern of $-\epsilon$ receptor with brief channel-openings. This had a major open time constant, $\text{Tau}_{\text{open1}}$, of $0.14 \pm 0.01 \text{ ms}$ ($n = 5$, at $30 \mu\text{M}$; Fig. 28 A). The second gating mode (termed as ‘b’) resembled the gating pattern observed with wt AChR, where channel-openings occurred mainly in clusters, with a major open time constant, $\text{Tau}_{\text{open2}}$, of $1.9 \pm 0.62 \text{ ms}$ ($n = 3$; Fig. 28 A). The fractions of channel-openings associated to the two dominant open time constants were similar in all cases to those observed in recordings with either $-\epsilon$ or wt AChRs, respectively.

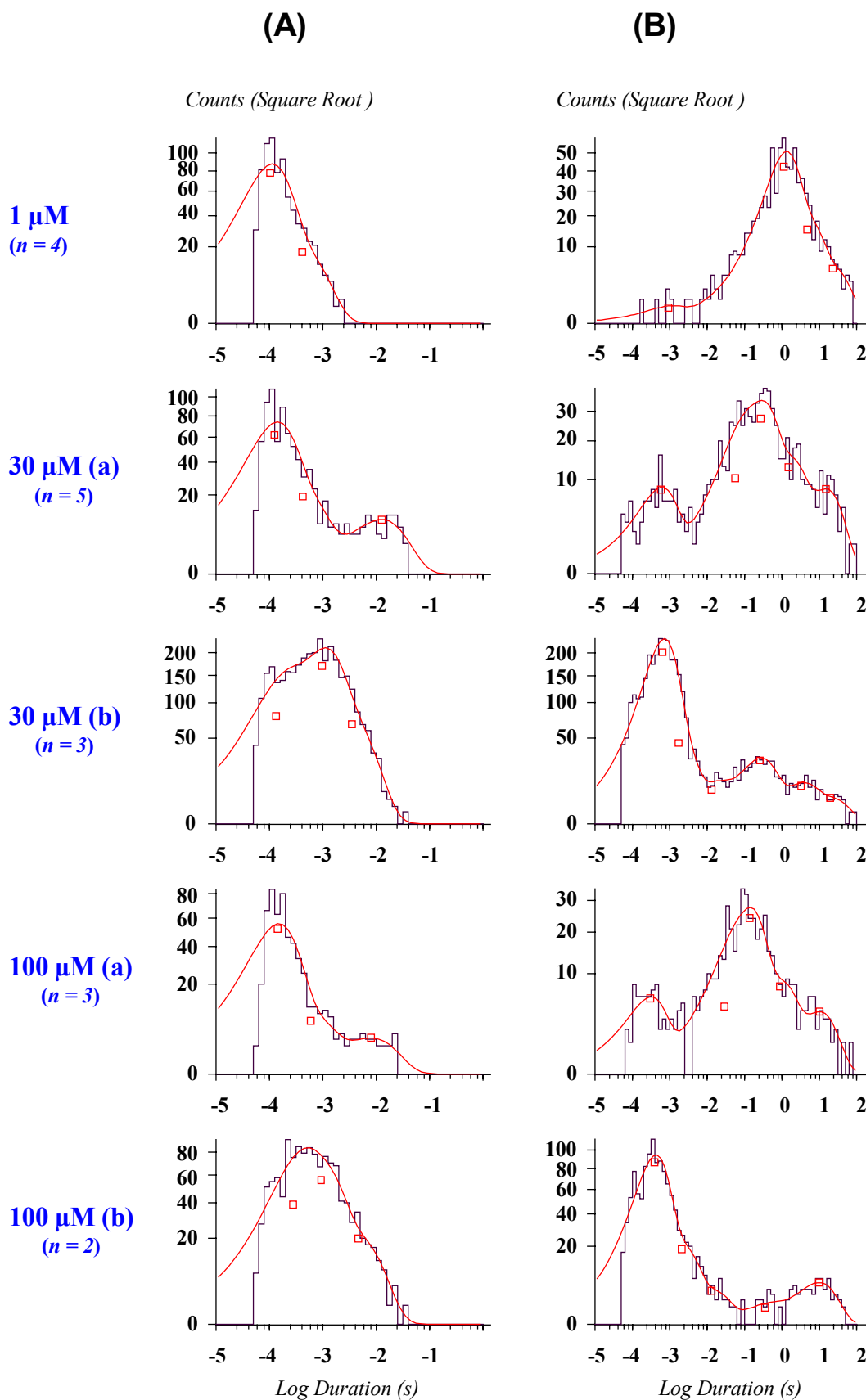


Fig. 28 Summary of open (**A**) and close (**B**) time distributions obtained for the $\epsilon 1030\text{delC}$ AChR at the indicated ACh concentrations; (a) stands for gating pattern with brief events, whereas (b) represents the gating mode with bursts of openings.

However, the $\epsilon 1030\text{delC}$ -containing AChR exhibited in bursts an additional faster open time constant ($\text{Tau}_{\text{open}1} : 0.16 \pm 0.04$ ms), which represented 22 ± 5 % of all apparent open times at $30 \mu\text{M}$ (Fig. 28 A). As mutation caused transient switches between two gating modes in the same recording, it was no surprise to observe the additional faster open time constant in the open time distribution histogram.

The close time distribution of the first gating mode ('a') revealed few closings in bursts, the majority of them being longer than 30 ms (82.54 ± 4.39 %, $n = 5$), as observed with $-\epsilon$ receptor (Table 2).

Type	% Closings > 30 ms	No. of Closings	No. of Openings	Rec. time (min)	n	Comments
WT	1.76 ± 0.46	40407	40528	50	9	
$-\epsilon$	73.87 ± 5.18	2250	2228	48	6	
$\epsilon 1030\text{delC}$	82.54 ± 4.39	167	172	24	5	(a)
$\epsilon 1030\text{delC}$	11.25 ± 1.64	3334	3342	27	3	(b)

Table 2 Percentage of closings between bursts (% Closings > 30 ms) for wt, $-\epsilon$, and $\epsilon 1030\text{delC}$ AChRs, respectively; (a) stands for gating pattern with brief events, whereas (b) represents the gating mode with bursts of openings. ACh concentration: $30 \mu\text{M}$. Holding potential: -100 mV.

In contrast, the gating mode in bursts ('b') exhibited mainly brief channel close times occurring in clusters (~ 80 %), and with increasing of ACh concentration from 30 to $100 \mu\text{M}$, the major close time constant shifted towards shorter durations, from 0.64 ms to 0.39 ms, respectively (Fig. 28 B). Only 11.25 ± 1.64 % ($n = 3$) were interburst closings (Table 2). In this mode ('b'), the receptor exhibited a high open probability that was similar to the one obtained with wt AChR at an agonist concentration of $30 \mu\text{M}$: 0.553 ± 0.06 ($n = 3$) vs. 0.66 ± 0.021 ($n = 9$; Fig. 31). However, the overall number of channel-openings was reduced by ~ 9 -fold compared to wt AChR, during a total recording time of 51 min (Table 2).

Mutant $\epsilon 1101\text{insT}$ exhibited a gating pattern with very brief and infrequent channel-openings (Fig. 29 A and B). The open time distribution revealed a major open time constant, $\text{Tau}_{\text{open}1}$, of 0.14 ± 0.04 ms, which represented 97.6 ± 0.2 % of all apparent open times ($n = 4$; Fig. 29 C). In the close time distribution, only 2 ± 0.9 % ($n = 2$) and 3 % ($n = 1$) were closings within bursts ($\text{Tau}_{\text{close}1} : 0.29 \pm 0.16$ ms; $\text{Tau}_{\text{close}2} : 3.69$ ms; Fig. 29 D). The majority of the closing intervals were longer than 30 ms, and the distribution exhibited a dominant component at ~ 600 ms that accounted for ~ 50 % of all close time durations (Fig. 29 D). The open probability within the total recording time for mutant $\epsilon 1101\text{insT}$ was very low: $1.2 \pm 0.32 \cdot 10^{-4}$ ($n = 4$, at $30 \mu\text{M}$; see Fig. 32).

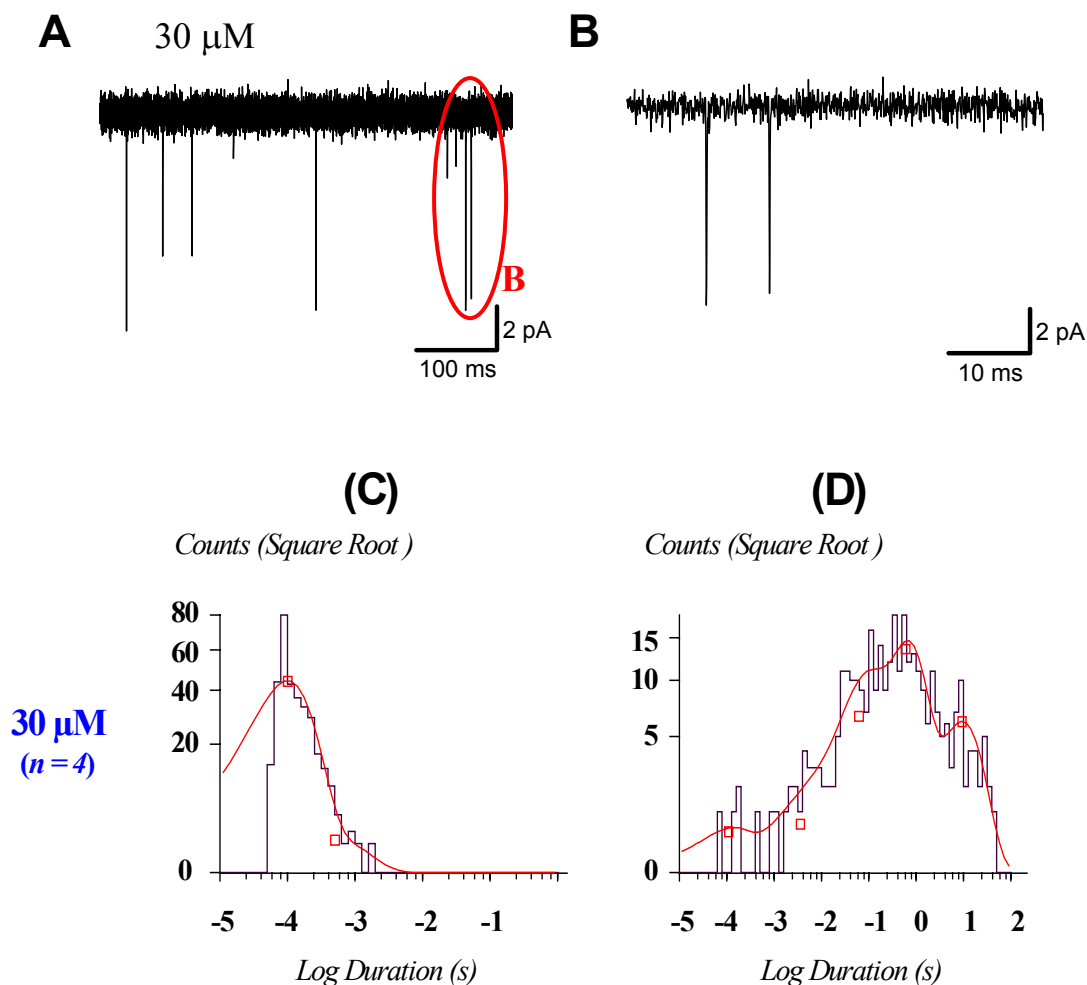


Fig. 29 Single-channel opening events recorded from a $\epsilon 1101\text{insT}$ AChR (**A** and **B**), and summary of open (**C**) and close (**D**) time distributions, obtained at an agonist concentration of 30 μM ; **B** represents the magnification of the encircled area of **A**. Holding potential: -100 mV.

3.2.3.4 The spontaneous activity of AChR

Spontaneous openings of AChR in the absence of ACh have been reported in the literature for mouse, rat, and bovine AChRs (Jackson, 1984, 1986; Jaramillo et al., 1988; Jackson et al., 1990; Zhou et al., 1999a,b; Grosman et al., 2000). To test whether these spontaneous channel-openings also occur in human AChR and to estimate their contribution in our recordings, we performed recordings in the absence of ACh, for wt and ϵ -subunit lacking AChRs.

In the absence of the agonist and within the total recording time, wt and $-\epsilon$ AChRs exhibited very low open probability values of $1.6 \pm 0.6 \cdot 10^{-4}$ ($n = 5$) and $1.3 \pm 0.6 \cdot 10^{-4}$ ($n = 5$), respectively (see Table 3 and Fig. 32). These values were in any case smaller than the values obtained at low ACh concentrations (1 – 10 μM) for both types of receptors (Table 3).

The channel-openings were very brief and had a duration of ~ 0.23 ms in $\sim 84\%$ of all open times (Fig. 30 A-C). Furthermore, twice as many opening events were recorded from $-\varepsilon$ AChR than from wt receptor (630 vs. 315; see also Fig. 30 C).

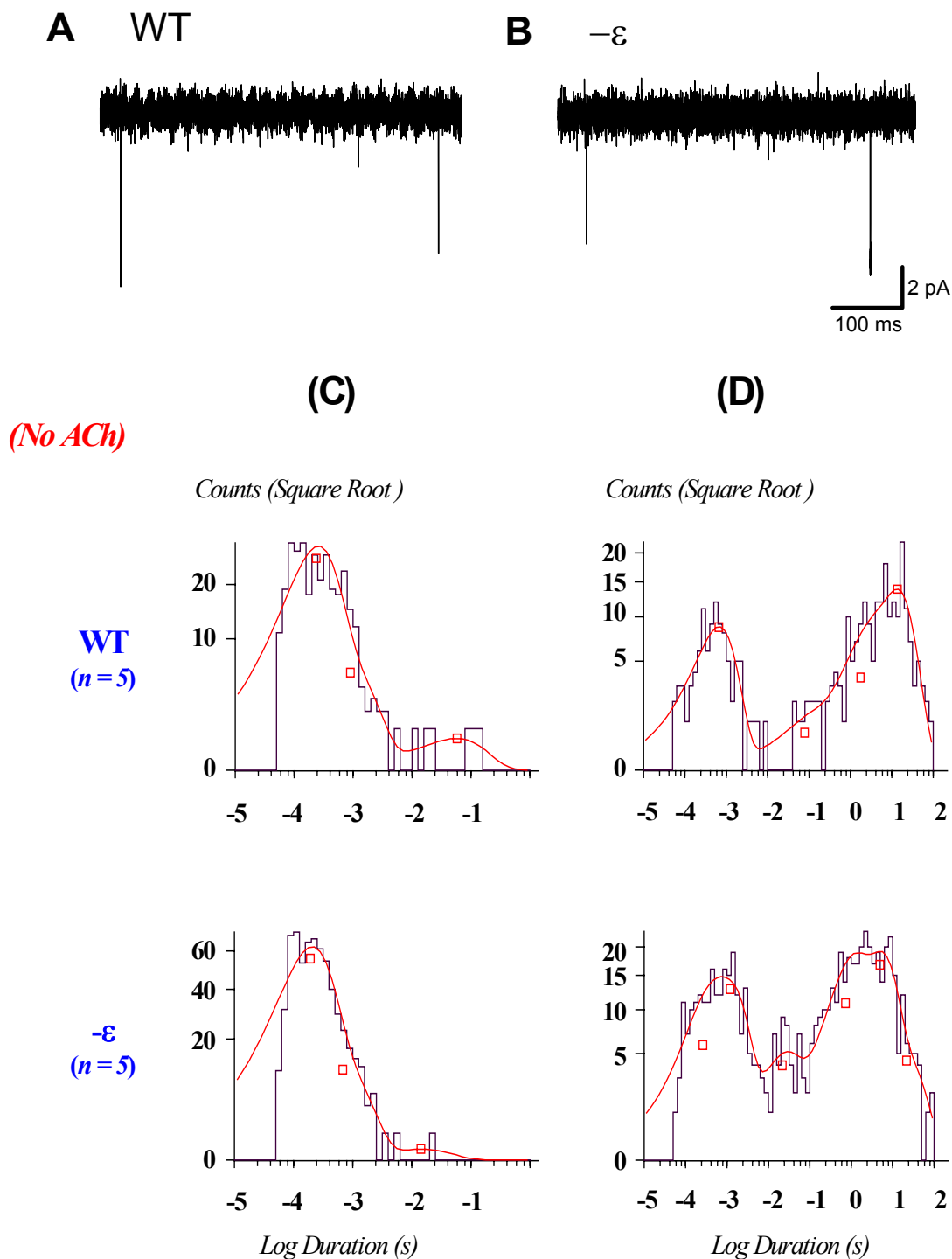


Fig. 30 Spontaneous single-channel opening events recorded from wt (A) and $-\varepsilon$ AChRs (B), respectively. Below, are given the corresponding open (C) and close (D) time distributions. Holding potential: -100 mV.

Interestingly, in the absence of ACh, ~ 32 % of the total close times were short closings with a duration of ~ 0.7 ms, in the case of wt receptor (Fig. 30 D). Some 68 % were closing intervals longer than 1 s. Similar values were obtained for $-\epsilon$ AChR as well ($P > 0.05$; see Fig. 30 D).

Taken together, these findings suggest that the spontaneous opening events in wt and $-\epsilon$ receptors occur even in the absence of ACh, however these openings occur very rarely, and therefore disturb very little our observations at very low ACh concentrations.

Type	[ACh; μ M]	P_o total rec. time	SEM	n	Total rec. time (min)
WT	0	1.60E-04	6.00E-05	5	17
WT	1	7.31E-03	4.46E-03	3	30
WT	10	2.93E-02	4.20E-03	7	24
WT	30	4.32E-02	5.22E-03	9	50
WT	100	2.28E-01	1.06E-01	4	30
$-\epsilon$	0	1.30E-04	6.00E-05	5	20
$-\epsilon$	10	4.56E-04	1.65E-04	4	16
$-\epsilon$	30	9.80E-04	3.50E-04	6	48
$-\epsilon$	100	5.09E-03	1.71E-03	7	39

Table 3 Open probability (P_o) values within the total recording time obtained for wt, and $-\epsilon$ AChRs, in the absence or presence (at the indicated concentrations) of agonist. Holding potential: -100 mV.

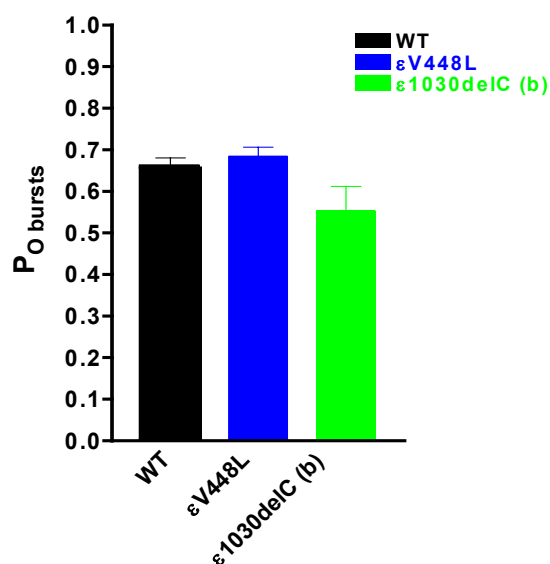


Fig. 31 Open probability (P_o) within bursts (between 0.04 and 30 ms) exhibited by wt, ϵ V448L, and ϵ 1030delC AChRs at an ACh concentration of 30 μ M. Holding potential: -100 mV. In the case of mutant ϵ 1030delC AChR, the P_o value is given for the gating mode with bursts of openings ('b'; $n = 3$ cells).

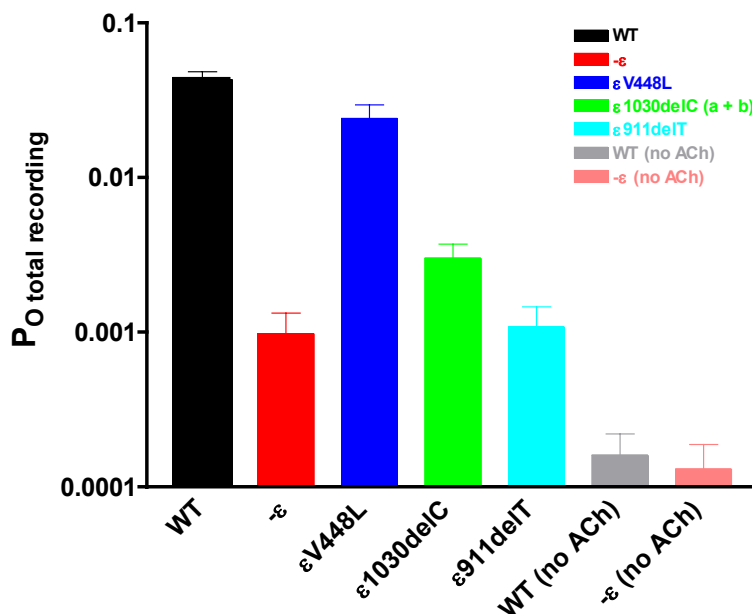


Fig. 32 Open probability (P_O) within the total recording time exhibited by wt, $-\epsilon$, and ϵ -mutant AChRs at an agonist concentration of 30 μM ACh. Holding potential: -100 mV. The P_O values were plotted on a logarithmic ordinate. In the case of $\epsilon 1030\text{delC}$ AChR, the P_O value represents the overall open probability when the receptor switched between the two distinct gating modes ('a' + 'b'; $n = 8$ cells), during a total recording time of 51 min.

3.2.4 The correlation between the whole-cell- and the single-channel data

As mentioned in Materials and Methods section 2.3.1.1.2, we introduced the current density (pA / pF) parameter, as a normalization of current responses to the cell surface. We did this, to correct for variation in current magnitude due to differences in cell size. On examining the data, we observed that the current density values obtained for $-\epsilon$, and ϵ -mutant AChRs were significantly reduced in comparison to wt receptor (Table 4 A and Fig. 17).

In whole-cell configuration, the recordings are taken from large populations of channels ($I_{max} = N \cdot P_O \cdot i$, see section 3.1.1). It was therefore difficult to tell if the reduction in the current density was a contribution of one or a combination of the parameters, number of functional channels (N), open probability (P_O) and / or unitary current (i).

To address this question, we have further investigated the ϵ -mutant receptors at single-channel level. A comparison of the data obtained in whole-cell- and single-channel mode is shown in Table 4.

The number of cells transfected with wt and ϵ -mutant AChRs, which responded to ACh application in whole-cell configuration was very similar to the values calculated from single-channel recordings (compare Table 4 A with 4 B). These data indicate that the ϵ -mutations

from our study did not reduce the current density by altering the number of functional channels that responded to agonist application. Furthermore, the unitary current values were similar in all cases, suggesting that mutations did not affect the size of the ion flux through the open channel (see Results section 3.2.2).

(A)

Type	% of cells resp. to ACh	No. of cells tested	Current density (pA / pF)
WT	53	160	292.53 ± 9.08
-ε	29	95	36.46 ± 2.64
εV448L	50	24	223.29 ± 29.96
ε1030delC	41	70	82.85 ± 11.2
ε911delT	19	74	13.57 ± 1.83
ε1101insT	28	36	65.47 ± 14.81

(B)

Type	% of cells resp. to ACh	No. of cells tested	$P_{O \text{ total rec. time}}$	$P_{O \text{ bursts}}$	i (pA)	$I_{\text{max bursts}}$
WT	68	246	0.0432	0.66	7.24	4.77
-ε	39	134	0.0010	-	7.73	-
εV448L	64	33	0.0241	0.68	6.56	4.49
ε1030delC	45	186	0.0030	0.55	8.01	4.43
ε911delT	36	73	0.0011	-	6.44	-
ε1101insT	36	22	0.0001	-	8.54	-

Table 4 The correlation between the whole-cell- and the single-channel data. The current density (pA / pF ± SEM) values inferred from whole-cell recordings are given in **A**. The macroscopic current (I_{max} , pA) values calculated from single-channel recordings are given in **B**. P_O and i (pA) values were obtained at an ACh concentration of 30 μM and a holding potential of -100 mV.

In terms of the last analyzed parameter, P_O , mutants ε911delT and ε1101insT showed during the total recording time similar low open probabilities ($P_{O \text{ total rec. time}}$) as the -ε receptor (Table 4 B, and also Fig. 32). Most of the opening events recorded from both occurred as isolated events and very few of them were clustered. This is why in their case we could not calculate the open probability in bursts ($P_{O \text{ bursts}}$).

Additionally, the mutant εV448L opened mainly in bursts with a gating pattern similar to wt receptor (Table 4 B, and Fig. 31), and therefore its current density value was statistically not different from that of the latter (Table 4 A). The mutant ε1030delC, which switched between bursts and isolated opening events, exhibited a $P_{O \text{ total rec. time}} \sim 15$ -fold smaller than that of wt AChR, and ~ 3 -fold larger than observed with -ε receptor (Table 4 B).

In conclusion, our findings suggest that the drastic reduction of the current density with the AChRs carrying the ε-truncating mutations is very likely to be the result of the low probability of channel-opening.

3.2.5 Summary of the single-channel data

As observed, the mutants expanded to some extent the distributions for channel-opening and closing time constants. Thus, inspection of the open and close time distributions revealed briefer opening events and prolonged closings for ϵ -mutant receptors compared to wild-type receptors. Only mutant ϵ V448L showed gating kinetics similar to wt receptor. Mutant ϵ 1030delC exhibited kinetic components of both, the individual wt and the ϵ -subunit lacking AChRs. Mutants ϵ 911delT and ϵ 1101insT showed gating kinetics similar to $-\epsilon$ AChR.

The low open probability exhibited by the individual receptors carrying the ϵ -truncating mutations is most probably responsible for the significant reduction of their current density observed in whole-cell recordings.

4 Discussion

4.1 CMS mutations and their localization

Mutations in the AChR ϵ -subunit gene are the most common cause of congenital myasthenic syndrome (CMS) characterized by deficiency of AChR at the motor endplate (Engel et al., 1996a; Ohno et al., 1997; Ohno et al., 1998a,b; Middleton et al., 1999; Croxen et al., 1999; Abicht et al., 1999; Abicht et al., 2000; Sieb et al., 2000a,b; Croxen et al., 2001). The mutations are found along the length of the ϵ -subunit gene, including the promoter region (Nichols et al., 1999; Ohno et al., 1999; Abicht et al., 2002), and result in frameshifts or nonsense codons that truncate the subunit polypeptide chain. This results in loss of residues essential for AChR assembly or function.

In the present study, we investigated two recently by Sieb and colleagues (2000a) identified mutations in the ϵ -subunit gene, ϵ 911delT, and ϵ 1030delC. These mutations are located at the end of the M₃ transmembrane domain and in the cytoplasmic loop between TM3-4, respectively. We were interested in investigating the molecular mechanism underlying AChR deficiency in these cases since ϵ -subunits expressed from these mutant alleles contain domains thought to be essential for AChR function.

The functional consequences of these mutations were investigated using patch-clamp recordings in whole-cell- and cell-attached configuration. Three related CMS-linked mutations all located in the TM3-4 cytoplasmic region, ϵ 1101insT, ϵ 1206ins19 and ϵ 1293insG, were included in the study to identify the role of specific regions in TM3-4 loop in AChR function. All mutations are frameshifting and are predicted to truncate the ϵ -subunit of AChR, generating a protein product with impaired functionality.

A common finding for all mutations located within the TM3-4 loop was a functional reduction of the underlying receptor via two mechanisms: reduction in number of receptors expressed on the cell surface and interference with channel-gating. In addition, mutant ϵ 1030delC introduced a switch in the gating mode of the receptor with characteristics resembling those of wt, as well as ϵ -subunit lacking AChR, while mutation ϵ 911delT, located at the end of TM₃, completely prevented formation of functional receptors.

4.2 *Structure, formation and membrane insertion of the AChR*

The AChR belongs to the ligand-gated ion channel superfamily that shares many structural features. These pentameric receptors are usually comprised of several different subunits arranged in a circle like structure to form a central pore, the ion channel (Karlin, 2002; see Introduction section 1.2.1.1). Within the endoplasmic reticulum (ER), the different subunits of the receptor are assembled and processed to the mature protein. The ability to distinguish between correctly assembled receptors and intermediate-building steps is of utmost importance to ensure reliable and stable signal transduction processes. Incorrectly folded proteins cannot be assembled and are retained and degraded within the ER, and only physiological active complexes with the correct stoichiometry are transported to the cell surface (Smith et al., 1987; Verrall et al., 1992; Blount et al., 1990; Gu et al., 1991). The AChR is comprised of four different subunits with a stoichiometry of $2\alpha_1\beta_1\gamma\delta$ for the fetal form, and $2\alpha_1\beta_1\epsilon\delta$ for the adult form of the receptor. Within the ER, the receptor is assembled in a step-like fashion where the $\alpha_1\text{-}\delta$, $\alpha_1\text{-}\gamma$ and $\alpha_1\text{-}\epsilon$ subunits form heterodimers that interact with the β_1 subunit to form the final pentameric structure. In skeletal muscle, assembly of AChR is an inefficient process and more than 90 % of newly synthesized AChR subunits are incorrectly folded (Smith et al., 1987; Gu et al., 1991). Single or incomplete associated subunits are retained within the ER and degraded (Smith et al., 1987; Merlie et al., 1983; Blount et al., 1990). Further, transport of all subunits to the cell surface is prevented if transcript for the α -subunit is erroneous (Black et al., 1987; Gu et al., 1989). A vital point for regulation of cell surface expression is the control of exit from the ER, however, currently little is known about the regulation of these steps. Recently, Wang et al. (2002) identified a conserved signal sequence (PLYFxxN motif) within the M_1 domain of all AChR subunits that controls incorporation of the mature functional protein into the cell membrane. In fully assembled pentamers, the signal sequence is hidden inside the protein (close to the pore-forming region) and allows transport to the cell surface. In contrast, if the signal sequence is accessible to the lumen, these subunits will not be assembled and are subject to degradation. The signal sequence therefore serves as quality control in the process of receptor formation and membrane insertion.

Several structural elements within the ϵ -subunit have been identified that may influence function of the receptor by controlling interaction with other subunits or translocation to the cell membrane. Recent studies on the AChR ϵ -subunit resulted in the proposal that the N-terminal domain mediates the initial subunit associations, whereas signals in its C-terminus

half are required for subsequent subunit interactions (Eertmoed and Green, 1999). In addition, studies of a three amino acid deletion in the β -subunit have identified a region in the cytoplasmic loop between M₃ and M₄ where the secondary structure is crucial for interaction between the β - and δ -subunits (Quiram et al., 1999).

A single cysteine residue within the carboxyl-terminal region at position 470 was recently identified by Ealing and co-workers (2002) and has been suggested to play a crucial role in surface expression of adult AChR. Robust surface expression was seen only when the ϵ -subunit contained the C470 residue but was completely lost when C470 was deleted or mutated to serine (S470). Fluorescent labeling of the ϵ -subunit showed that the mutant ϵ -subunits 1369delG or C470S are retained within the ER. The interaction partner(s) of the C-terminus ϵ C470 are currently not known. The authors suggested that the loss of ϵ C470 partially reduces the efficiency of the steps involved in the initial α - ϵ subunit association and affect subsequent steps in pentamer assembly, transfer from the ER and incorporation into the plasma membrane. It is further possible that C470 might be involved in formation of a disulphide bond in addition to that of the N-terminal extracellular cysteine-loop structure that is common to all members of this ion channel superfamily. Ealing et al. (2002) concluded that all truncating mutations that occur before position C470 would lead to a complete loss of the AChR protein. The findings from the present study do not support this hypothesis.

4.3 Mutation ϵ 911delT in the M₃ segment leads to loss of function

Aim of the work was to gain insights into the molecular mechanism underlying AChR deficiency in postsynaptic CMS due to truncating mutations of the ϵ -subunit. The initial characterization of human wild-type muscle AChR ($2\alpha_1, \beta_1, \epsilon, \delta$) and the ϵ -subunit lacking AChR ($2\alpha_1, \beta_1, \delta$) set the framework that allowed the interpretation of functional effects of the CMS mutations.

AChRs lacking the ϵ -subunit could be easily distinguished from wt receptors based on their biophysical properties (largely reduced current density, rapid desensitization kinetics, complete desensitization). On the single-channel level, the AChR lacking the ϵ -subunit exhibited a different gating pattern compared to wt receptor. The number of opening events was about 40-fold reduced and the open channel duration was only 1/5 of that observed with wt AChR (see Results section 3.2.3.2). In contrast, the single-channel conductances for wt and $-\epsilon$ AChRs were very similar, with a value of 61 pS. Similar values have been previously reported for wt human muscle AChR (Newland et al., 1995; Ohno et al., 1997). A larger

conductance of 78 pS has been reported for mouse AChR (Ohno et al., 1995) and it is very likely to be due to species differences (but see below section 4.4.1).

The AChR that contained the frameshifting mutation in transmembrane domain 3 - $\epsilon 911\text{delT}$ - exhibited biophysical properties that resembled those observed with AChR lacking the ϵ -subunit. The current density of $\epsilon 911\text{delT}$ -containing receptors was below that seen with ϵ -lacking AChR, suggesting a severe interference with cell surface expression of the receptor. Single-channel recordings further revealed biophysical properties for $\epsilon 911\text{delT}$ similar to those observed with ϵ -lacking AChR, indicating a loss of function of the receptor containing the mutated ϵ -subunit. The deletion $\epsilon 911\text{delT}$ leads to a frameshift in the predicted amino acid sequence, causing a premature stop codon after 60 missense codons, and would preserve only the first 15 amino acids of the large intracellular loop. This would indicate that critical elements controlling receptor formation / expression are located downstream of position 911. The data suggest that homozygous expression of $\epsilon 911\text{delT}$ is very likely to result in a loss of function. To date, no case report of a homozygous presence of mutation $\epsilon 911\text{delT}$ has been published.

Patients that are heterozygous for mutation $\epsilon 911\text{delT}$ show marked reduction in the number of secondary synaptic clefts in association with reduced AChR density at the neuromuscular junctions with signs of a myasthenic syndrome (Sieb et al., 1998). Affected family members were heteroallelic for the $\epsilon 911\text{delT}$ and $\epsilon \text{IVS4} + 1\text{G} \rightarrow \text{A}$, a splice-site mutation at the junction between exon 4 and intron 4 (Sieb et al., 2000a). The latter produces a stop codon at the N-terminal loop that results in loss of all four transmembrane segments of the ϵ -subunit. These findings would support the idea that homozygous expression of $\epsilon 911\text{delT}$ is very likely to result in a severe myasthenic phenotype.

4.4 Mutations within the TM3-4 cytoplasmic loop

4.4.1 Mutation $\epsilon 1101\text{insT}$

Mutation $\epsilon 1101\text{insT}$ leads to a shift in the reading frame and the production of a stop codon that truncates 2/3 of the cytoplasmic loop between TM_3 and TM_4 , as well as the remaining C-terminus part. The AChRs containing the $\epsilon 1101\text{insT}$ mutation were functional but showed a reduction in current density to $\sim 22\%$ of wt receptor level. This finding is in line with previous studies, showing an approximately 4-fold reduction in α -bungarotoxin binding to AChR carrying the $\epsilon 1101\text{insT}$ mutation compared to wt receptor (Engel et al., 1996a; Sieb et

al., 2000b). In single-channel recordings, ϵ 1101insT AChR exhibited very short open lifetimes, and long closing intervals, as well as reduced open probability compared to wt AChR. Our findings appear to be in contrast to a previous study by Engel et al. (1996a) on the same mutation ϵ 1101insT, which had apparently no influence on the kinetic properties of the receptor. The discrepancy between the results of the two studies of mutant ϵ 1101insT could arise from species differences, as in the study by Engel et al. (1996a) the mutation was investigated in *mouse* AChR. In fact, the same group showed that *human* and *mouse* AChR containing ϵ L296F exhibit significant differences in single-channel gating properties (Engel et al., 1996b). The ϵ -subunit mutation L296F, when introduced in *mouse* AChR, resulted in an approximately 3-fold reduction in channel open duration compared to that obtained from *human* AChR. Similarly, species-related functional differences have been described for epithelial Na^+ channels. In a structure-function study of *human* epithelial Na^+ channels (ENaC), Snyder and co-workers (1999) performed a cysteine screen of the pore-lining regions of α , β and γ -subunits. For position β G520C, they reported a strong inhibition by a thioreactive agent (MTSET) that resulted from covalent modification of the introduced cysteine. In contrast, *mouse* epithelial Na^+ channels carrying the corresponding cysteine modification (β G525C) showed no modulation by MTSET (Li et al., 2003).

The findings with ϵ 1101insT AChR provide evidence that the C-terminus, that includes residue C470, is not crucial for maturation and functional expression of the AChR as proposed by Ealing et al. (2002). In the study by the latter, truncation of the C-terminus up to amino acid 470 resulted in retention of the protein within the ER. These truncated proteins still contained the full TM3-4 loop and the complete TM₄ segment. As ϵ 1101insT-containing AChRs form functional channels, it is possible that parts of the TM₄ segment or the TM3-4 loop, that are still present in the C470 mutant, allow interaction with structural elements within the ER that cause the retention of the receptor.

4.5 Structural elements within the TM3-4 loop that influence channel-gating

4.5.1 Role of mutations ϵ 1293insG and ϵ 1206ins19

The M₃-M₄ cytoplasmic loop of the ϵ -subunit is the least conserved structure of all AChR subunits. Several studies have investigated the role of an amphipathic α -helix (HA) that is located at the C-terminus of the M₃-M₄ cytoplasmic loop (Finer-Moore and Stroud, 1984; Bouzat et al., 1994; Milone et al., 1998a; Akk and Steinbach, 2000; Wang et al., 2000). The

HA region extends from residues 376 to 435 of the homologous human ϵ -subunit, and displays stripes of hydrophobic and positively and negatively charged residues along its length. The actual location of the HA region with respect to the membrane or the rest of the cytoplasmic loop is not known. Recently, a projection from the cytoplasmic side of each subunit has been identified that has helical content, so it may be that the HA region projects into the cytoplasm and interacts with the intracellular loops from other subunits as well (Miyazawa et al., 1999).

This region has significant impact on the gating properties of the associated receptor. First evidence was presented by Bouzat et al. (1994) showing that the gating properties of AChR could be modulated by the HA region of the ϵ -subunit. Gating of AChR could be switched from “adult” (short opening, fast channel-closing) to “fetal” (long opening, slow channel-closing) gating pattern, when the HA region within the ϵ -subunit was replaced by that of the γ -subunit. Two additional fast-channel mutations that have been identified in CMS patients are located in HA region. One of these is an in-frame duplication of the six residues, STRNQE (ϵ 1154ins18; Milone et al., 1998a), and the other is a point mutation, ϵ A411P (Wang et al., 2000). Both mutations corrupt the fidelity of gating of the receptor channels so that they open and close with irregular kinetics. The tandem duplication causes abrupt switches between efficient and inefficient channel-gating with individual activation modes. Such changes in gating modes are very uncommon and usually not observed in normal receptors. In contrast, mutation ϵ A411P does not cause mode switching within individual activation episodes, but instead results in activation episodes with a large range of open probabilities. These mutants show, in addition to the loss in gating fidelity, a marked reduction in receptor expression (Milone et al., 1998a; Wang et al., 2000), and both features jeopardize the safety margin of neuromuscular transmission.

Two of the truncating mutations investigated in the present study, ϵ 1206ins19 and ϵ 1293insG, are located within the HA region of the long cytoplasmic loop. Similar to the changes in gating properties described above, the two mutations showed in whole-cell recordings altered biophysical properties with speed-up in the time course, as well as enhanced degree of receptor desensitization. As neither one of the mutations has been characterized on the single-channel level, it remains speculative what the underlying mechanism for the observed kinetic changes might be.

In addition to the alterations in channel-gating, the two mutants also caused a marked reduction in current density, however, significantly above the level observed with ϵ -subunit lacking AChR. If the reduction in current density is the result of alteration in channel-gating

or reduction in the number of receptors expressed on the cell surface is unclear. Previous studies showed an approximately 4-fold reduction in α -bungarotoxin binding of ϵ 1206ins19 and ϵ 1293insG AChR, respectively (Ohno et al., 1998b; Engel et al., 1996a; Croxen et al., 2001), suggesting a reduction in surface expression. This might be the reason why no single-channel activity could be recorded from cells expressing ϵ 1293insG AChRs (Engel et al., 1996a).

In addition to changes in channel-gating and surface expression, mutant ϵ 1293insG also reduced the receptor sensitivity to ACh by approximately 5-fold. It is likely that the observed change in ACh affinity is due to a change in ACh association or dissociation constant. Previous studies from CMS patients with slow-channel syndrome identified two mutations within the α -subunit that enhance ACh affinity of the receptor (Engel et al., 1996b; Milone et al., 1997). The mutations N217K and V249F are located within TM₁ and TM₂ of the α -subunit, respectively, quite distant to the ACh binding site. The increase in ACh affinity by these mutations is mainly due to a reduction in the ACh dissociation rate constant (Engel et al., 1996b; Milone et al., 1997). The location of ϵ 1293insG within the TM3-4 loop is even further away from the ACh binding site and would suggest that these mutations may exert their effect through structures that link the channel gate to the binding site.

4.6 Mutation ϵ 1030delC elicits switch in gating pattern

Mutation ϵ 1030delC leads to a shift in the reading frame and produces after 20 residues a stop codon. The resulting protein carries only 1/3 of the cytoplasmic loop between TM₃ and TM₄. Similar to the above-described mutants, ϵ 1030delC also affected gating properties and current density of the underlying receptors. The latter was reduced to \sim 1/3 of wt receptor level.

In the whole-cell mode, the mutant exhibited gating kinetics with two patterns. At low agonist concentrations ($< 1 \mu\text{M}$), the time course of desensitized receptors was substantially slower than that of ϵ -lacking receptors (see Fig. 16 A), whereas at higher agonist concentrations the time course was indistinguishable from that of the latter. This change in speed of desensitization was even more pronounced for wt AChR, whereas for $-\epsilon$ receptor only marginal. In single-channel recordings, mutant ϵ 1030delC exhibited switches in the gating kinetics between two distinct modes within individual activation episodes. The two modes resembled properties observed with wild-type (channel-openings that occurred in bursts with high open probability) and ϵ -lacking AChRs (brief and isolated opening events), respectively. This switch in the gating mode might explain the different kinetic pattern in desensitization

kinetics. It is very likely that at higher agonist concentrations, the gating mode corresponding to the $-\epsilon$ receptor is prevailing, whereas at lower concentrations a mixture between wt and $-\epsilon$ receptor gating is prevailing.

Switches in gating mode have so far only been reported for mutations located within the HA motif of the TM3-4 cytoplasmic loop (see above). The findings with $\epsilon 1030\text{delC}$ suggest that also other regions within the TM3-4 loop may influence the gating properties of the receptor. The overall changes in TM3-4 structure that are caused by these mutations are presently unclear. Taken together, the findings suggest that part(s) of the cytoplasmic loop are able to interact with the gating machinery of the receptor and influence the gating process. A systematic study of the individual residues within the TM3-4 loop may enhance our understanding in the contribution of individual TM3-4 regions in channel-gating.

To date, there is no report of a patient found to express $\epsilon 1030\text{delC}$ homozygous. The functional consequences of $\epsilon 1030\text{delC}$ would predict loss of function in the underlying AChR. The identified affected patient was heterozygous for $\epsilon 1030\text{delC}$ and a mutation $\epsilon R64X$, a truncating mutation within the first third of the N-terminus (Ohno et al., 1997). Muscle biopsies from this patient showed reduction in ACh binding sites, paucity of the secondary synaptic clefts, as well as reduced endplate size (Sieb et al., 2000a). The parents, each of them carrying one mutation, neither were affected nor exhibited morphological changes. This would suggest that in a heterozygous situation the predicted loss of function by either $\epsilon 1030\text{delC}$ or $\epsilon R64X$ could be compensated by the healthy allele. However, when both alleles carry predicted loss of function mutations, the inherent rescue by the fetal γ -subunit is not sufficient to compensate for the functional loss.

4.7 Outlook for treatment of CMS patients

In patients carrying such CMS truncating mutations, the number of AChRs available at the postsynaptic regions of the motor endplate drastically decreases upon sustained muscular activity, as the mutant receptors desensitize more rapidly and in greater numbers, during prolonged exposure to ACh. Additionally, because of the low open probability, the markedly attenuated postsynaptic response to ACh compromises the safety margin of the neuromuscular transmission. All this finally leads to generalized weakness and fatigability of voluntary muscles including those controlling movement, eye movement, swallowing, and breathing. Increasing the postsynaptic response is therefore a suitable therapy. Indeed, these CMS patients generally respond well to the combined use of 3,4-diaminopyridine (3,4-DAP), which

increases the number of quanta released by nerve impulse, and to anticholinesterases, which increase the availability of ACh in the synaptic cleft. The synaptic transmission is enhanced as follows: 3,4-DAP selectively blocks the voltage-gated K^+ channels, and that prolongs the nerve action potentials. As a result, the voltage-gated Ca^{2+} channels remain activated for longer periods, and that allows greater influx of Ca^{2+} at the presynaptic terminal. Theoretically, this chain of physiological events results in additional ACh release. Pyridostigmine (Mestinon) is the most commonly used acetylcholinesterase inhibitor. It reversibly binds to acetylcholinesterase enzyme and slows the breakdown of ACh, raising its concentration at the junctional folds and increasing its probability of remaining attached to functional receptors. This leads to endplate potentials (EPPs) with a more rapid rise time, higher amplitude and thus a greater likelihood of generating action potentials in previously blocked muscle fibers. Patients with a normal density of AChRs on the junctional folds respond best, as a decreased density of receptors on the folds entails a proportionate reduction in the number of AChRs that can be activated by any given quantum (Engel et al., 2003b). All these demonstrate how understanding of fundamental mechanistic steps that are altered in the disease can lead to rational clinical therapies.

4.8 Summary

In summary, with one exception, namely ϵ V448L AChR, all the investigated mutants exhibited acceleration of the desensitization decay and increase in the degree of desensitization, as well as reduced current density compared to wt receptor. Furthermore, the mutations did not affect the size of the ion flux through the open receptors (the *slope conductance*), and only slightly reduced the percentage of cells expressing individual AChRs. Receptors carrying the ϵ -truncating mutations opened mainly with brief and isolated events, similar to ϵ -lacking receptor, and exhibited very low probability of opening in clusters. Only mutant ϵ 1030delC induced switches between the kinetic modes of wt and $-\epsilon$ AChRs, however the majority of the events were brief and isolated. The reduction in the overall number of opening events is very likely to be the main factor that accounts for the reduced current density observed with the ϵ -mutant receptors from the present study.

From all mutations, only deletion mutation ϵ 911delT, located at the end of TM₃, completely prevented formation of functional receptors, whereas in the presence of the other truncating mutations, the AChRs were still functional but exhibited altered kinetic properties as described above.

The present findings are consistent with the notion that mutations causing postsynaptic CMS due to AChR deficiency are concentrated in the ϵ -subunit of the receptor. There are two possible reasons for that: one likely reason is that persistent low-expression level of the embryonic γ -subunit-containing AChR can partially compensate for the absence of the ϵ -subunit (Engel et al., 1996a,b; Ohno et al., 1997; Milone et al., 1998b; Croxen et al., 2001). Patients harboring null mutations in subunits other than ϵ might not survive due to the lack of a substituting subunit. In addition, the gene encoding the ϵ -subunit, and especially exons encoding the long cytoplasmic loop, has a high GC content (61.2 %) that could predispose to DNA rearrangements (Middleton et al., 1999).

Appendix

The patch-clamp technique

i. General remarks

The patch-clamp technique is an extremely powerful and versatile method that allows the recording of macroscopic whole-cell- or microscopic single-channel currents flowing across biological membranes through ion channels. With no other technique, it is possible to observe the functioning of a single protein molecule in a lipid bilayer. Neher and Sakmann applied this technique (starting with 1976) to record for the first time ion currents through single channels in cell membranes, in the pico-Ampere range ($1 \text{ pA} = 10^{-12} \text{ A}$). Since then, several developments improved its applicability to virtually all biological preparations such as animal and plant cells, bacteria, yeast and cell organelles. Others had measured similar single-channel events in reconstituted lipid bilayers. For their discovery and development of this technique and its vast applicability, Neher and Sakmann were awarded the 1991 Nobel Prize in Physiology or Medicine (see the Nobel Lectures: Neher, 1992; Sakmann, 1992). In patch-clamp experiments, a small patch of membrane is tightly sealed to a $1 \mu\text{m}$ diameter glass micropipette tip, allowing the measurement of membrane potential or membrane current across the patch of membrane (Fig. I).

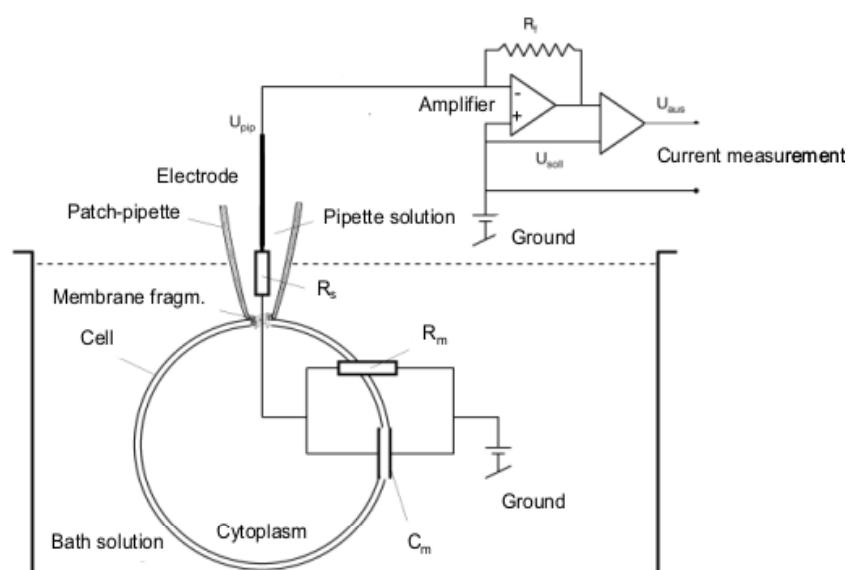
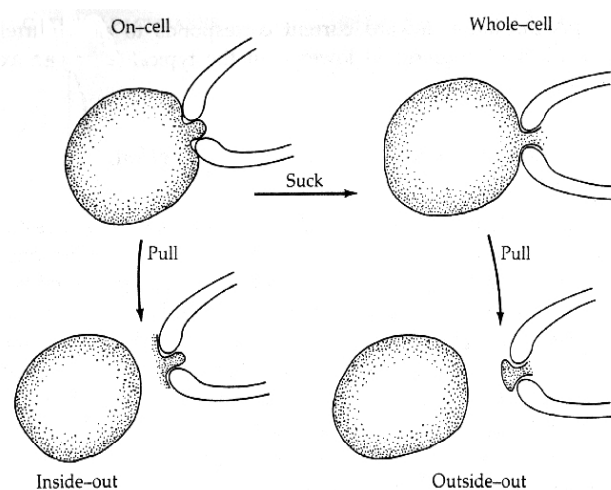


Fig. I A simple scheme of a patch-clamp experiment.

If the piece of membrane contains a single channel, then the currents through that individual channel dominate the measured current across the membrane patch. Observations of single-channel recordings give insight into the mechanisms responsible for transmembrane currents. Paired with cell and molecular biological approaches, the patch-clamp technique constitutes an indispensable pillar of modern cell biology. There are two approaches of this technique: one is the **voltage-clamp** procedure, that applies a voltage across the cell membrane and the resulting current is a direct measure of ion movements across a known membrane (Fig. I). The second approach is the **current-clamp** procedure, in which a current is applied as a stimulus and the ensuing changes in membrane potential are measured.

ii. Five patch-clamp measurement configurations

Neher and Sakmann and their co-workers soon discovered a simple way to improve the patch-clamp recording technique. They used glass pipettes with super-clean ("fire-polished") tips in filtered solutions and applied slight under-pressure in the pipette. This procedure caused tight sealing of the membrane against the pipette tip measured in terms of resistance: $G\Omega$ sealing, (giga = 10^9). This measurement configuration is called **cell-attached patch (CAP)** (Fig. II), which allowed the recording of single-channel currents from the sealed patch with the intact cell still attached. The cell-attached measurement leaves the cell largely intact, and allows one to observe channels open and close, or to record action potentials extracellularly.



(Modified from Hamill et al., 1981)

Fig. II Patch-clamp configurations.

This giga-seal procedure allowed Neher and Sakmann and their co-workers to obtain three other measurement configurations, including one for intracellular voltage- and current-clamp:

while maintaining the tight seal, a short pulse of suction or voltage breaks the membrane patch between the pipette solution and the cytoplasm (Hamill et al., 1981), without loss of the glass-to-membrane seal. Thus, an electrical connection is established between measuring pipette and cell, with the pipette-cell assembly well insulated against the outside bath. In this so-called **whole-cell (WC)** configuration (Fig. II), the applied pipette potential extends into the cell to voltage-clamp the plasma membrane. There is rapid diffusional exchange and equilibration between patch pipette and cell (Neher et al., 1983; Pusch and Neher, 1988). This provides control over the composition of the medium inside the cell. A cell can easily be loaded with ions, chelators, second messengers, fluorescent probes, etc., simply by including these substances in the measuring pipette (Neher, 1992). However, this exchange also implies that the internal milieu is disturbed, and that signaling cascades may be disrupted, because the contents of the recording pipette solution will begin to alter the composition of the cell cytoplasm (Hille, 2001). Alternatively, the amplifier could be used to inject current into the cell to current-clamp the cell membrane and to record voltage, for example to study action potentials of small excitable cells. Another achievement of the WC-configuration was the possibility to perfuse the intracellular compartment with the defined pipette solution. Although the WC-clamp configuration is no longer a clamp of a small membrane patch, electrophysiologists continued to refer to the WC-clamp configuration as a variant of the patch-clamp technique, probably because the WC-clamp starts with giga-sealing a small membrane patch. The giga-seal cell-attached patch, sometimes called an "on-cell" patch, can be excised from the cell by suddenly pulling the pipette away from the cell. Often the cell survives this hole-punching procedure by resealing of the damaged membrane, so that the excision can be repeated on the same cell. The excised patch is called an **inside-out patch (IOP)** (Fig. II), because the inside of the plasma membrane is now exposed to the external salt solution. In the excised patches, membrane patches are removed from their natural environment for optimal control of solution composition on both sides of the membrane. For example, this allows one to expose the cytoplasmic side to defined solutions in order, for example, to test for intracellular factors that control membrane channel activity. Another type of excised patch can be obtained, but now from the WC-configuration rather than the cell-attached configuration. It is the **outside-out patch (OOP)**, which is excised from the WC-configuration by slowly pulling the pipette away from the WC (Fig. II). This maneuver first defines a thin fiber that eventually breaks to form a vesicle at the tip of the pipette. The configuration obtained is a micro-WC configuration, which allows one to study small populations of channels or single channels and to readily manipulate the "tiny cell" to

different bathing solutions for rapid perfusion. The fifth configuration is the **permeabilized-patch WC-configuration (ppWC)** (not shown), in which the CAP is not actually ruptured for direct access to the inside of the cell, but made permeable by adding artificial ion channels (monovalent cation channel-forming antibiotics) via the pipette solution (Horn and Marty, 1988). Examples of such antibiotics are amphotericin and nystatin, both produced by microorganisms. The great advantage of this configuration is that it allows intracellular voltage- and current-clamp measurements on relatively intact cells, i.e. cells with a near normal cytoplasmic composition. This is in contrast to the perfused WC-configuration.

iii. The patch-clamp setup

A patch-clamp setup consists of the amplifier main unit (1, in Fig. III), with the integrated interface board, the computer system (2), the head-stage (or probe; 3), and the microscope (4) with the cell chamber (5). The amplifier main unit contains the power supply, the signal processing electronics, the analog / digital and digital / analog converters and the connectors for analog and digital input / output. The probe is contained in a small enclosure, designed to be mounted on a micromanipulator (6) and directly attached to the recording electrode through a pipette holder (7). The recording electrode, which will advance inside a glass-pipette (that contains the intracellular recording solution), is an Ag / AgCl electrode allowing ionic currents flowing in the pipette solution to be seen as electrical currents by the amplifier head-stage. A second Ag / AgCl electrode in the bath solution is connected to the head-stage ground terminal that is directly connected to the signal ground of the main unit. The micromanipulator and the micromanipulator unit – consisting of the keypad (8) and the control system (9) – control the movement of the pipette holder in the submicrometer range. The microscope is mounted on an appropriate vibration isolation table (10), to dump out undesired microscopic movements and vibrations. The cell chamber (or cell bath) is mounted onto the stage of the microscope, and will contain the extracellular solution that will feed the cells patched during experiments. A perfusion pump (not with this setup) may be used for continuously running the extracellular solution through the cell chamber during recordings. The microscope and the vibration isolation table are placed into a Faraday cage (11), used as a shield against the electromagnetic radiation present in the environment. Because of the extreme sensitivity of the setup components, all surfaces that will be near the probe input are grounded, in order to minimize the noise interference during recordings. The microscope and its stage are also grounded, because they constitute typical conducting surfaces nearest the

pipette and holder. In experiments that deal with fluorescent cells, a fluorescence lamp (12) is also used. In experiments in which a fast application of a certain drug is desired, the setup is additionally equipped with a fast-pressure application system (13), directly controlled by a voltage command valve control system (14). To continuously monitoring recordings, an oscilloscope is usually used (15, in Fig. III).

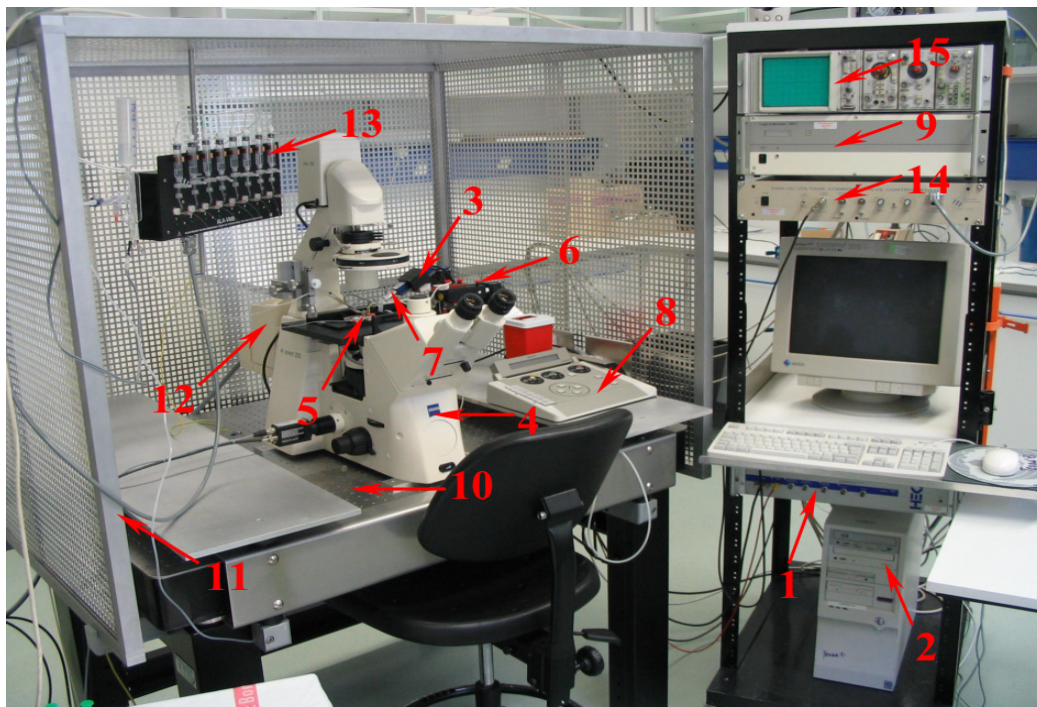


Fig. III Patch-clamp setup.

iv. The main steps during a patch-clamp experiment

Initially, the electrode is brought down and introduced into the bath with positive pressure applied to the pipette. The cell is then approached carefully, and, as the pipette tip presses the cell, the positive pressure is removed and gentle suction is applied, until the giga-seal is formed. After the formation of the giga-seal, which represents the cell-attached configuration, the suction is removed. If single-channel currents (in the range of a few pA) are the object of the study, the procedure stops here, and the recording is started. When ion currents of the entire cell are desired, after the cell-attached configuration is attained, by applying short pulses of suction or voltage to the interior of the pipette, the cell membrane is ruptured and the whole-cell mode is obtained. The recording can be started, and an average response of all channels present into the cell membrane can be obtained (usually, in the range of hundreds or thousands of pA).

References

Abicht A., Stucka R., Karcagi V., Herczegfalvi A., Horvath R., Mortier W., Schara U., Ramaekers V., Jost W., Brunner J., Janssen G., Seidel U., Schlotter B., Müller-Felber W., Pongratz D., Rüdell R., and Lochmüller H. (1999) A common mutation (ϵ 1267delG) in congenital myasthenic patients of Gypsy ethnic origin. *Neurology*: 53(7): 1564-9.

Abicht A., Stucka R., Song I. H., Karcagi V., Kugler K., Baumgarten-Walczak A., Stier C., Pongratz D., Mortier W., Müller-Ferber W., and Lochmüller H. (2000) Genetic analysis of the entire AChR ϵ -subunit gene in 52 congenital myasthenic families. *Acta Myol*: 19: 23–27.

Abicht A., Stucka R., Schmidt C., Briguet A., Hopfner S., Song I. H., Pongratz D., Müller-Felber W., Ruegg M. A., and Lochmüller H. (2002) A newly identified chromosomal microdeletion and an N-box mutation of the AChR ϵ gene cause a congenital myasthenic syndrome. *Brain*: 125(Pt 5): 1005-13.

Aidley D. J. (1989) The physiology of excitable cells. 3rd Ed. University Press, Cambridge, England.

Akk G., and Steinbach J. H. (2000) Structural elements near the C-terminus are responsible for changes in nicotinic receptor gating kinetics following patch excision. *J Physiol*: 527 Pt 3: 405-17.

Anderson C. R., and Stevens C. F. (1973) Voltage clamp analysis of acetylcholine produced endplate current fluctuations at frog neuromuscular junction. *J Physiol*: 235(3): 655-91.

Anderson D. J., Blobel G., Tzartos S., Gullick W., and Lindstrom J. (1983) Transmembrane orientation of an early biosynthetic form of acetylcholine receptor δ -subunit determined by proteolytic dissection in conjunction with monoclonal antibodies. *J Neurosci*: 3(9): 1773-84.

Bear M. F., Connors B. W., and Pardiso M. A. (2001) Neuroscience: Exploring the Brain. 2nd Ed. Lippincott Williams and Wilkins, Philadelphia, USA.

- Beeson D., Newland C., Croxen R., Buckel A., Li F. Y., Larsson C., Tariq M., Vincent A., and Newsom-Davis J.** (1998) Congenital myasthenic syndromes. Studies of the AChR and other candidate genes. *Ann N Y Acad Sci*: 841: 181-3.
- Bhattacharyya B. J., Day J. W., Gundeck J. E., Leonard S., Wollmann R. L., and Gomez C. M.** (1997) Desensitization of mutant acetylcholine receptors in transgenic mice reduces the amplitude of neuromuscular synaptic currents. *Synapse*: 27(4): 367-77.
- Black R., Goldman D., Hochschwender S., Lindstrom J., and Hall Z. W.** (1987) Genetic variants of C2 muscle cells that are defective in synthesis of the α -subunit of the acetylcholine receptor. *J Cell Biol*: 105(3): 1329-36.
- Blount P., and Merlie J. P.** (1990) Mutational analysis of muscle nicotinic acetylcholine receptor subunit assembly. *J Cell Biol*: 111(6 Pt 1): 2613-22.
- Bouzat C., Bren N., and Sine S. M.** (1994) Structural basis of the different gating kinetics of fetal and adult acetylcholine receptors. *Neuron*: 13(6): 1395-402.
- Butler D. H., and McNamee M. G.** (1993) FTIR analysis of nicotinic acetylcholine receptor secondary structure in reconstituted membranes. *Biochim Biophys Acta*: 1150(1): 17-24.
- Cachelin A. B., and Colquhoun D.** (1989) Desensitization of the acetylcholine receptor of frog endplates measured in a Vaseline-gap voltage clamp. *J Physiol*: 415: 159-88.
- Colquhoun D., and Sakmann B.** (1981) Fluctuations in the microsecond time range of the current through single acetylcholine receptor ion channels. *Nature*: 294(5840): 464-6.
- Colquhoun D., and Sakmann B.** (1985) Fast events in single-channel currents activated by acetylcholine and its analogues at the frog muscle endplate. *J Physiol*: 369: 501-57.
- Colquhoun D., Cachelin A. B., Marshall C. G., Mathie A., and Ogden D. C.** (1990) Function of nicotinic synapses. *Prog Brain Res*: 84: 43-50.

Colquhoun D., Unwin N., Shelley C., Hatton C. J., and Sivilotti L. (2003) In Burger's Medical Chemistry, Vol II "Drug Discovery and Drug Development", Chapter 11 ("Nicotinic Acetylcholine Receptors": 357 - 405). Ed. Abraham, D., J. Wiley, New York.

Corringer P. J., Le Novere N., and Changeux J. P. (2000) Nicotinic receptors at the amino acid level. *Annu Rev Pharmacol Toxicol*: 40: 431-58.

Croxen R., Newland C., Betty M., Vincent A., Newsom-Davis J., and Beeson D. (1999) Novel functional ϵ -subunit polypeptide generated by a single nucleotide deletion in acetylcholine receptor deficiency congenital myasthenic syndrome. *Ann Neurol*: 46(4): 639-47.

Croxen R., Young C., Slater C., Haslam S., Brydson M., Vincent A., and Beeson D. (2001) Endplate γ - and ϵ -subunit mRNA levels in AChR deficiency syndrome due to ϵ -subunit null mutations. *Brain*: 124(Pt 7): 1362-72.

Croxen R., Vincent A., Newsom-Davis J., and Beeson D. (2002) Myasthenia gravis in a woman with congenital AChR deficiency due to ϵ -subunit mutations. *Neurology*: 58(10): 1563-5.

Cully D. F., Vassilatis D. K., Liu K. K., Paress P. S., Van der Ploeg L. H., Schaeffer J. M., and Arena J. P. (1994) Cloning of an avermectin-sensitive glutamate-gated chloride channel from *Caenorhabditis elegans*. *Nature*: 371(6499): 707-11.

Dionne V. E., and Leibowitz M. D. (1982) Acetylcholine receptor kinetics. A description from single-channel currents at snake neuromuscular junctions. *Biophys J*: 39(3): 253-61.

Donger C., Krejci E., Serradell A. P., Eymard B., Bon S., Nicole S., Chateau D., Gary F., Fardeau M., Massoulie J., and Guicheney P. (1998) Mutation in the human acetylcholinesterase-associated collagen gene, COLQ, is responsible for congenital myasthenic syndrome with endplate acetylcholinesterase deficiency (Type Ic). *Am J Hum Genet*: 63(4): 967-75.

Ealing J., Webster R., Brownlow S., Abdelgany A., Oosterhuis H., Muntoni F., Vaux D. J., Vincent A., and Beeson D. (2002) Mutations in congenital myasthenic syndromes reveal

an ϵ -subunit C-terminal cysteine, C470, crucial for maturation and surface expression of adult AChR. *Hum Mol Genet*: 11(24): 3087-96.

Eertmoed A. L., and Green W. N. (1999) Nicotinic receptor assembly requires multiple regions throughout the γ -subunit. *J Neurosci*: 19(15): 6298-308.

Elenes S., and Auerbach A. (2002) Desensitization of diliganded mouse muscle nicotinic acetylcholine receptor channels. *J Physiol*: 541(Pt 2): 367-83.

Engel A. G., and Biesecker G. (1982) Complement activation in muscle fiber necrosis: demonstration of the membrane attack complex of complement in necrotic fibers. *Ann Neurol*: 12(3): 289-96.

Engel A. G. (1993a) The investigation of congenital myasthenic syndromes. *Ann N Y Acad Sci*: 681: 425-34.

Engel A. G., Hutchinson D. O., Nakano S., Murphy L., Griggs R. C., Gu Y., Hall Z. W., and Lindstrom J. (1993b) Myasthenic syndromes attributed to mutations affecting the ϵ -subunit of the acetylcholine receptor. *Ann N Y Acad Sci*: 681: 496-508.

Engel A. G. (1994) Congenital myasthenic syndromes. *Neurol Clin*: 12(2): 401-37.

Engel A. G., Ohno K., Bouzat C., Sine S. M., and Griggs R. G. (1996a) Endplate acetylcholine receptor deficiency due to nonsense mutations in the ϵ -subunit. *Ann Neurol*: 40: 810-17.

Engel A. G., Ohno K., Milone M., Wang H. L., Nakano S., Bouzat C., Pruitt J. N., Hutchinson D. O., Brengman J. M., Bren N., Sieb J. P., and Sine S. M. (1996b) New mutations in acetylcholine receptor subunit genes reveal heterogeneity in the slow-channel congenital myasthenic syndrome. *Hum Mol Genet*: 5(9): 1217-27.

Engel A. G. (1999a) Congenital myasthenic syndromes. *J Child Neurol*: 14(1): 38-41.

- Engel A. G., Ohno K., and Sine S. M.** (1999b) Congenital myasthenic syndromes: recent advances. *Arch Neurol*: 56(2): 163-7.
- Engel A. G., Ohno K., and Sine S. M.** (2003a) Congenital myasthenic syndromes: progress over the past decade. *Muscle Nerve*: 27(1): 4-25.
- Engel A. G., Ohno K., and Sine S. M.** (2003b) Sleuthing molecular targets for neurological diseases at the neuromuscular junction. *Nat Rev Neurosci*: 4(5): 339-52.
- Engel A. G., Ohno K., and Sine S. M.** (2003c) Congenital myasthenic syndromes: A diverse array of molecular targets. *J Neurocytol*: 32(5-8): 1017-37.
- Finer-Moore J., and Stroud R. M.** (1984) Amphipathic analysis and possible formation of the ion channel in an acetylcholine receptor. *Proc Natl Acad Sci U S A*: 81(1): 155-9.
- Flucher B. E., and Daniels M. P.** (1989) Distribution of Na⁺ channels and ankyrin in neuromuscular junctions is complementary to that of acetylcholine receptors and the 43 kDa protein. *Neuron*: 3(2): 163-75.
- Franke C., Parnas H., Hovav G., and Dudel J.** (1993) A molecular scheme for the reaction between acetylcholine and nicotinic channels. *Biophys J*: 64(2): 339-56.
- Gomez C. M., Maselli R., Gundeck J. E., Chao M., Day J. W., Tamamizu S., Lasalde J. A., McNamee M., and Wollmann R. L.** (1997) Slow-channel transgenic mice: a model of postsynaptic organellar degeneration at the neuromuscular junction. *J Neurosci*: 17(11): 4170-9.
- Gomez C. M., Maselli R. A., Groshong J., Zayas R., Wollmann R. L., Cens T., and Charnet P.** (2002) Active calcium accumulation underlies severe weakness in a panel of mice with slow-channel syndrome. *J Neurosci*: 22(15): 6447-57.
- Grosman C., and Auerbach A.** (2000) Kinetic, mechanistic, and structural aspects of unliganded gating of acetylcholine receptor channels: a single-channel study of second transmembrane segment 12' mutants. *J Gen Physiol*: 115(5): 621-35.

Grosman C., and Auerbach A. (2001) The dissociation of acetylcholine from open nicotinic receptor channels. *Proc Natl Acad Sci U S A*: 98(24): 14102-7.

Gu Y., Ralston E., Murphy-Erdosh C., Black R. A., and Hall Z. W. (1989) Acetylcholine receptor in a C2 muscle cell variant is retained in the endoplasmic reticulum. *J Cell Biol*: 109(2): 729-38.

Gu Y., Forsayeth J. R., Verrall S., Yu X. M., and Hall Z. W. (1991) Assembly of the mammalian muscle acetylcholine receptor in transfected COS cells. *J Cell Biol*: 114(4): 799-807.

Hamill O. P., Marty A., Neher E., Sakmann B., and Sigworth F. J. (1981) Improved patch-clamp techniques for high-resolution current recording from cells and cell-free membrane patches. *Pflugers Arch*: 391(2): 85-100.

Hatton C. J., Shelley C., Brydson M., Beeson D., and Colquhoun D. (2003) Properties of the human muscle nicotinic receptor, and of the slow-channel myasthenic syndrome mutant ϵ L221F, inferred from maximum likelihood fits. *J Physiol*: 547(Pt 3): 729-60.

Hille B. (2001) Ionic channels of excitable membranes. 3rd Ed., *Sinauer Associates, Inc.*, Sunderland, Massachusetts, USA.

Horn R., and Marty A. (1988) Muscarinic activation of ionic currents measured by a new whole-cell recording method. *J Gen Physiol*: 92(2): 145-59.

Jackson M. B. (1984) Spontaneous openings of the acetylcholine receptor channel. *Proc Natl Acad Sci U S A*: 81(12): 3901-4.

Jackson M. B. (1986) Kinetics of unliganded acetylcholine receptor channel-gating. *Biophys J*: 49(3): 663-72.

Jackson M. B. (1988) Dependence of acetylcholine receptor channel kinetics on agonist concentration in cultured mouse muscle fibers. *J Physiol*: 397: 555-83.

- Jackson M. B., Imoto K., Mishina M., Konno T., Numa S., and Sakmann B.** (1990) Spontaneous and agonist-induced openings of an acetylcholine receptor channel composed of bovine muscle α -, β -, and δ -subunits. *Pflugers Arch*: 417(2): 129-35.
- Jaramillo F., Vicini S., and Schuetze S. M.** (1988) Embryonic acetylcholine receptors guarantee spontaneous contractions in rat developing muscle. *Nature*: 335(6185): 66-8.
- Jones S. F., and Kwanbunbumpen S.** (1970a) The effects of nerve stimulation and hemicholinium on synaptic vesicles at the mammalian neuromuscular junction. *J Physiol*: 207(1): 31-50.
- Jones S. F., and Kwanbunbumpen S.** (1970b) Some effects of nerve stimulation and hemicholinium on quantal transmitter release at the mammalian neuromuscular junction. *J Physiol*: 207(1): 51-61.
- Kao P. N., and Karlin A.** (1986) Acetylcholine receptor binding site contains a disulfide cross-link between adjacent half-cystinyl residues. *J Biol Chem*: 261(18): 8085-8.
- Karlin A., Holtzman E., Yodh N., Lobel P., Wall J., and Hainfeld J.** (1983) The arrangement of the subunits of the acetylcholine receptor of *Torpedo californica*. *J Biol Chem*: 258(11): 6678-81.
- Karlin A.** (1993) Structure of nicotinic acetylcholine receptors. *Curr Opin Neurobiol*: 3(3): 299-309.
- Karlin A., and Akabas M. H.** (1995) Toward a structural basis for the function of nicotinic acetylcholine receptors and their cousins. *Neuron*: 15(6): 1231-44.
- Karlin A.** (2002) Emerging structure of the nicotinic acetylcholine receptors. *Nat Rev Neurosci*: 3(2): 102-14.
- Katz B., and Thesleff S.** (1957) A study of the desensitization produced by acetylcholine at the motor endplate. *J Physiol*: 138(1): 63-80.

Katz B. (1966) Nerve, Muscle, and Synapse. *Ed. McGraw-Hill, New York.*

Kraner S., Laufenberg I., Strassburg H. M., Sieb J. P., and Steinlein O. K. (2003) Congenital myasthenic syndrome with episodic apnea in patients homozygous for a CHAT missense mutation. *Arch Neurol: 60(5): 761-3.*

Li J., Sheng S., Perry C. J., and Kleyman T. R. (2003) Asymmetric organization of the pore region of the epithelial sodium channel. *J Biol Chem: 278(16): 13867-74.*

Lindstrom J. (2000) The structures of neuronal nicotinic receptors. In Handbook of Experimental Pharmacology (Clementi F., Fornasari D., Gotti C., eds), vol. 144: 101- 162. *Springer-Verlag, Berlin-Heidelberg.*

Lindstrom J. (2001) Nicotinic Acetylcholine Receptors. Encyclopedia of Life Sciences / *Macmillan Publishers Ltd., Nature Publishing Group, London, England.*

Lindstrom J. M. (2000) Acetylcholine receptors and myasthenia. *Muscle Nerve: 23(4): 453-77.*

Martin A. R. (1994) Amplification of neuromuscular transmission by postjunctional folds. *Proc. R. Soc. Lond: B 258: 321-26.*

Maselli R., Chen M., Chen T. Y., Kong D. Z., Agius M. A., Bowe C., Wollman R. L., and Gomez C. M. (2002) Severe low-affinity fast-channel syndrome due to a heteroallelic nonsense/missense mutation in the acetylcholine receptor ϵ -subunit. *Neurology: 58(Suppl 3): A228.*

Merlie J. P., Sebbane R., Gardner S., Olson E., and Lindstrom J. (1983) The regulation of acetylcholine receptor expression in mammalian muscle. *Cold Spring Harb Symp Quant Biol: 48 Pt 1: 135-46.*

Middleton L. T. (1996) Congenital myasthenic syndromes. 34th ENMC International Workshop, 10-11 June 1995. *Neuromuscul Disord: 6(2): 133-6.*

Middleton L., Ohno K., Christodoulou K., Brengman J., Milone M., Neocleous V., Serdaroglu P., Deymeer F., Ozdemir C., Mubaidin A., Horany K., Al-Shehab A., Mavromatis I., Mylonas I., Tsingis M., Zamba E., Pantzaris M., Kyriallis K., and Engel A. G. (1999) Chromosome 17p-linked myasthenias stem from defects in the acetylcholine receptor ϵ -subunit gene. *Neurology*: 53(5): 1076-82.

Milone M., Wang H. L., Ohno K., Fukudome T., Pruitt J. N., Bren N., Sine S. M., and Engel A. G. (1997) Slow-channel myasthenic syndrome caused by enhanced activation, desensitization, and agonist binding affinity attributable to mutation in the M₂ domain of the acetylcholine receptor alpha subunit. *J Neurosci*: 17(15): 5651-65.

Milone M., Wang H. L., Ohno K., Prince R., Fukudome T., Shen X. M., Brengman J. M., Griggs R. C., Sine S. M., and Engel A. G. (1998a) Mode switching kinetics produced by a naturally occurring mutation in the cytoplasmic loop of the human acetylcholine receptor ϵ -subunit. *Neuron*: 20(3): 575-88.

Milone M., Ohno K., Fukudome T., Shen X. M., Brengman J., Griggs R. C., and Engel A. G. (1998b) Congenital myasthenic syndrome caused by novel loss-of-function mutations in the human AChR ϵ -subunit gene. *Ann N Y Acad Sci*: 841: 184-8.

Mishina M., Takai T., Imoto K., Noda M., Takahashi T., Numa S., Methfessel C., and Sakmann B. (1986) Molecular distinction between fetal and adult forms of muscle acetylcholine receptor. *Nature*: 321(6068): 406-11.

Miyazawa A., Fujiyoshi Y., Stowell M., and Unwin N. (1999) Nicotinic acetylcholine receptor at 4.6 Å resolution: transverse tunnels in the channel wall. *J Mol Biol*: 288(4): 765-86.

Neher E., and Sakmann B. (1976) Single-channel currents recorded from membrane of denervated frog muscle fibers. *Nature*: 260(5554): 799-802.

Neher E., Marty A., and Fenwick E. (1983) Ionic channels for signal transmission and propagation. *Prog Brain Res*: 58: 39-48.

Neher E. (1992) Nobel Lecture. Ion channels for communication between and within cells. *EMBO J*: 11(5): 1672-9.

Newland C. F., Beeson D., Vincent A., and Newsom-Davis J. (1995) Functional and non-functional isoforms of the human muscle acetylcholine receptor. *J Physiol*: 489(Pt 3): 767-78.

Nichols P., Croxen R., Vincent A., Rutter R., Hutchinson M., Newsom-Davis J., and Beeson D. (1999) Mutation of the acetylcholine receptor ϵ -subunit promoter in congenital myasthenic syndrome. *Ann Neurol*: 45(4): 439-43.

Ohno K., Hutchinson D. O., Milone M., Brengman J. M., Bouzat C., Sine S. M., and Engel A. G. (1995) Congenital myasthenic syndrome caused by prolonged acetylcholine receptor channel-openings due to a mutation in the M₂ domain of the ϵ -subunit. *Proc Natl Acad Sci U S A*: 92(3): 758-62.

Ohno K., Wang H. L., Milone M., Bren N., Brengman J. M., Nakano S., Quiram P., Pruitt J. N., Sine S. M., and Engel A. G. (1996) Congenital myasthenic syndrome caused by decreased agonist binding affinity due to a mutation in the acetylcholine receptor ϵ -subunit. *Neuron*: 17(1): 157-70.

Ohno K., Quiram P. A., Milone M., Wang H. L., Harper M. C., Pruitt J. N., Brengman J. M., Pao L., Fischbeck K. H., Crawford T. O., Sine S. M., and Engel A. G. (1997) Congenital myasthenic syndromes due to heteroallelic nonsense/missense mutations in the acetylcholine receptor ϵ -subunit gene: identification and functional characterization of six new mutations. *Hum Mol Genet*: 6(5): 753-66.

Ohno K., Anlar B., Özdirim E., Brengman J. M., and Engel A. G. (1998a) Frameshifting and splice-site mutations in the acetylcholine receptor ϵ -subunit gene in three Turkish kinships with congenital myasthenic syndromes. *Ann N Y Acad Sci*: 841: 189-94.

Ohno K., Anlar B., Özdirim E., Brengman J. M., DeBleecker J. L., and Engel A. G. (1998b) Myasthenic syndromes in Turkish kinships due to mutations in the acetylcholine receptor. *Ann Neurol*: 44(2): 234-41.

- Ohno K., Anlar B., and Engel A. G.** (1999) Congenital myasthenic syndrome caused by a mutation in the Ets-binding site of the promoter region of the acetylcholine receptor ϵ -subunit gene. *Neuromuscul Disord*: 9(3): 131-5.
- Ohno K., Tsujino A., Brengman J. M., Harper C. M., Bajzer Z., Udd B., Beyring R., Robb S., Kirkham F. J., and Engel A. G.** (2001) Choline acetyltransferase mutations cause myasthenic syndrome associated with episodic apnea in humans. *Proc Natl Acad Sci U S A*: 98(4): 2017-22.
- Ohno K., Engel A. G., Shen X. M., Selcen D., Brengman J., Harper C. M., Tsujino A., and Milone M.** (2002) RAPSIN mutations in humans cause endplate acetylcholine-receptor deficiency and myasthenic syndrome. *Am J Hum Genet*: 70(4): 875-85.
- Ortells M. O., and Lunt G. G.** (1995) Evolutionary history of the ligand-gated ion channel superfamily of receptors. *Trends Neurosci*: 18(3): 121-7.
- Pusch M., and Neher E.** (1988) Rates of diffusional exchange between small cells and a measuring patch pipette. *Pflugers Arch*: 411(2): 204-11.
- Quiram P., Ohno K., Milone M., Patterson M. C., Pruitt N. J., Brengman J. M., Sine S. M., and Engel A. G.** (1999) Mutation causing congenital myasthenia reveals acetylcholine receptor β/δ subunit interaction essential for assembly. *J Clin Invest*: 104: 1403-1410.
- Reynolds J. A., and Karlin A.** (1978) Molecular weight in detergent solution of acetylcholine receptor from *Torpedo californica*. *Biochemistry*: 17(11): 2035-8.
- Ruff R. L.** (1996) Sodium channel slow inactivation and the distribution of sodium channels on skeletal muscle fibers enable the performance properties of different skeletal muscle fiber types. *Acta Physiol Scand*: 156(3): 159-68.
- Sakmann B., Patlak J., and Neher E.** (1980) Single acetylcholine-activated channels show burst-kinetics in presence of desensitizing concentrations of agonist. *Nature*: 286(5768): 71-3.

Sakmann B. (1992) Nobel Lecture. Elementary steps in synaptic transmission revealed by currents through single ion channels. *EMBO J*: 11(6): 2002-16.

Salpeter M. M. (1987) In the Vertebrate Neuromuscular Junction. Ed. John Wiley & Sons Inc., New York.

Schofield P. R., Darlison M. G., Fujita N., Burt D. R., Stephenson F. A., Rodriguez H., Rhee L. M., Ramachandran J., Reale V., and Glencorse T. A. (1987) Sequence and functional expression of the GABA_A receptor shows a ligand-gated receptor super-family. *Nature*: 328(6127): 221-7.

Shen X. M., Ohno K., Fukudome T., Brengman J. M., and Engel A. G. (1999) Deletion of a single codon from the long cytoplasmic loop of the AChR subunit gene causes brief single-channel currents. *Soc Neurosci Abstr*: 25: 1721.

Shen X. M., Tsujino A., Ohno K., Brengman J. M., Gingold M., and Engel A. G. (2000) A novel fast-channel congenital myasthenic syndrome caused by a mutation in the Cys-loop domain of the acetylcholine receptor ϵ -subunit. *Neurology*: 54(Suppl3): A138.

Shen X. M., Ohno K., Milone M., Brengman J. M., Spilsbury P. R., and Engel A. G. (2001) Fast-channel syndrome. *Neurology*: 56(Suppl. 3): A60.

Shen X. M., Ohno K., Fukudome T., Tsujino A., Brengman J. M., De Vivo D. C., Packer R. J., and Engel A. G. (2002) Congenital myasthenic syndrome caused by low-expressor fast-channel AChR δ -subunit mutation. *Neurology*: 59(12): 1881-8.

Shen X. M., Ohno K., Tsujino A., Brengman J. M., Gingold M., Sine S. M., and Engel A. G. (2003) Mutation causing severe myasthenia reveals functional asymmetry of AChR signature cysteine loops in agonist binding and gating. *J Clin Invest*: 111(4): 497-505.

Sieb J. P., Dorfler P., Tzartos S., Wewer U. M., Ruegg M. A., Meyer D., Baumann I., Lindemuth R., Jakschik J., and Ries F. (1998) Congenital myasthenic syndromes in two kinships with endplate acetylcholine receptor and utrophin deficiency. *Neurology*: 50(1): 54-61.

- Sieb J. P., Kraner S., Rauch M., and Steinlein O. K.** (2000a) Immature endplates and utrophin deficiency in congenital myasthenic syndrome caused by ϵ -AChR subunit truncating mutations. *Hum Genet*: 107(2): 160-4.
- Sieb J. P., Kraner S., Schrank B., Reitter B., Goebel T. H., Tzartos S. J., and Steinlein O. K.** (2000b) Severe congenital myasthenic syndrome due to homozygosity of the 1293insG ϵ -acetylcholine receptor subunit mutation. *Ann Neurol*: 48(3): 379-83.
- Sigworth F. J., and Sine S. M.** (1987) Data transformations for improved display and fitting of single-channel dwell time histograms. *Biophys J*: 52(6): 1047-54.
- Sine S. M., Claudio T., and Sigworth F. J.** (1990) Activation of Torpedo acetylcholine receptors expressed in mouse fibroblasts. Single-channel current kinetics reveal distinct agonist binding affinities. *J Gen Physiol*: 96(2): 395-437.
- Sine S. M., Ohno K., Bouzat C., Auerbach A., Milone M., Pruitt J. N., and Engel A. G.** (1995) Mutation of the acetylcholine receptor α -subunit causes a slow-channel myasthenic syndrome by enhancing agonist-binding affinity. *Neuron*: 15(1): 229-39.
- Sine S. M., Shen X. M., Wang H. L., Ohno K., Lee W. Y., Tsujino A., Brengmann J., Bren N., Vajsar J., and Engel A. G.** (2002) Naturally occurring mutations at the acetylcholine receptor binding site independently alter ACh binding and channel-gating. *J Gen Physiol*: 120(4): 483-96.
- Smith M. M., Lindstrom J., and Merlie J. P.** (1987) Formation of the α -bungarotoxin binding site and assembly of the nicotinic acetylcholine receptor subunits occur in the endoplasmic reticulum. *J Biol Chem*: 262(9): 4367-76.
- Snyder P. M., Olson D. R., and Bucher D. B.** (1999) A pore segment in DEG / ENaC Na⁺ channels. *J Biol Chem*: 274(40): 28484-90.
- Stroud R. M., McCarthy M. P., and Shuster M.** (1990) Nicotinic acetylcholine receptor superfamily of ligand-gated ion channels. *Biochemistry*: 29(50): 11009-23.

Takeuchi A., and Takeuchi N. (1960) On the permeability of endplate membrane during the action of transmitter. *J Physiol (Paris)*: 154: 52-67.

Tsunoyama K., and Gojobori T. (1998) Evolution of nicotinic acetylcholine receptor subunits. *Mol Biol Evol*: 15(5): 518-27.

Uchitel O., Engel A. G., Walls T. J., Nagel A., Bril V., and Trastek V. F. (1993a) Congenital myasthenic syndrome attributed to an abnormal interaction of acetylcholine with its receptor. *Ann N Y Acad Sci*: 681: 487-95.

Uchitel O., Engel A. G., Walls T. J., Nagel A., Atassi M. Z., and Bril V. (1993b) Congenital myasthenic syndromes: II. Syndrome attributed to abnormal interaction of acetylcholine with its receptor. *Muscle Nerve*: 16(12): 1293-301.

Unwin N. (1993) Nicotinic acetylcholine receptor at 9 Å resolution. *J Mol Biol*: 229(4): 1101-24.

Unwin N. (1995) Acetylcholine receptor channel imaged in the open state. *Nature*: 373(6509): 37-43.

Verrall S., and Hall Z. W. (1992) The N-terminal domains of acetylcholine receptor subunits contain recognition signals for the initial steps of receptor assembly. *Cell*: 68(1): 23-31.

Vincent A., Newland C., Croxen R., and Beeson D. (1997) Genes at the junction-candidates for congenital myasthenic syndromes. *Trends Neurosci*: 20(1): 15-22.

Vincent A., Beeson D., and Lang B. (2000) Molecular targets for autoimmune and genetic disorders of neuromuscular transmission. *Eur J Biochem*: 267(23): 6717-28.

Wang H. L., Ohno K., Milone M., Brengman J. M., Evoli A., Batocchi A. P., Middleton L. T., Christodoulou K., Engel A. G., and Sine S. M. (2000) Fundamental gating mechanism of nicotinic receptor channel revealed by mutation causing a congenital myasthenic syndrome. *J Gen Physiol*: 116(3): 449-62.

- Wang J. M., Zhang L., Yao Y., Viroonchatapan N., Rothe E., and Wang Z. Z.** (2002) A transmembrane motif governs the surface trafficking of nicotinic acetylcholine receptors. *Nat Neurosci*: 5(10): 963-70.
- Witzemann V., Schwarz H., Koenen M., Berberich C., Villarroel A., Wernig A., Brenner H. R., and Sakmann B.** (1996) Acetylcholine receptor ϵ -subunit deletion causes muscle weakness and atrophy in juvenile and adult mice. *Proc Natl Acad Sci U S A*: 93(23): 13286-91.
- Wood S. J., and Slater C. R.** (2001) Safety factor at the neuromuscular junction. *Prog Neurobiol*: 64(4): 393-429.
- Xie Y., and Cohen J. B.** (2001) Contributions of Torpedo nicotinic acetylcholine receptor γ Trp-55 and δ Trp-57 to agonist and competitive antagonist function. *J Biol Chem*: 276(4): 2417-26.
- Zheng Y., Hirschberg B., Yuan J., Wang A. P., Hunt D. C., Ludmerer S. W., Schmatz D. M., and Cully D. F.** (2002) Identification of two novel *Drosophila melanogaster* histamine-gated chloride channel subunits expressed in the eye. *J Biol Chem*: 277(3): 2000-5.
- Zhou M., Engel A. G., and Auerbach A.** (1999a) Serum choline activates mutant acetylcholine receptors that cause slow-channel congenital myasthenic syndromes. *Proc Natl Acad Sci USA*: 96(18): 10466-71.
- Zhou M., Grosman C., and Auerbach A.** (1999b) Single-channel properties of the ϵ -less acetylcholine receptor channel. *Biophys J*: 76: A371 (Abstr.).

Eidesstattliche Erklärung

An Eides Statt versichere ich, dass ich diese Arbeit selbst und ohne jede unerlaubte Hilfe angefertigt habe, und dass diese oder eine ähnliche Arbeit noch keiner anderen Stelle zur Prüfung vorgelegen hat.

Bonn, November 2004

Cristian Gurgui

Curriculum Vitae

CRISTIAN GURGUI

Phone: +49 (0) 1632963758
christian.gurgui@ukb.uni-bonn.de

Personal Data

Name, First Name	GURGUI, CRISTIAN
Born	December 31 st , 1977
In	Bucharest, Romania
Family status	Single
Nationality	Romanian

Education

09/02 – 10/04	University of Bonn, Institute of Physiology II, Germany PhD thesis: “ <i>Functional consequences of ϵ AChR subunit truncating mutations linked to Congenital Myasthenic Syndrome</i> ”
10/01 – 08/02	University of Bonn, Kekulé Institute of Organic Chemistry and Biochemistry, Germany Master thesis: “ <i>The physiological significance of intracellular sphingosine-1-phosphate. Knock out of sphingosine-1-phosphate lyase by RNA interference in Swiss 3T3 fibroblasts</i> ”
09/00 – 06/02	University of Bucharest, Faculty of Biology, Romania Master of Biochemistry and Molecular Biology
09/99 – 06/00	Physical Chemistry Department, Faculty of Chemistry, Romania Diploma thesis: “ <i>Characterization through Cyclic Voltammetry of Some New Synthesized Coumarin Derivatives, biologically active</i> ”
09/96 – 06/00	University of Bucharest, Faculty of Chemistry, Romania Head subject: Technological Biochemistry
09/92 – 06/96	High School “Dimitrie Leonida“, Bucharest, Romania Baccalaureate: June 1996
09/84 – 06/92	Primary School No. 82, Bucharest, Romania

Bonn, Nov 2004